UNIVERSITY OF HAWAII
LIBRARY

Journal of MOLECULAR BIOLOGY

EDITOR-IN-CHIEF: J. C. KENDREW

Volume II, Number 4, October 1960

ACADEMIC PRESS LTD., LONDON
ACADEMIC PRESS INC., NEW YORK

JOURNAL OF MOLECULAR BIOLOGY

EDITOR-IN-CHIEF

J. C. KENDREW, Peterhouse, Cambridge, England

EDITORIAL BOARD

P. DOTY, Department of Chemistry, Harvard University, Cambridge, Mass., U.S.A.
A. F. HUXLEY, Physiological Laboratory, University of Cambridge, England.
R. L. SINSHEIMER, Division of Biology, California Institute of Technology, Pasadena, Cal., U.S.A.
J. D. WATSON, Biological Laboratories, Harvard University, Cambridge, Mass., U.S.A.
M. H. F. WILKINS, Physics Department, King's College, London, England.

ADVISORY BOARD

S. BENZER, Purdue University, U.S.A.
M. CALVIN, University of California, Berkeley, U.S.A.
F. H. C. CRICK, University of Cambridge, England.
J. F. DANIELLI, King's College, London, England.
A. ENGSTRÖM, Karolinska Institutet, Stockholm, Sweden.
A. D. HERSHEY, Carnegie Institute, Cold Spring Harbor, U.S.A.
F. JACOB, Pasteur Institute, Paris, France.
A. KORNBERG, Stanford University, Stanford, California, U.S.A.
C. LEVINTHAL, Massachusetts Institute of Technology, Cambridge, Mass., U.S.A.
S. E. LURIA, Massachusetts Institute of Technology, Cambridge, Mass., U.S.A.
D. MAZIA, University of California, Berkeley, U.S.A.
P. B. MEDAWAR, University College, London, England.
L. E. ORGEL, University of Cambridge, England.
M. F. PERUTZ, University of Cambridge, England.
R. D. PRESTON, University of Leeds, England.
G. N. RAMACHANDRAN, University of Madras, India.
A. RICH, Massachusetts Institute of Technology, Cambridge, Mass., U.S.A.
G. SCHRAMM, Max-Planck Institut, Tübingen, Germany.
F. S. SJØSTRAND, Karolinska Institutet, Stockholm, Sweden.
I. WATANABE, University of Tokyo, Japan.
R. C. WILLIAMS, University of California, Berkeley, U.S.A.

Published by Academic Press Inc. (London) Limited

Volume II, 1960: 100*s*. ($14.00)

Subscription orders should be sent to Academic Press Inc. (London) Limited, 17 Old Queen Street, London, S.W.1, with the exception of those originating in the U.S.A., Canada, Central America, and South America; these should be sent to Academic Press Inc., 111 Fifth Avenue, New York 3, N.Y.

Copyright © 1960, by Academic Press Inc. (London) Limited

J. Mol. Biol. (1960) **2**, 171-188

Configurational Properties of Tobacco Mosaic Virus Ribonucleic Acid

Helga Boedtker

Conant Laboratory, Harvard University, Cambridge, Mass., U.S.A.

(*Received 5 April 1960*)

The configuration of nearly monodisperse tobacco mosaic virus (TMV) ribonucleic acid (RNA) of molecular weight 2·0 ± 0·1 million was studied at 20 to 25°C in 0·1 M-sodium phosphate buffer, pH 6·8, by light scattering, sedimentation, viscosity, optical rotary dispersion, and optical absorbance measurements. Results show that the partly helical configuration stable under these conditions behaves hydrodynamically as a randomly coiled polymer chain. The RNA chain becomes more compact when solutions are heated briefly to temperatures as high as 80°C and cooled rapidly, or allowed to stand at 25°C for 2 days, no change in molecular weight or distribution being observed under these conditions.

The helix-coil transition was observed by optical rotary dispersion measurements at 21 and 71°C, the critical wave length changing from 2500 to 3100 Å, and by relative absorbance-temperature profiles as a function of both monovalent and divalent counterion concentrations. Mg^{2+} was found to be about 25,000 times more effective than Na^{+} in stabilizing the helical regions of RNA. However, the addition of Na^{+} to solutions of RNA containing Mg^{2+} does not increase but *decreases* the helix stability. If the ratio of Na^{+} to Mg^{2+} is high enough (about 1500) the temperature of the helix-coil transition is determined by the Na^{+} rather than by the Mg^{2+} concentration.

The helix-coil transition was also studied by measuring both the absorbance and the sedimentation coefficient as a function of the concentration of added sodium. The observation that a marked increase in sedimentation coefficient coincides with the increase in hypochromicity led to the suggestion that the configurational transition is reflected by a large change in the overall spatial arrangement of the segments of the RNA chain and not just by local variations along the chain. From the sharpness of the distribution of sedimentation coefficients throughout the transition region, it seems likely that all the RNA molecules from TMV behave identically, as expected from their uniform primary chemical structure.

1. Introduction

The existence of a secondary structure in RNA has recently been demonstrated by using several methods that are sensitive to base-paired helical structures and that have been calibrated by means of synthetic polynucleotides of known configuration (Doty, Boedtker, Fresco, Haselkorn & Litt, 1959; Doty, Boedtker, Fresco, Hall & Haselkorn, 1959). The secondary structure was identified as short helical regions in which base pairs united two neighbouring parts of the single RNA strand. This particular disposition of hydrogen bonding was necessary to explain changes in absorbance at 2580 Å and optical rotation upon heating; it offered an equally adequate means of accounting for other data which showed the presence of a large number of

intramolecular hydrogen bonds, irrespective of whether or not they were periodically arranged as is required for secondary structure. Examples of this second type of observation include the reduced reactivity of the bases with formaldehyde (Hall & Doty, 1959; Doty *et al.*, 1959) and the highly constricted form of the RNA chain in solution (Boedtker, 1959; Hall & Doty, 1958).

If the RNA chain consists of short helical regions alternating with flexible unbonded regions, it is to be expected that the molecular properties as reflected in the sedimentation coefficient and viscosity will be a sensitive index of the relative amount of secondary structure. It should therefore be possible to observe significant changes in these properties when the helical regions are destroyed by increasing the temperature or decreasing the ionic strength. Preliminary evidence that the dimensions of tobacco mosaic virus (TMV) RNA are very temperature dependent (Boedtker, 1959) has been confirmed (Gavrilova, Spirin & Belozerskii, 1959; Spirin, Gavrilova, Bresler & Mossevitsky, 1959). Moreover it has been reported that the ionic strength dependence of the viscosity of *Escherichia coli* ribosomal RNA is greater than could be explained in terms of the expansion of a typical polyelectrolyte (Cox & Littauer, 1959). It was of interest, therefore, to study these hydrodynamic changes quantitatively and to correlate them if possible with the hypochromic changes associated with the helix-coil transition.

In studying the helix-coil transition, particular attention has been given to the effect of divalent counterions on the RNA configuration. Previously evidence had been presented suggesting that the presence of small amounts of divalent cations strongly favor the existence of the partly helical form of RNA (Haschemeyer, Singer & Fraenkel-Conrat, 1959), but the nature of the interaction between these ions and RNA was uncertain. Therefore we wished to determine whether a divalent ion such as Mg^{2+} plays a special role, qualitatively different from that of monovalent ions, in stabilizing the helical regions of RNA.

TMV RNA is uniquely suited to a detailed study of secondary structure since it consists of a single molecular species of high molecular weight and relatively stable RNA. Before presenting the results on the helix-coil transition, some further studies on the molecular weight and the configuration of TMV RNA will be presented.

2. Materials

TMV was prepared by the procedure previously described (Boedtker & Simmons, 1958). All samples were examined by flow birefringence and sedimentation measurements thereby establishing that at least 95% of the preparation consisted of particles of uniform size. The virus was then stored in either 0·02 M-sodium phosphate buffer at pH 7·3, or in 0·001 M-EDTA (ethylenediaminetetra-acetate) at pH 7·5. RNA was prepared from TMV solutions having a concentration of 1 to 2 g/100 ml.

With one exception, all RNA samples were prepared by the Schramm method (Gierer & Schramm, 1956 *a* & *b*) using redistilled phenol. From 5 to 25 ml. of TMV solution were shaken with an equal volume of water-saturated phenol at 5°C for 7 min. The layers were separated by centrifuging for 8 min at 7000 ***g***, and then carefully pipetting off the upper layer. The process was repeated twice with smaller volumes of phenol and shorter shaking times. The final solution was shaken several times with 3 volumes of ether, and then nitrogen was bubbled through the solution to remove the ether. The preparation required 1 hr, whereupon RNA solutions were either frozen or used immediately. As reported previously (Boedtker, 1959), freezing has no measurable effect on the properties of RNA. The yields obtained were seldom better than 60% because an appreciable fraction of the RNA was lost while separating the layers.

3. Molecular Properties of TMV RNA

(a) *Molecular weight*

Although the physical properties of RNA isolated by heat denaturation of TMV have been studied in some detail (Boedtker, 1959), relatively few physical data are available on RNA prepared by phenol extraction. For this reason the molecular weight and distribution of RNA prepared by both methods was measured and the results compared. It is known from absorbance measurements that TMV RNA exhibits a maximum helical character at room temperature if the ionic strength is 0·2 or higher. Therefore the physical properties were studied in 0·1 M-sodium phosphate buffer in which the ratio of the disodium to the monosodium salt was either 1 : 1 (pH 6·8) or 13 : 7 (pH 7·1). The details of the methods used have been described previously (Boedtker, 1959), and will not be repeated here.

The results of molecular weight determinations by light scattering and sedimentation-viscosity on three different phenol preparations (P–20, P–24, P–25) as well as on one heat preparation (H–28) are summarized in Table 1. With the exception of P–24,

TABLE 1

Molecular weight of TMV RNA

Sample	$[\eta]$	$S_{20°,w}$	$M_{[\eta],S}\times10^{-6}$	$M_{l.s.}\times10^{-6}$
H–28	0·612†	30·3†	1·78	1·70†
P–20	1·18	26·0	1·97	2·15
P–24	1·10	28·2	2·14	—
P–25	1·15	26·1	1·95	—

† Measured at 6°C.

all the intrinsic viscosities were calculated from the η_{sp}/c(100 ml./g) value obtained at a single concentration, corrected to zero concentration by using the Huggins' equation with $k' = 0{\cdot}32$, the latter value having been obtained from measurements on P–24.

Of the two light scattering results reported here, only that for P–20 was obtained by measuring several concentrations of RNA (Fig. 1). The second virial coefficient obtained in this case ($B = 2{\cdot}4\times10^{-4}$) was not used to correct the results obtained on H–28 because the latter was measured at a lower temperature and under conditions where the molecule is more compact (note the viscosity).

The molecular weight from sedimentation-viscosity data was calculated by means of the Flory-Mandelkern equation (assuming $\Phi^{1/3}P^{-1} = 2{\cdot}5\times10^{6}$, and the partial specific volume, $\bar{v} = 0{\cdot}578$). An average value of $2{\cdot}03\pm0{\cdot}08\times10^{6}$ was obtained for the three phenol preparations in excellent agreement with the light scattering result. Within the limits of experimental error and uncertainty, therefore, these samples consist of molecules which have the maximum possible molecular weight predicted for RNA prepared from monodisperse TMV with a phosphorus content of 0·45% (Knight & Woody, 1958) and a molecular weight of 39 million (Boedtker & Simmons, 1958).

The molecular weight of H–28 appears to be somewhat lower than that obtained for the phenol preparations. However, if the light scattering results are corrected to

zero concentration by assuming a modest concentration dependence ($B = 1 \times 10^{-4}$), the molecular weight is increased to 1·88 million. This value, combined with the sedimentation-viscosity data on H–28, results in a $\Phi^{1/3}P^{-1}$ of 2·42 rather than $2{\cdot}5 \times 10^6$. Since a lower value of $\Phi^{1/3}P^{-1}$ is consistent with the more compact configuration of RNA observed (see Table 1) when the measurements are carried out at low temperature (6°C), the correct molecular weight of H–28 is probably about 1·9 million.

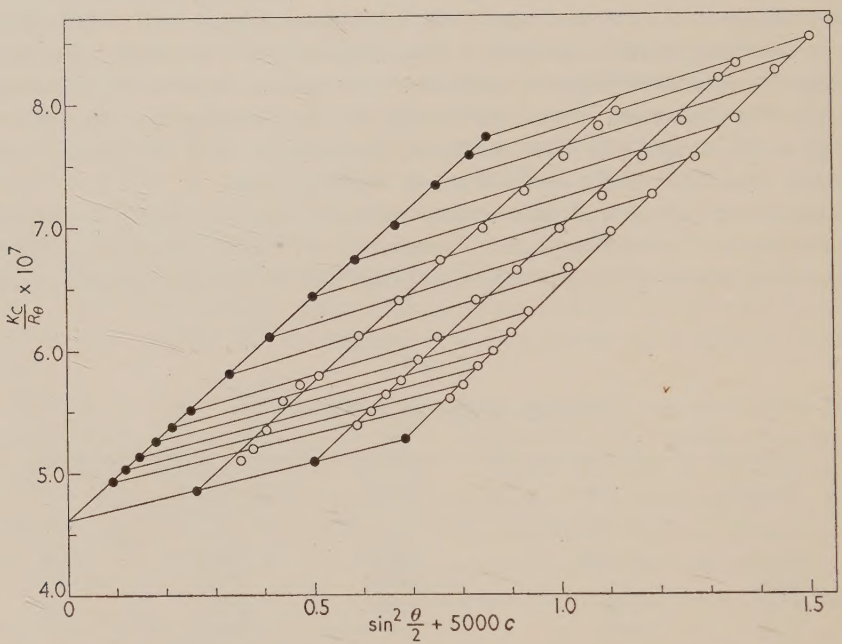

FIG. 1. Light scattering results on RNA P–20 in 0·1 M-sodium phosphate(1 : 1) at 21°C. ○, experimental points; ●, extrapolated data.

The remaining difference in the molecular weight obtained for RNA prepared by the two methods can be attributed to a slight difference in the distribution of sedimentation coefficients. In the phenol preparations, more than 85% of the molecules sedimented with a single sharp boundary at concentrations of about 0·004 g/100 ml. (ultraviolet absorption optics). In the heat preparation, only 70% exhibited the same sedimentation coefficient.

Although there are no major differences in the molecular properties of RNA prepared by the two methods, an important difference in stability was observed, phenol-prepared RNA being definitely more stable. Solutions could be stored at 5°C for 4 days, or exposed to temperatures as high as 80°C for 10 min with no decrease in sedimentation coefficient (see below). It was this enhanced stability, so important in physical measurements, which led to the use of phenol prepared samples for further study.

(b) *The random coil configuration*

The configuration of TMV, calf liver and *E. coli* ribosomal RNA in solution has previously been reported to be similar to that of a randomly-coiled solvent-immobilizing polymer chain (Boedtker, 1959; Hall & Doty, 1958; Littauer & Eisenberg, 1959). This conclusion is based in part on the great flexibility of the molecule as

shown by the readiness with which it expands as the temperature is increased or the ionic strength is decreased. Since it is now known that RNA undergoes a transition from a partly helical to a random form under these conditions, such evidence should not be applied to elucidate the configuration of the molecule in the helical form. Information about the configuration can be obtained, however, by comparing results obtained from light scattering and viscosity, and by studying the molecular weight dependence of the light scattering radius of gyration, the sedimentation coefficient, and the intrinsic viscosity.

First, we compare the radius of gyration obtained from light scattering measurements with that calculated from the viscosity using the Flory-Fox equation. The results given in Table 2 show that the dimensions obtained from the two methods are

TABLE 2

Radius of gyration of TMV RNA

Sample	Measured by light scattering	Calculated from viscosity
H–28	340 ± 20 Å	323 Å
P–20	398 ± 20	407

in excellent agreement. Since the Flory-Fox equation applies to randomly coiled polymer chains, this agreement suggests that the coil model is an accurate representation of the configuration of RNA. Thus the helical regions appear to be randomly located in the chain and do not seem to alter the Gaussian distributions of segments characteristic of randomly coiled chains.

Further support for this model is found in the molecular weight dependence of the radius of gyration obtained from light scattering measurements. If RNA is a random coil without excluded volume effects, the ratio of the molecular weight to the radius of gyration should be a constant. In practice, one measures the weight average molecular weight, M_w, and the z-average radius $(R_g)_z$, the two averages being identical of course if the sample is monodisperse as it is initially. As RNA degrades, however, the distribution becomes the most probable distribution (Montroll & Simha, 1940) in which the z-average is 1·5 times greater than the weight average. Therefore, as the molecular weight decreases one would expect $M_w/(R_g^2)_z$ to decrease and approach two-thirds of that of the original sample. The results obtained on two samples are given in Table 3. RNA P–20 was degraded by allowing it to stand at 25°C for several days; H–28 was degraded by heating it to 75°C first for 5 min, then for 10 min, and finally to 90° for 5 min.

In both cases the ratio $M_w/(R_g^2)_z$ decreases as expected. The limiting value is reached in the one case ($2/3 \times 13{\cdot}6 = 9{\cdot}1$) but not in the other where the degradation has not proceeded far enough to permit the limiting value of the ratio to be attained. The slightly higher values of the ratio obtained for sample H–28 can be explained by the fact that R_g^2 was measured at 6°C in this case and at 25°C in the former. Some expansion with temperature is expected. Thus, within the probable error of

these measurements, the degradation of RNA produces a change in the weight-to-size ratio in agreement with that expected for a uniform random coil.

A third test of the adequacy of the random coil model is the molecular weight

TABLE 3

The molecular weight dependence of the radius of gyration

Sample	$M_w \times 10^{-6}$	$(R_g)_z$ in Å	$\frac{M_w}{(\overline{R_g^2})_z}$
P–20	2·15	398	13·6
	1·64	370	12·0
	1·25	328	11·6
	0·775	274	10·3
	0·530	242	9·1
H–28	1·70	340	14·7
	1·32	322	12·8
	1·04	288	12·6
	1·00	284	12·5

dependence of the sedimentation coefficient and intrinsic viscosity. Calf liver ribosomal RNA in 0·01 M-phosphate buffer, pH 7·1, clearly behaves in the manner predicted for a randomly-coiled single-chain molecule (Hall & Doty, 1958). In order to determine if TMV RNA would exhibit similar behavior, samples of RNA were allowed

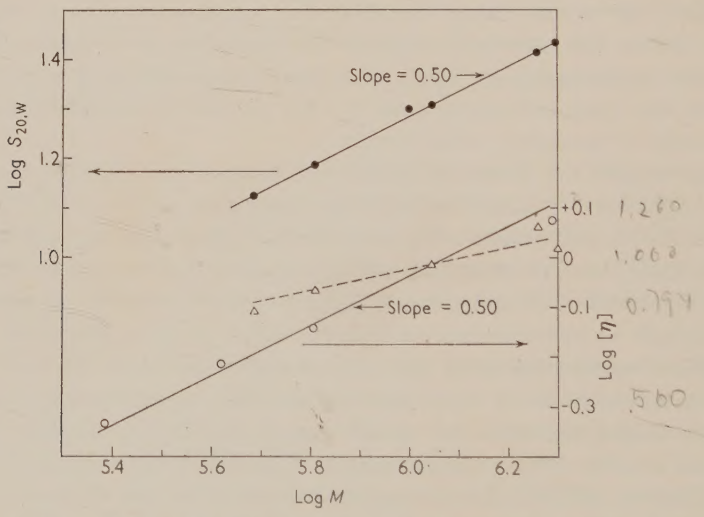

FIG. 2. Sedimentation- and viscosity-molecular weight relation. 0·1M-sodium phosphate (1 : 1). Measurements made at 25°C.

to degrade slowly by letting them stand at 25°C or heating them briefly to 56°C. In one case (P–20), the sample was kept in a thermostated light scattering cell at 25°C. Portions were withdrawn at regular intervals and the sedimentation coefficient measured. It was thus possible to obtain the sedimentation coefficient as a function of molecular weight. The other samples (P–25, P–29) were kept in a viscometer. In

one case the solutions were kept at 25°C; in the other, they were heated at 56°C for varying times and then returned to 25°C. In both cases, the viscosity and sedimentation coefficient were measured at 25°C. From the sedimentation-molecular weight relationship obtained in the first set of experiments, the sedimentation coefficient in the second and third sets could be converted into the corresponding value of the molecular weight. As a result it was possible to express the viscosity as a function of molecular weight. The results are shown in Fig. 2.

If RNA behaves as a randomly coiled single chain, the slope of the log-log plot of the sedimentation coefficient *versus* molecular weight should have a value between 0·4 and 0·5, and that of the viscosity *versus* molecular weight should be between 0·5 and 0·8. Moreover, these two constants are uniquely related: thus, if one is 0·5 the other must be 0·5 also. Therefore the observed sedimentation-molecular weight relation (slope of 0·5) is compatible with the random coil model and in agreement with the results obtained by Hall & Doty (1958).

However, the results for the viscosity-molecular weight relation (dashed line, slope of 0·26) which were obtained when the temperature was maintained at 25°C throughout the experiment were not consistent with the concept that RNA is behaving as a random coil. Even though the data cover only a fourfold change in molecular weight, the deviation of the slope from the minimum possible one for random coils (0·5) is sufficiently great to lie outside experimental error. A possible explanation for this result is that the higher concentration required to measure the viscosity (approximately 1 mg/ml.) prevents the chains from diffusing apart until several bonds have broken. Such "aggregates" would then dissociate when the solutions are diluted to measure the sedimentation coefficient. To check this possibility, a second viscosity experiment was carried out in which the RNA was degraded by heating to 56°C. At this temperature more than half of the hydrogen bonds have been broken and aggregation would be less likely. The results shown as the full line in Fig. 2 do indeed give a slope of 0·5 for the viscosity-molecular weight relation. It appears therefore that the anomalous viscosity-molecular weight relation originally obtained can be attributed to aggregation. Under conditions which favor the dissociation of aggregates, however, the viscosity-molecular weight relation of TMV RNA is compatible with that expected for a randomly coiled single chain.

Thus in four independent ways the physical properties of TMV RNA show the behavior expected of a random coil and so in a hydrodynamic sense this identification can be considered established. That is, the dimension measured by light scattering agrees with that calculated from the viscosity assuming the coil model, and the molecular weight dependence of the light scattering radius of gyration, the sedimentation coefficient, and the intrinsic viscosity are characteristic of macromolecules having a Gaussian distribution of chain elements.

(c) *The effect of heating on configuration*

The investigation of the configuration of TMV RNA was complicated by a slight variability of the sedimentation coefficient of freshly prepared RNA. The values given in Table 1 for the three phenol preparations range from 26 to 28 s, a difference too great to be attributed to experimental error. At first one might assume that the variation simply reflected differences in the molecular weight of the samples due to different degrees of degradation during the preparation. The fact that the distribution of sedimentation coefficients was equally sharp in all cases however, indicated that a

different explanation should be sought. In reviewing data obtained on measurements designed to test the thermal stability of TMV RNA, it was found that a small but consistent increase in sedimentation coefficient is observed when RNA solutions are exposed to elevated temperatures. The results obtained for five different samples are given in Table 4.

TABLE 4

Effect of thermal treatment on sedimentation of RNA

Sample	Thermal treatment	Initial $S_{20°,w}$	Final $S_{20°,w}$
P–9	30 min at 40°C	27·6	27·8
P–12	30 min at 55°C	27·2	27·7
P–12	30 min at 70°C	26·2	28·1
P–15	45 min at 70°C	25·9	28·5
P–15	15 min at 70°C	25·9	29·7
P–17	5 min at 80°C	27·9	29·4
P–25	43 hr at 25°C	26·1	27·3
average		26·5	28·3

Because an *increase* in sedimentation coefficient is observed in each case, we are confident that the variation does not reflect a degradation. Moreover, in one case it was possible to demonstrate that the increase is not due to aggregation. The results obtained on P–25 where both the sedimentation and viscosity were measured at 25°C are given in Table 5. It is evident that the slight increase in sedimentation coefficient is compensated for by a 10% drop in viscosity, and as a result the molecular weight calculated from $[\eta]$ and $S_{20°,w}$ is approximately constant for the first 43 hr.

TABLE 5

Evidence for a configurational change at 25°C in TMV RNA

Time	$S_{20°,w}$	$[\eta]$	$M \times 10^{-6}$
Initial	26·1	1·15	1·95
19 hr	26·0	1·13	1·93
43 hr	27·3	1·05	2·00

The variation in sedimentation coefficient thus indicates that the RNA chains undergo internal rearrangements to form more compact configurations. Because this phenomenon occurs slowly at low temperatures where half of the molecule is in a partly helical configuration and rapidly at high temperatures where all the hydrogen bonds have been broken, it would seem that the more compact configuration is the thermodynamically more stable one. Since, in spite of this greater stability, it is not the most probable one, i.e. it is not the one formed when RNA is first extracted from the virus at 5°C, there must be a steric factor favoring the formation of a slightly more expanded form at low temperatures.

It should be noted in passing that the thermal treatment which produces a more compact configuration of the RNA chain is almost inevitably accompanied by a sharp drop in biological activity (Boedtker & Watson, unpublished results). But since we have ruled out the possibility of breaking primary valence bonds under these conditions, and since it is unlikely that depurinization can occur at the lower temperatures, the two most commonly accepted explanations for the loss of infectivity fail here. The physical or chemical reasons of this inactivation thus remain a mystery.

Finally, it should be emphasized that the results in Fig. 2 and Table 5 make it clear that viscosity studies of the enzymatic degradation of RNA cannot provide a reliable means of determining the number of chains making up TMV RNA. Viscosity results are at best an insensitive function of the molecular weight, and in the initial and most important stages of the degradation process, the viscosity is a wholly inaccurate reflection of the molecular weight. This does not, of course, rule out the possibility of proving that RNA is single stranded in low salt where the secondary structure is minimal (Littauer & Eisenberg, 1959), but it does open to question earlier results on TMV RNA (Gierer, 1958), in which the intrinsic viscosity in 0·02 M-sodium phosphate at 5°C was presumed to be proportional to the first power of the molecular weight.

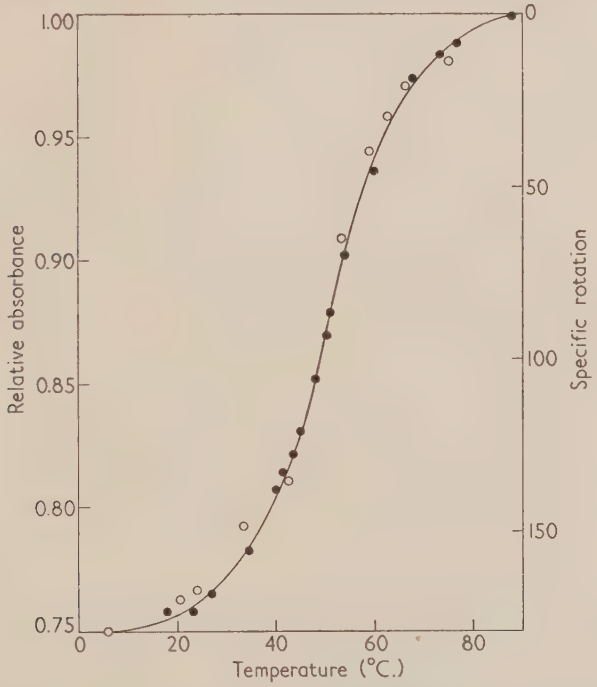

FIG. 3. Relative absorbance and specific rotation as a function of temperature. RNA P–7 in 0·1 M-sodium phosphate (1 : 1). ●, relative absorbance at 2580 Å; ○, specific rotation at 5890 Å.

4. The Helix-Coil† Transition

(a) *Optical rotation*

The existence of the partly helical configuration of TMV RNA described above was first established by studying the temperature dependence of the specific rotation and absorbance (Doty *et al.*, 1959). New and more complete data are shown in Fig. 3 where

† The term "coil" is used throughout this section to denote the highly extended, disorganized form of TMV RNA in which there is no interaction between neighboring parts of the molecule.

it is seen that the two curves essentially coincide if the ordinate scales are properly adjusted. These two superimposed curves can be interpreted if compared with the corresponding data for the polyadenylic + polyuridylic two-stranded helical complex, poly (A+U). Such a comparison shows that the relative absorbance and optical rotation at the high temperature plateau is the same for TMV RNA and for poly (A+U). The low temperature plateau for poly (A+U) corresponds to 100% helix (Felsenfeld & Rich, 1957) and is lower than that obtained for TMV RNA. By using the absorbance and specific rotation scales as a calibration of the percent helix, the low temperature values of TMV RNA can be interpreted. The low temperature absorbance of RNA is 61·8% and the specific rotation is 60·5% of the change exhibited by poly (A+U).† The fact that these two values arrived at independently agree permits us to conclude that the configurational transition observed in RNA *is* a helix-coil transition similar to that in poly (A+U). That is, the transition observed is not simply the result of a change in the amount of interaction between bases randomly arranged, but specifically a transition from a partly helical form to a random

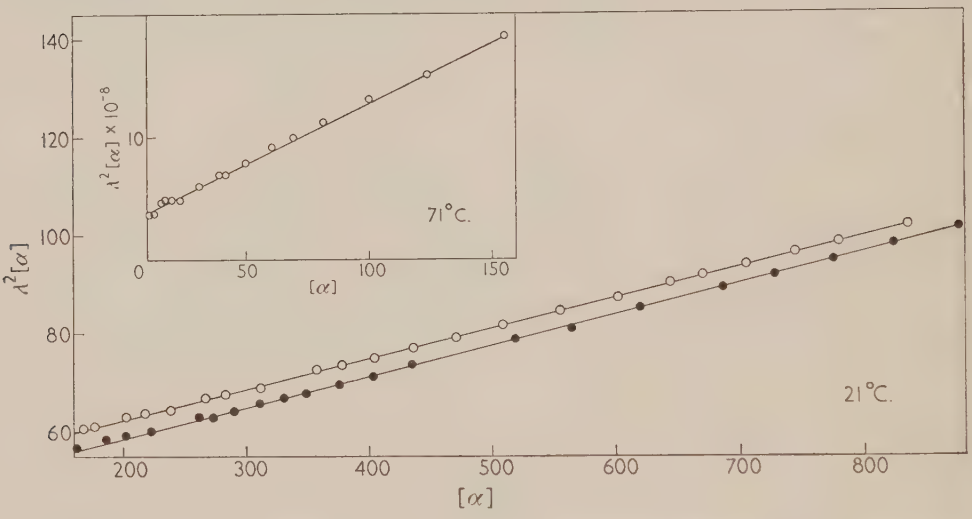

Fig. 4. Optical rotary dispersion of RNA P–8 in 0·1 M-sodium phosphate (1 : 1), concentration of 0·355 g/100 ml.

A. 71°C, $\lambda_c = 3100$ Å.

B. 21°C, ●, before heating, $\lambda_c = 2510$ Å; ○, after heating, $\lambda_c = 2490$ Å.

one. A comparison of the thermally induced absorbance changes alone would not have justified this conclusion. However, the fact that the same interpretation can be made from a comparison of the optical rotation changes, which reflect the main chain conformation, is strong evidence that the thermally induced changes in RNA are similar to those in poly (A+U).

To explore this transition further, optical rotary dispersion measurements were made in 0·1 M-sodium phosphate buffer, pH 6·8 at both 21° and 71°C. The results shown in Fig. 4 cover a wavelength range from 5890 to 3400 Å. At both temperatures, the dispersion follows the Drude equation, but the critical wavelength, λ_c, changes reversibly from 2500 to 3100 Å upon going from the lower to the higher temperature.

† Of course this comparison should be based on the properties of both poly (A+U) and polyguanylic and polycytidylic acid. When data on the two stranded poly (G+C) helical complex become available, the helical content of TMV RNA may have to be revised.

These results are in qualitative agreement with those obtained by Haschemeyer *et al.* (1959), who obtained a value of 2400 Å in salt and 2830 Å in water. However, since the concentrations required to measure the dispersion preclude counterion concentrations less than 5 to 10 mM, only a part of the helix-coil transition can be observed in this way (see below), and the smaller range of λ_c in this other work is therefore understandable. Unfortunately, sufficient data on synthetic polynucleotides to obtain a quantitative correlation between λ_c and the percent helix are not yet available, but it is hoped that such a correlation will soon be possible.

(b) *Absorbance*

Relative absorbance measurements as a function of temperature provide a profile of the stability of the helical regions in RNA. It had previously been reported that

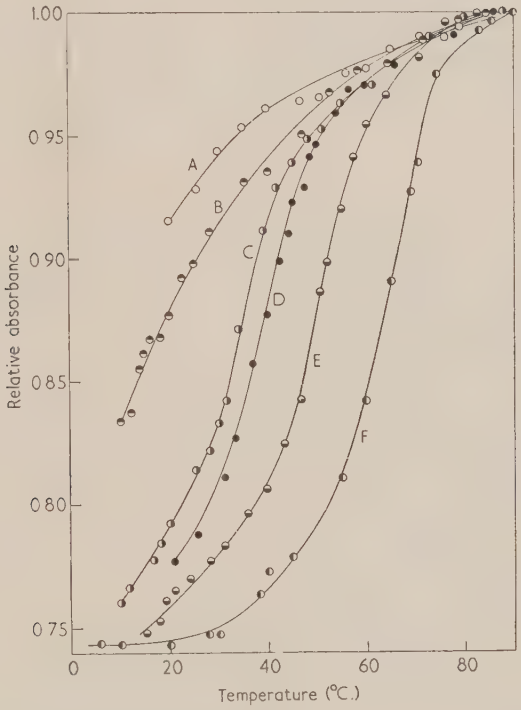

FIG. 5. Relative absorbance-temperature profiles as a function of concentration of added sodium. (RNA concentration approximately 15 μg/ml.)

A. 0·06 mM-Na^+
B. 0·17 mM-Na^+
C. 15 mM-Na^+
D. 34 mM-Na^+
E. 153 mM-Na^+
F. 1430 mM-Na^+

the absorbance depends on ionic strength (Hall & Doty, 1958; Boedtker, 1959). We have extended these studies to lower counterion concentrations to see if all the helical regions could be removed at room temperature. In the absorbance data discussed below, the results are expressed relative to the absorbance of TMV RNA at 90°C in 0·1 M-sodium phosphate buffer (1 : 1), which is taken as unity. This value is equal to 0·922 of the absorbance of hydrolyzed RNA. The RNA concentrations used were between 10 and 20 μg/ml. Hence the counterion concentration, assuming no binding, was at least 0·03 mM-Na^+.

Relative absorbance-temperature profiles are shown in Fig. 5 for concentrations of added Na^+ from 0·06 to 150 mM. As observed before, the mean melting temperature, T_m, decreases with decreasing salt concentration. At the lower salt concentration, however, it is impossible to determine T_m accurately because only part of the transition is accessible above 0°C. The relative absorbance at 20°C, however, is 0·745 in 1430 mM, 0·792 in 15 mM, and 0·915 in 0·06 mM-Na^+. Since on this scale, 100% helix would correspond to a relative absorbance of 0·665 (see above), we can estimate that the percent helix decreases from 66·5 to 18·2% over the salt concentration investigated. Thus one-third of helical regions persist, even at the lowest counterion concentration practically encountered. The remaining helical content might be reduced a little further by removing all added salt, thereby reducing the total Na^+ concentration from 0·09 to 0·03 mM. However, the absorbance is already almost independent of the concentration of added Na^+ in this region of salt concentration, and the conclusion remains that some secondary structure is maintained at room temperature. Thus a salt-free solution of TMV RNA does not correspond to a non-helical configuration, but rather to an intermediate state with significant helical content, the actual amount depending on the concentration of RNA since this in turn controls the Na^+ concentration.

(c) *The effect of divalent cations*

The absorbance data just described were all obtained in salt solutions in which the cations were monovalent, specifically Na^+. The absence of significant concentrations of divalent cations was assumed because redistilled phenol and EDTA were used in the preparation of RNA. Moreover, the decrease in absorbance at 20°C on going from 0·1 to 150 mM-Na^+ was 21%, in agreement with maximum change observed by Haschemeyer *et al.* (1959) for TMV RNA preparations which were found to be uncontaminated by divalent metal ions. Additional evidence that the 21·5% helical content in 0·1 mM-Na^+ is not due to divalent metal ions was obtained by measuring the absorbance at 20°C in the presence of EDTA. (See below.)

Because the results described in the preceding section indicated that the helical regions of TMV RNA were stabilized by modest concentrations of monovalent cations, divalent ions do not seem to be essential to the formation of secondary structure in RNA. Nevertheless, the presence of small quantities of such ions in RNA solutions has been reported (Wacker & Vallee, 1959; Loring & Waritz, 1957), and the possibility remained that they play some special role in stabilizing RNA. Therefore, we wanted to obtain quantitative data on the effect of a divalent ion such as Mg^{2+} on the absorbance-temperature profile. By studying the effect of Mg^{2+} both in the presence and absence of Na^+ ions, it might be seen whether or not the interaction between Mg^{2+} and RNA occurred at a specific site unaffected by Na^+ ions.

The relative absorbance-temperature profile obtained in 1·0 mM-EDTA (2·8 mM-Na^+) is shown in curve A of Fig. 6. It is clear that a significant fraction, again approximately one-third, of the helical regions remain at 20°C. To test if the absorbance is sensitive to the Na^+ concentration, the EDTA concentration was diluted 50-fold with double-distilled water so that the added Na^+ concentration was approximately equal to the counterion concentration. The absorbance increased only 2%. EDTA does not, therefore, appreciably reduce the helical content of RNA at 20°C. This supports the conclusion that about one-third of the helical regions are indeed stable at room temperature in the absence of any added salt.

To find out how a divalent ion like Mg^{2+} would effect the results just presented, absorbance-temperature profiles were obtained at several concentrations of Mg^{2+}. It is seen in Fig. 6 (curves B, C, E, and F) that the hypochromicity and the mean melting temperature, T_m, both increase as the concentration of Mg^{2+} increases.

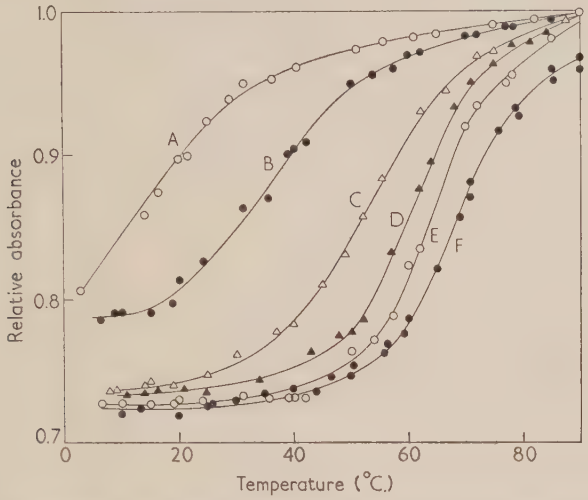

Fig. 6. Effect of Mg^{2+} on the relative absorbance-temperature profile. RNA concentration approximately 15 μg/ml.

A. 1 mM EDTA, pH 7·4 (2·8 mM-Na^+)
B. 0·001 mM-Mg^{2+}
C. 0·01 mM-Mg^{2+}
D. 1 mM-Mg^{2+} and 10 mM-sodium phosphate buffer (1 : 1)
E. 0·1 mM-Mg^{2+}
F. 1 mM-Mg^{2+}

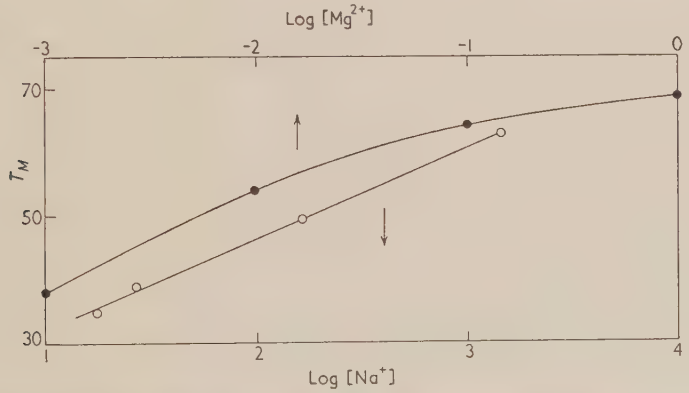

Fig. 7. Mean melting temperature, T_m, as a function of the concentration of added Na^+, ○, and Mg^{2+}, ●, in mM.

However, the hypochromicity at 20°C nears its maximum value in 0·01 mM-Mg^{2+} when the RNA concentration is approximately $1{\cdot}2\times10^{-5}$ g/ml. That is, 94% of the observed decrease in absorbance is reached when there is one Mg^{2+} per three RNA phosphates, in agreement with results obtained by Zubay & Doty (1958) and Staehelin (1959).

A comparison of the dependence of T_m on Na^+ and Mg^{2+} concentrations is made in Fig. 7, where T_m is plotted against the log of m-moles of added counterion. The concentration scales are shifted by four. It is clear that it would require a shift of about

4·4 units to bring the two sets of data into coincidence. This means that it requires about 25,000 times higher concentrations of Na^+ than Mg^{2+} to achieve a comparable helix stability. Such a difference seems too great to be explained in terms of the higher charge density of the Mg^{2+}. The possibility that the interaction between RNA and Mg^{2+} is more than an electrostatic one was therefore explored.

First the effect of EDTA on the Mg^{2+}-RNA interaction was studied by measuring the relative absorbance-temperature profile of Mg-RNA in the presence of EDTA and comparing the T_m obtained with that in the absence of EDTA. From the T_m observed, it was possible to obtain an estimate of the amount of Mg^{2+}, if any, which remained "bound" by RNA after the addition of EDTA. The results obtained are summarized in Table 6.

TABLE 6

Effect of EDTA on the Mg^{2+}-RNA interaction

mM-Mg^{2+}	mM-EDTA	mM-EDTA/mM-Mg^{2+}	T_m°C	Residual mM-Mg^{2+} "bound" by RNA
1·0	1·0	1	62	0·032
0·1	0·1	1	50	0·0033
0·1	1·0	10	19	0
0·01	0·1	10	19	0

Since the concentration of RNA was approximately the same (15 μg/ml.) in each case, there seems to be no relation between the residual Mg^{2+} "bound" by RNA and the concentration of RNA. Indeed, it appears that EDTA is 100% efficient in binding the Mg^{2+} present providing it is at least ten times more concentrated than the latter. This shows that RNA binds Mg^{2+} much less strongly than EDTA does.

To determine if the Mg^{2+}-RNA complex was reversible, the relative absorbance-temperature profile was measured in the presence of Na^+. Comparison of curve F and curve D of Fig. 6 shows that T_m is lowered 9°C if 10 mM-NaH_2PO_4-Na_2HPO_4 (1 : 1) is added to 1·0 mM-Mg^{2+}. The fact that the melting temperature is lowered 9°C *although the total cation concentration is actually increased*, certainly suggests that Na^+ can reversibly replace the Mg^{2+} "bound" by RNA, and thus diminish the effect Mg^{2+} has on the stability of the helical regions. The reversible interplay of Na^+ and Mg^{2+} is also seen in that the same T_m is observed if the Mg^{2+} is added to the RNA solution containing the Na^+.

Additional information on the effectiveness with which Na^+ can compete with Mg^{2+} was obtained from relative absorbance-temperature measurements before and after the addition of 0·1 mM-Mg^{2+} to RNA in different concentrations of sodium phosphate buffer. The results presented in Fig. 8 show that the T_m is increased 9°C in 15 mM, 2°C in 34 mM, and less than 1°C in 150 mM-Na^+. Consequently T_m in 34 mM-Na^+ plus 0·1 mM-Mg^{2+} (43°C) is actually lower than that obtained in 15 mM-Na^+ plus 0·1 mM-Mg^{2+} (44°C), a lower total cation concentration. To check that the effect observed was entirely due to the added Na^+, and not the result of the phosphate buffer, a control was run in which 150 mM-NaCl was substituted for sodium phosphate. The T_m in NaCl was the same as that observed in phosphate, confirming the results

described above. Thus it seems clear that if the Na^+ concentration is high enough, Na^+ can and does interfere with the helix stabilizing effects of Mg^{2+}.

Nevertheless, even when the Na^+ concentration is high enough so that T_m is determined by Na^+ rather than by Mg^{2+}, the latter still has a noticeable effect on the breadth of the helix-coil transition. In Fig. 8 (C), for example, the absorbance-temperature profile shows that Mg^{2+} has narrowed the transition region even though T_m is the same as it was without Mg^{2+}. Such a result indicates that there is less variation in the average helix stability but offers no insight into the mechanism by which Mg^{2+} accomplishes this.

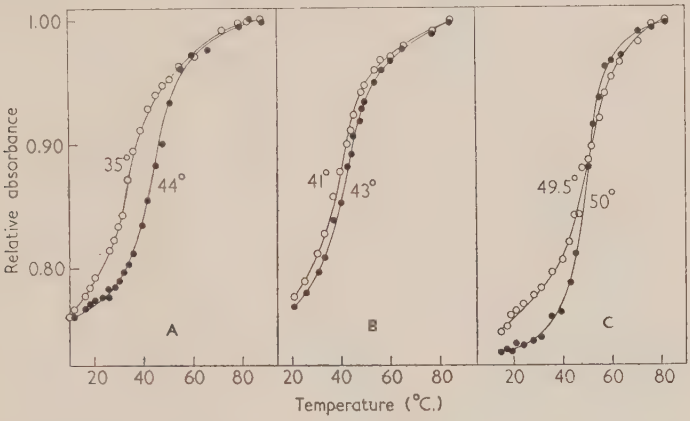

FIG. 8. Effect of 0·1 mM-Mg^{2+} in the presence of Na^+ on the relative absorbance-temperature profile; ○, without Mg^{2+}; ●, with Mg^{2+}.

A. 15 mM-Na^+, pH 6·7 B. 34 mM-Na^+, pH 7·1 C. 153 mM-Na^+, pH 7·1

The inhibition of the Mg^{2+}-RNA interaction by Na^+ suggests that the binding sites or at least the points of influence are the phosphates and not the bases, in agreement with the views expressed by others (Shack & Bynum, 1959; Felsenfeld & Huang, 1959, 1960). Although there is as yet no convincing evidence as to the type of interaction being observed, two general conclusions can be drawn. First we see that the interaction between RNA and Mg^{2+} is much more specific than that between RNA and Na^+ because we find that Mg^{2+} is some 25,000 times more effective than Na^+ in stabilizing the helical regions. And second, we see that the interaction is nevertheless relatively weak because it is fully reversible. The addition of EDTA or simply of Na^+ lowers the helix stability to that which would be observed in the absence of Mg^{2+}. The effect as determined by T_m is already significant if the EDTA concentration is equal to that of the Mg^{2+}, or if the Na^+ concentration is 15 times greater than that of the Mg^{2+}. By the time that the ratio of EDTA/Mg^{2+} is ten or of Na^+/Mg^{2+} is 1500, Mg^{2+} no longer has a measurable effect on T_m.

(d) *Sedimentation*

Thus far we have only observed the helix-coil transition by optical methods sensitive to the arrangement of small regions of the RNA chain. Once it was established that at least two-thirds of this transition could be observed by varying the cation concentration at a single temperature, the study of the hydrodynamic properties accompanying the transition became feasible. It was thus possible to make measurements such as sedimentation velocity, at the normal temperatures (20° to 25°C) and observe

the transition without the complications which result from the partial degradation of RNA at high temperature.

By measuring the sedimentation coefficient and absorbance at 21°C over a wide range of Na^+ concentration, it should be possible to see how the overall configuration of the RNA molecule is altered as the helical regions are destroyed. In one set of experiments, the Na^+ concentration was varied from 0·2 to 150 mM. A striking ninefold change in sedimentation coefficient was observed, from $S_{20°,w} = 3{\cdot}26$ to 28·2 s. More significant, however, was the fact that the increase in sedimentation coefficient closely paralleled the increase in hypochromicity; this can be seen in Fig. 9. It is evident,

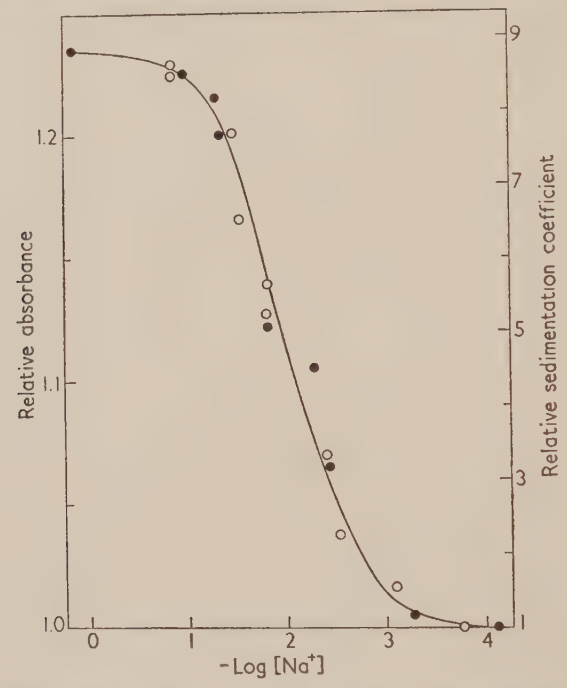

FIG. 9. Relative absorbance and sedimentation coefficients as a function of concentration of added Na^+. Measurements at 21°C. ●, decrease in absorbance at 2580 Å relative to that in 0·1 mM-Na^+; ○, increase in $S_{20°,w}$ relative to that in 0·18 mM-Na^+ ($S_{20°,w} = 3{\cdot}26$ s).

therefore, that the helix-coil transition is accompanied by a very large change in the average spatial arrangement of the segments making up the RNA chains. Although part of this expansion from a very compact form to a highly extended one results from the expected behavior of any polyelectrolyte, the transition is too large and occurs over too narrow a range of ionic strength to be explicable in terms of electrostatic repulsion only. Moreover, the increase in sedimentation coefficient occurs over the identical range of Na^+ concentration over which the absorbance goes to its maximum value at 20°C. Since the increase in absorbance has already been associated with a breakdown of the secondary structure in RNA, the decrease in sedimentation coefficient can be identified primarily with the helix-coil transition.

It was naturally of interest to see how the *distribution* of sedimentation coefficients would vary as RNA molecules were taken from the partly helical to the disordered configuration. Previous reports had stated that the distribution was considerably broader the lower the salt concentration (Haschemeyer *et al.*, 1959). Our results, as

can be seen in Fig. 10, did not confirm this. The sedimentation patterns show that the distribution of sedimentation coefficients was equally narrow regardless of the salt concentration. This would indicate that all the RNA molecules obtained from TMV have the same chemical composition and sequence. If this were not so, one should have observed a polydispersity of shape reflecting a variation in the stability of helical regions in different molecules, and hence a broadening of the distribution of sedimentation coefficients in the transition region. This result was of course expected because of the identity of the RNA molecules.

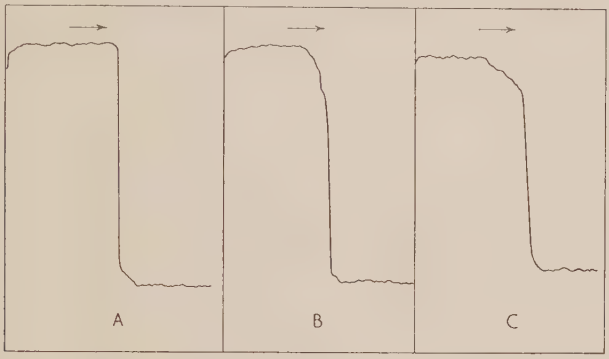

FIG. 10. Ultraviolet ultracentrifuge patterns for RNA P–22, sedimenting at 39,460 rev/min at a concentration of approximately 40 μg/ml., at 21°C.

A. 0·8 mM-Na^+, after 144 min. B. 4·5 mM-Na^+, after 64 min.
C. 153 mM-Na^+, after 24 min.

It can thus be seen that a spectrum of configurations is available to TMV RNA, each one of which can be identified by a sedimentation coefficient and by a definite value of the specific rotation and of the relative absorbance. By virtue of the identity of the RNA molecules in this case, we can associate with each configuration a particular helical content. It would appear that such an identification is more accurate and realistic than the somewhat misleading nomenclature of RNA I and RNA II (Haschemeyer *et al.*, 1959). Not only are there more than two RNA configurations, but RNA I as characterized at room temperature is not wholly a random molecule, and RNA II is certainly not 100% helical. Finally it cannot be over-emphasized that the partly helical form of RNA can be formed reversibly by suitably adjusting the temperature and *monovalent* salt concentration. Although there is no doubt that divalent cations are remarkably efficient in stabilizing the helical regions, they are not essential to the maximal development of the helical content.

I wish to thank Dr. Jacques R. Fresco and Mr. Joseph Eigner for their helpfulness, both in discussions and instrumentation. I would also like to acknowledge the excellent technical assistance I received from Mr. George Michaels on some of this work. And I wish again to thank Professor Paul Doty for his interest and suggestions, which made a vital contribution to this investigation. This investigation was supported by the U.S. Public Health Service through grants A 2396 and C 2171.

REFERENCES

Boedtker, H. (1959). *Biochim. biophys. Acta*, **32**, 519.
Boedtker, H. & Simmons, N. S. (1958). *J. Amer. Chem. Soc.* **80**, 2550.
Cox, R. A. & Littauer, U. Z. (1959). *Nature*, **184**, 818.

Doty, P., Boedtker, H., Fresco, J. R., Hall, B. D. & Haselkorn, R. (1959). *Ann. N.Y. Acad. Sci.* **81**, 693.
Doty, P., Boedtker, H., Fresco, J. R., Haselkorn, R. & Litt, M. (1959). *Proc. Nat. Acad. Sci., Wash.* **45**, 482.
Felsenfeld, G. & Huang, S. (1959). *Biochim. biophys. Acta*, **34**, 234.
Felsenfeld, G. & Huang, S. (1960). *Biochim. biophys. Acta*, **37**, 425.
Felsenfeld, G. & Rich, A. (1957). *Biochim. biophys. Acta*, **26**, 457.
Gavrilova, L. P., Spirin, A. S. & Belozerskii, A. N. (1959). *Proc. Acad. Sci., U.S.S.R.* **126**, 1121.
Gierer, A. (1958). *Z. Naturf.* **13b**, 485.
Gierer, A. & Schramm, G. (1956*a*). *Nature*, **177**, 702.
Gierer, A. & Schramm, G. (1956*b*). *Z. Naturf.* **11b**, 339.
Hall, B. D. & Doty, P. (1958). *Microsomal Particles and Protein Synthesis*, ed. by R. B. Roberts, p. 27. New York, London: Pergamon Press.
Hall, B. D. & Doty, P. (1959). *J. Mol. Biol.* **1**, 111.
Haschemeyer, R., Singer, B. & Fraenkel-Conrat, H. (1959). *Proc. Nat. Acad. Sci., Wash.* **45**, 313.
Knight, C. A. & Woody, B. R. (1958). *Arch. Biochem. Biophys.* **78**, 460.
Littauer, U. Z. & Eisenberg, H. (1959). *Biochim. biophys. Acta*, **32**, 320.
Loring, H. S. & Waritz, R. S. (1957). *Science*, **125**, 646.
Montroll, E. W. & Simha, R. (1940). *J. Chem. Phys.* **8**, 721.
Shack, J. & Bynum, B. S. (1959). *Nature*, **184**, 635.
Spirin, A. S., Gavrilova, L. P., Bresler, S. E. & Mossevitsky, M. I. (1959). *Biochimia*, **24**, 938.
Staehelin, M. (1959). *Experientia*, **15**, 413.
Wacker, W. E. C. & Vallee, B. L. (1959). *J. Biol. Chem.* **234**, 3257.
Zubay, G. & Doty, P. (1958). *Biochim. biophys. Acta*, **29**, 47.

J. Mol. Biol. (1960) **2**, 189-196

The Structure of the Protein Shell of Turnip Yellow Mosaic Virus

H. E. Huxley

Medical Research Council, Department of Biophysics, University College London, England

AND

G. Zubay†

Medical Research Council Biophysics Research Unit, King's College, London, and Department of Biophysics, University College, London, England

(*Received 2 May 1960*)

Turnip yellow mosaic virus (TYMV) is an approximately spherical plant virus, having a diameter of 280 to 300 Å and containing 60% protein and 40% RNA; the protein is believed to form a spherical shell around a nucleic acid core. It has been shown previously by X-ray diffraction that the virus particles must have cubic symmetry, and it has been argued on theoretical grounds that viruses having cubic symmetry and containing a spherical shell of protein were likely to have that protein shell built up of subunits arranged in a polyhedron having either tetrahedral (23), octahedral (432) or icosahedral (532) symmetry elements. We have examined TYMV in the electron microscope by the negative staining method, and have found that regularly disposed subunits may be discerned on the surface of the particles. There appear to be 32 such subunits, arranged on or near the vertices of either a pentakis dodecahedron or a rhombic triacontahedron (or other polyhedra approximating to those forms). These are semi-regular polyhedra having 532 symmetry, the former having 60 identical triangular faces and the latter 30 identical rhombic faces; both have 32 vertices, which fall into two separate groups, 12 vertices lying on fivefold axes and 20 vertices lying on threefold axes. Thus the subunits occupy two different types of position, and can be of two different species. Because the subunits lie on rotation axes, they must contain the appropriate number of identical *structural* units. These results agree with the suggestion made on the basis of the X-ray results that the particles have 532 symmetry, but they conflict with the more tentative suggestion that the particular polyhedron involved contained 60 subunits placed at the vertices of a snub dodecahedron. A possible way in which the X-ray results can be reconciled with the present observations is suggested.

1. Introduction

Turnip yellow mosaic virus (TYMV) is a "small" and approximately spherical plant virus, having a radius of 140 to 150 Å, a molecular weight of about 5 million, and containing 40% RNA and 60% protein (Markham, 1951). Preparations of the virus also often contain a component ("top component") having the same size and shape as the intact virus, but containing no nucleic acid. It was suggested by Markham that the protein part was in the form of a spherical shell, enclosing a core of RNA;

†Now at The Rockefeller Institute, New York, 21, New York, U.S.A.

and this picture has been confirmed by later work (Schmidt, Kaesberg & Beeman, 1954).

The virus particles (and the nucleic-acid-free protein too) crystallize in a cubically shaped lattice (Bernal & Carlisle, 1948), and it has been shown subsequently that the lattice has cubic symmetry, and that the particles lie at the lattice points (Klug, Finch & Franklin, 1957).

It has been pointed out earlier by Hodgkin (1949) and by Low (1953) that such a result would require that the particles be built up of $12n$ identical structural units arranged so that the whole particle has at least the same symmetry as the lattice, and this argument has been further developed, and applied in detail to the case of a spherical shell of protein, by Crick & Watson (1956). The shell must possess at least four threefold axes and three twofold axes, arranged as in a tetrahedron, and this requirement places severe restrictions on the manner in which the structural units can be arranged. If all the structural units have identical surroundings, then they must either lie in groups of appropriate symmetry around the vertices of one of the 5 Platonic solids (the cube, tetrahedron, octahedron, icosahedron, or dodecahedron), or at the vertices of an icosahedron. In the special case of structural units arranged with equal distances between all neighbours, they must lie either on the vertices of one of the 13 Archimedean polyhedra, or at the vertices of an icosahedron.

A group of structural units arranged with appropriate symmetry around a rotation axis may be treated as an intermediate building block in the protein shell; we shall refer to such a group as a *subunit*.

Some of these arrangements possess extra symmetry elements over and above those required for cubic symmetry; these arrangements have either the symmetry 432 or else the non-crystallographic symmetry 532; this latter symmetry may show up in X-ray diffraction photographs as concentrations of reflections with high intensities in the appropriate directions. Such "spikes" of high intensity, suggestive of fivefold symmetry, were observed by Caspar (1956) in X-ray diagrams from bushy stunt virus, and Klug *et al.* (1957) have reported that they find regions of higher intensity X-ray reflections in directions indicative of 532 symmetry in the case of TYMV. They also showed that the presence of 432 symmetry can be excluded by the nature of the crystal structure; particles rotated through 90° about a twofold axis have to be distinguishable.

We have examined TYMV using the negative staining technique (Hall, 1955; Huxley, 1957; Brenner & Horne, 1959) employing a new procedure, described elsewhere (Huxley & Zubay, 1960), in which the sheets of phosphotungstic acid (PTA) containing the particles are formed over holes in the supporting film. This procedure is particularly useful in the case of TYMV, where the substructure on the surface of the particle otherwise shows up with rather low contrast; also, this method seems to produce less flattening of the particles, and the precise geometry of the arrangement of subunits is more likely to be accurately preserved. Unlike ribosomes, the virus particles did not require previous fixation.

2. Results

The general appearance of a favourable preparation is shown in Plate I(a) & (b). The particles often form fairly regular hexagonal arrays and their distance apart is about 230 to 240 Å. The apparent diameter of the particles is usually less, and measures 180 to 200 Å, the particles appearing not to be in contact. However, we

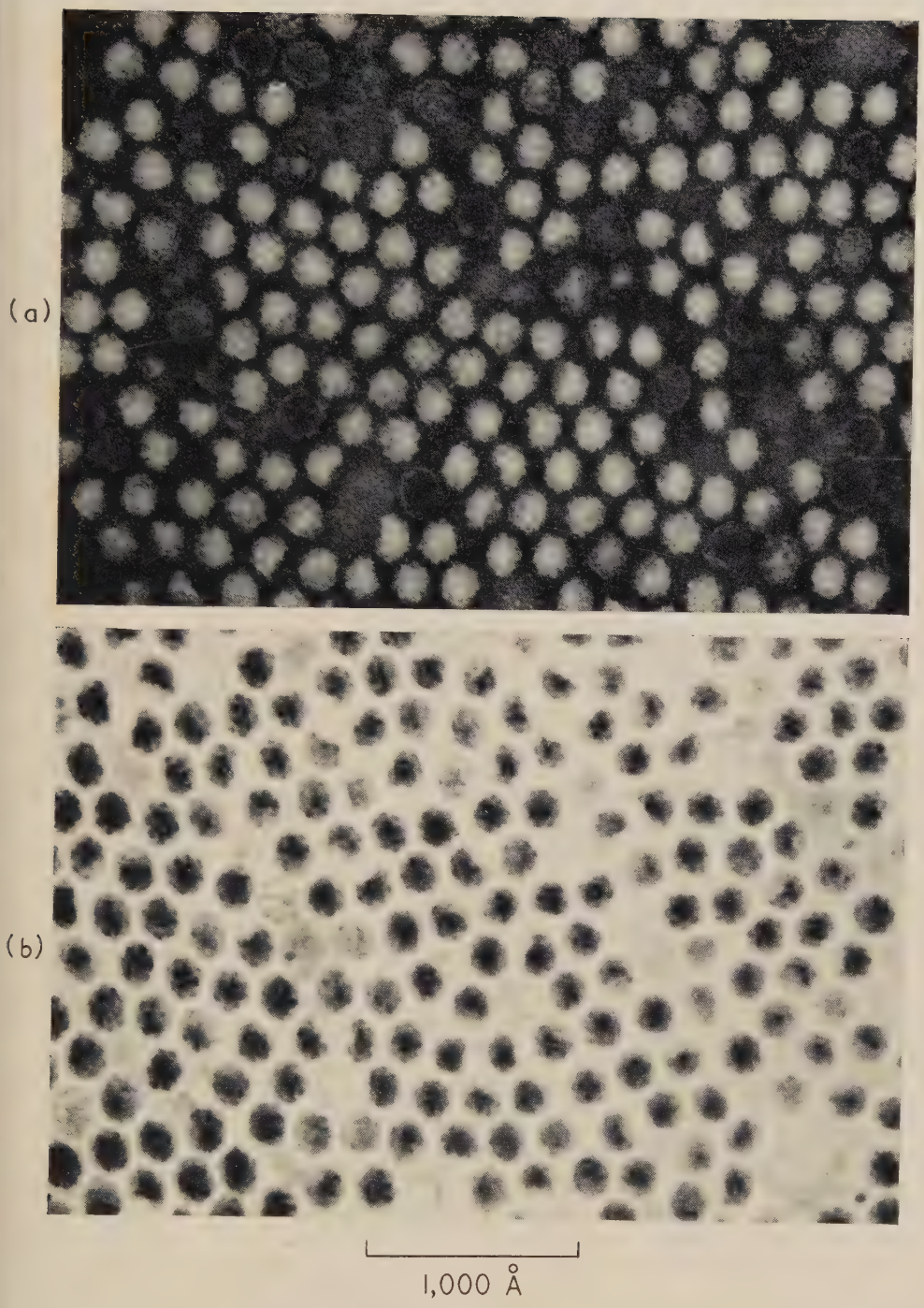

PLATE I(a). Typical appearance of an electron micrograph, printed in the normal way, of a preparation of TYMV "negatively stained" in a thin film of PTA. A number of "empty" particles may be seen. The virus particles appear not to be in contact with each other, but it is likely that this appearance arises because they are only partially immersed in the PTA, and that their true diameter is larger than it usually appears. A distinctive substructure appears in the particles, but it shows up with rather low contrast.

(b) Another TYMV preparation, negatively stained and photographed in the normal way, but printed in reversed contrast, by making a contact copy-print off a normal enlargement. This technique often helps the substructure of the virus particles to be seen more clearly.

Magnification × 300,000

[*To face page* 190

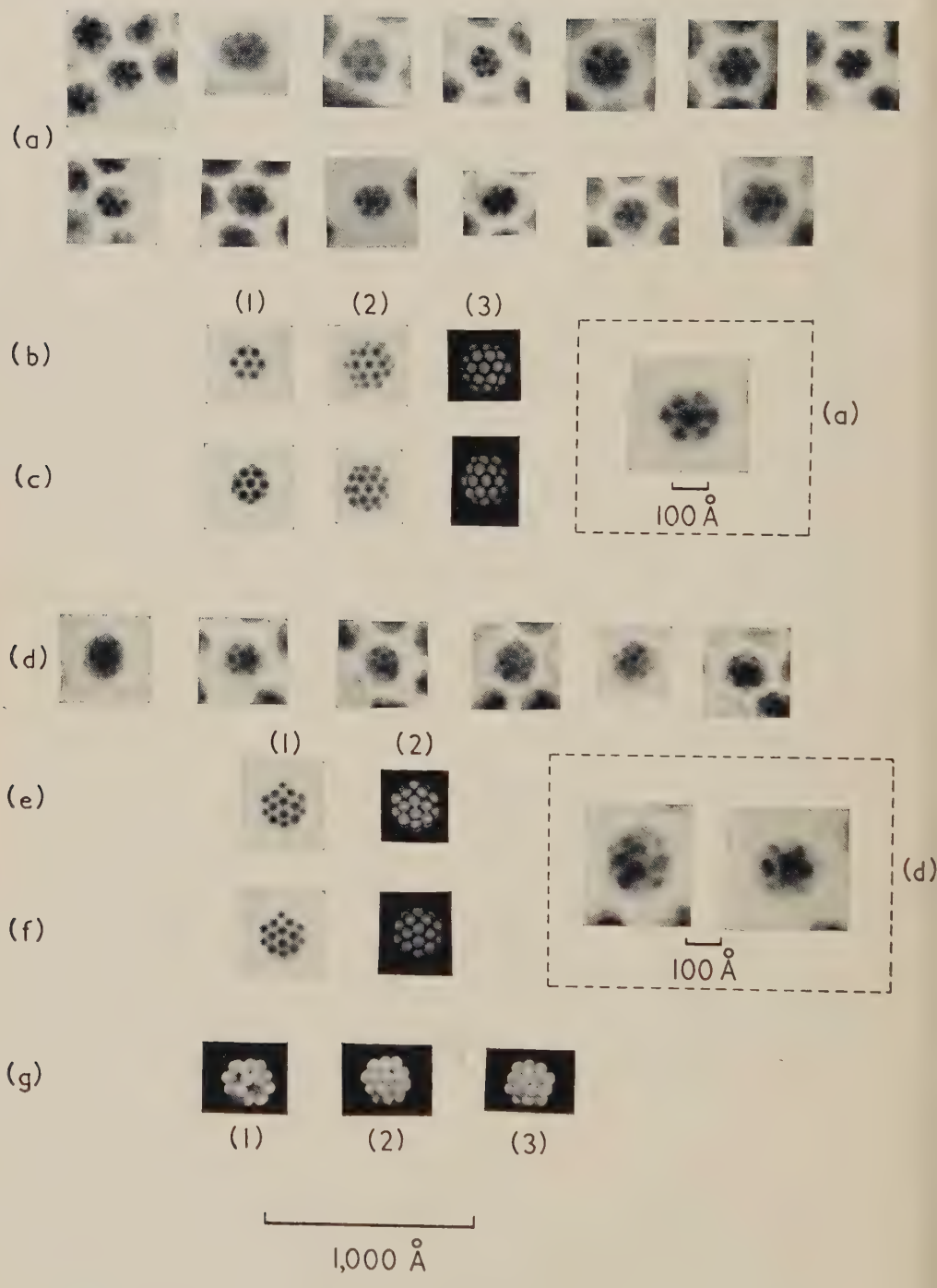
(a)
(1)
(2)
(3)
(b)
(c)
(a)
100 Å
(d)
(1)
(2)
(e)
(f)
(d)
100 Å
(g)
(1)
(2)
(3)
1,000 Å

PLATE II(a). A number of selected TYMV particles, in which the orientation is such as to show an hexagonal ring of 6 subunits about a central subunit ["6+1"] on a face of the particle immersed in the negative stain. We believe this view represents the appearance of the particle seen down a threefold axis. The micrographs are all reproduced at the same magnification, and the apparent differences in scale are due to different conditions of shrinkage and flattening during the preparation of the specimens. The larger groups were observed when the particles dried down onto a supporting film, the smaller ones when they dried down over holes.

Magnification × 300,000
(Inset × 500,000)

(b) Model in which the subunits are represented by ping-pong balls placed at the vertices of a rhombic triacontahedron, oriented to correspond to the view of particles in (a) above, and reproduced on the same scale for comparison.

(1) Printed through a mask so that only the group of subunits nearest to the observer is seen. Contrast reversed.
(2) Printed without mask, so that all the subunits on the side facing the observer are seen. Contrast reversed.
(3) Printed with normal contrast.

(c) As in (b), but with subunits at the vertices of a pentakis dodecahedron. Good agreement with the models is obtained if one supposes that the particles are less than half immersed in the negative stain, and that only the subunits on the submerged portion are visible.

(d) Selected TYMV particles showing two "intersecting" sets of [6+1] subunits (on the left-hand and right-hand side of the particle) having a common edge, 2 subunits near the centre of the particle being shared between the two sets. This corresponds, we believe, to a view of the particle looking along a direction in between 2 threefold axes, and is a particularly favourable one for it shows almost half (14 out of 32) of the total number of subunits present.

Magnification × 300,000
(Inset × 500,000)

(e) Model in the form of a rhombic triacontahedron, oriented to correspond to the view of particles in (d) above.

(1) Printed, without mask, with reversed contrast.
(2) Printed with normal contrast.

(f) As in (e), but with subunits at the vertices of a pentakis dodecahedron.

(g) Model built with subunits at the vertices of a truncated octahedron.

(1) Basic arrangement of 24 subunits, forming 8 rings of 6 subunits, two of which can be seen clearly.
(2) The same basic pattern, in the same orientation, but with 8 extra subunits added, one at the centre of each group of 6 subunits.
(3) Another view of (2).

The model shown in (2) and (3) has the same number of subunits (32) as in the rhombic triacontahedron and pentakis dodecahedron, but it has 432 symmetry instead of 532 symmetry, and can be eliminated by the results illustrated in Plate III.

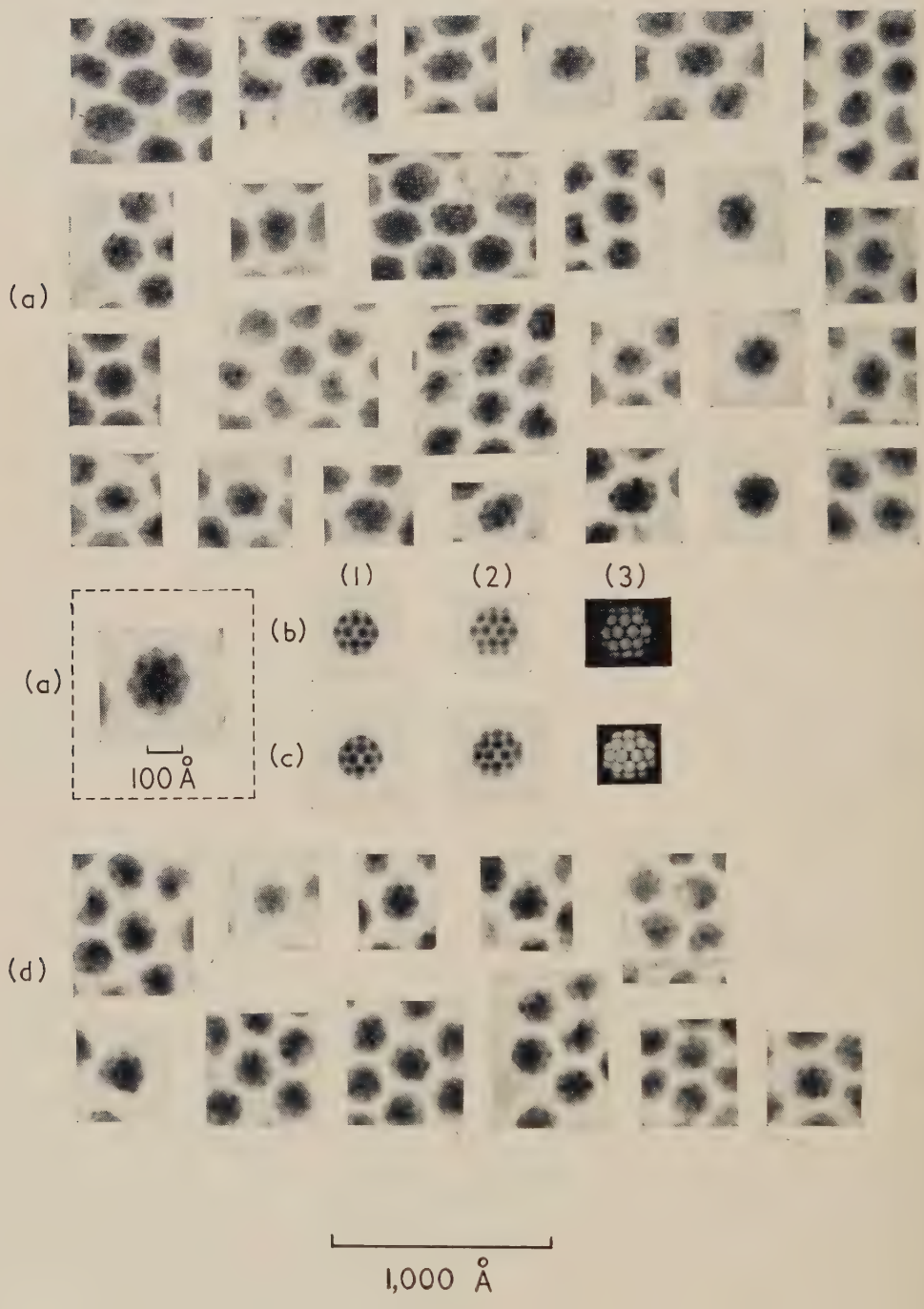
(a)
(1)
(2)
(3)
(b)
(a)
(c)
100 Å
(d)
1,000 Å

PLATE III(a). A number of selected areas from micrographs of negatively stained TYMV, in which particles show the diamond- or rhombus-shaped group of 4 subunits near the centre of the particle. In many instances this can be seen to be the central group of subunits in two *overlapping* sets of [6 + 1] subunits. We consider that this corresponds to a view of the particle looking down a twofold axis. A substantial number of examples are presented so that it can be seen that this is not a chance view arising from some local artifact.

Magnification × 300,000
(Inset × 500,000)

(b) Model with subunits at the vertices of a rhombic triacontrahedron, oriented to correspond to the particles in (a) above.

(1) Printed through a mask so as to exclude the subunits near the periphery of the projected view; reversed contrast.
(2) Printed without a mask; reversed contrast.
(3) Printed with normal contrast.

(c) As in (b), but with subunits at the vertices of a pentakis dodecahedron. Good agreement with the models is obtained if one supposes that the particles are less than half immersed in the negative stain, and that only the subunits on the submerged portion are visible.

(d) Selected examples of virus particles, seen in same view as in (a) (looking down the twofold axis), but chosen to show the group of 5 subunits around a central subunit near the top and bottom of the particle. In the models we have been considering, fivefold axes would pass through the centre of these groups.

Magnification × 300,000

believe that this is not really the case, that the particles are more probably in contact with each other, and that the effect arises because they are only partially immersed in the sheet of PTA, making in it an array of depressions which are not in contact with one another. (The "edges" of the particles seem too sharply defined for the effect to be explained in terms of contrast conditions near the peripheries of spherical or hemispherical depressions which *are* in contact with each other.) A diameter of 230 to 240 Å indicates substantial shrinkage from the wet dimensions of 280 to 300 Å, but agrees well with the interparticle distance of 228 Å deduced by Bernal & Carlisle (1948) from their X-ray measurements on crystals dried over P_2O_5. A number of particles show up merely as approximately circular rings. These presumably represent empty protein shells.

Most of the particles show well-marked evidence of regular substructure. The exact appearance of any particular particle would naturally depend on its orientation. We have attempted to derive from our pictures an exclusive arrangement of subunits on the surface of the particle, having cubic symmetry, which will account for all the different appearances seen. The arrangement we find is one in which the subunits are located, at least approximately, on the 32 vertices of either a pentakis dodecahedron or a rhombic triacontahedron, two very similar Archimedean dual solids (Cundy & Rollett, 1951) having 532 symmetry. We will outline the arguments by which this result was obtained.

The general appearance of the particles suggests that we are seeing the substructure on one side of the particle only. Thus, the minimum distance between subunits near the centre of the particle is approximately constant, i.e., there is no indication that we are looking at two superimposed sets of subunits, on top and bottom of the particle. Also, the number of subunits which can be counted at the periphery of the particles—10 or 11 generally—is incompatible with arrangements of regularly-disposed subunits in which the total number of subunits is only 14 or 15 (the maximum number seen). The mechanism by which the negative staining technique—and this procedure in particular—reveals surface detail on only one face of the particles needs investigation ; a plausible explanation might be that the particles are only partially immersed in the sheet of phosphotungstic acid, a possibility we have already mentioned in connection with the anomalous diameter of the particles.

If, then, only approximately half the subunits are visible, we can say that the total number of subunits is approximately 30 and that their characteristic separation, in these dried particles, is 65 to 75 Å.

Although the visible arrangement of subunits is variable, there are a number of highly characteristic patterns that recur again and again which we can use to construct a model of the structure. The first of these, and perhaps the most striking of all, consists of a set of 6 subunits arranged to form a regular hexagon around one central subunit. A number of particles showing this appearance is shown in Plate II(a). When seen in face view like this, the particle reveals very little of the other subunits which must be near the periphery so it would appear likely that this group of 7 subunits forms an approximate facet on the particle, from which other facets may slope back rather sharply. It is interesting to note that Steere (1957) found a somewhat similar appearance in TYMV studied by the frozen-replica technique. This aspect of the particle is the only one which shows threefold symmetry about the viewing direction, and it is reasonable to assume that we are looking down a threefold axis.

The next important clue is the occasional appearance of particles which show two adjoining hexagonal groups of subunits, having one edge in common. Such particles

are illustrated in Plate II(d). This is a very favourable perspective, for almost one half of the total number of subunits fit into this very simple geometric arrangement. Moreover, using the fact (known from the X-ray results) that the particles must have cubic symmetry, we can deduce that we are looking at the structure along a direction approximately bisecting the angle between two of the four tetrahedrally oriented threefold axes. We are therefore in a position to construct the whole particle. There must necessarily be a hexagon visible whenever we look down on a threefold axis, in either direction, giving 8 hexagons in all, and they must each share common edges with three adjacent hexagons, in the same way as the visible hexagons have a common edge. This fixes the number of subunits at 32, and it shows that, to a first approximation, the structure resembles an arrangement of subunits placed at the vertices and at the centres of the hexagonal faces of a truncated octahedron. A model built of ping-pong balls arranged in this manner is shown in Plate II(g).

This model accounts satisfactorily for the appearance of particles viewed in certain directions, but it has to be modified before it can account for all the arrangements seen. A prominent feature of many particles is a diamond- or rhombus-shaped set of 4 subunits near the centre of the particle, which in many instances may be seen to be the shared portion part of two overlapping groups of 6, each hexagonally arranged about a central subunit (Plate III(a)). This particular arrangement does not arise naturally in any view of the truncated octahedron. Conversely, a prominent feature of the truncated octahedron should be a set of 4 subunits at the corners of a square, and no such arrangement is visible in any particle we have examined. These difficulties arise from the fact that the truncated octahedron has 432 symmetry, while the particle we are seeing shows twofold axes and does not show fourfold axes. Furthermore, 432 symmetry is excluded by the X-ray data. It was therefore evident that a slightly different arrangement was required, which retained the (approximately) regular hexagons, suitably oriented to give cubic symmetry, and in which the number of subunits was still 32, but in which the square sets of subunits were transformed into diamonds so as to turn the fourfold axes into twofold axes. We found that this could be done by "puckering" the hexagonal sets of subunits, i.e., moving alternate ones up or down relative to the plane of the hexagon, and by trial and error we arrived at a configuration which gave the observed ratio (about 5 : 3) between the major and minor axes of the "diamonds". In this structure, the sets of 6 subunits still appear as simple hexagons, for the "puckering" is rather slight. But the most unexpected feature of the model which we had now built was that it had developed approximate fivefold axes, passing through the subunits at the acute angled corners of the " diamonds". This symmetry had arisen of its own accord, as it were, without having been "built-in" to the model by the initial assumptions about symmetry. On comparing this model, which we had deduced in largely empirical fashion, with all the regular and semi-regular polyhedra and their derivatives, we found that we had quite unwittingly constructed a very close approximation to either a pentakis dodecahedron or a rhombic triacontahedron (we are indebted to Dr. Klug for the suggestion that the possibility of a correspondence between the model we had built and the latter polyhedra might be examined). The pentakis dodecahedron is a semi-regular polyhedron having 60 identical triangular faces, 60 edges, and 32 vertices. It has 532 symmetry. The triangular faces have angles 68° 36′, 55° 42′, 55° 42′ and so are approximately equilateral. The "hexagonal" sets of vertices in projection are disposed accurately at 60° angles about the central member of the group, and the two types of vertex in the group differ in their distance from the centre by only about 5%. A model built of ping-

pong balls arranged in this manner is shown as viewed from various directions in Plates II(c), II(f) & III(c). The rhombic triacontahedron is a semi-regular polyhedron having 30 identical rhombic faces, 30 edges, and 32 vertices (see Fig. 1). It too has 532 symmetry. It may be looked on as a pentakis dodecahedron in which pairs of triangular faces had been bent until they were co-planar. The angles in the triangular sets of vertices are 63° 26′, 58° 17′, 58° 17′, again giving a close approximation to an equilateral triangle. Again, the angles in the hexagons are 60° in projection, and the two characteristic distances differ by only about 10%. A ping-pong ball model is shown in Plates II(b), II(e) & III(b).

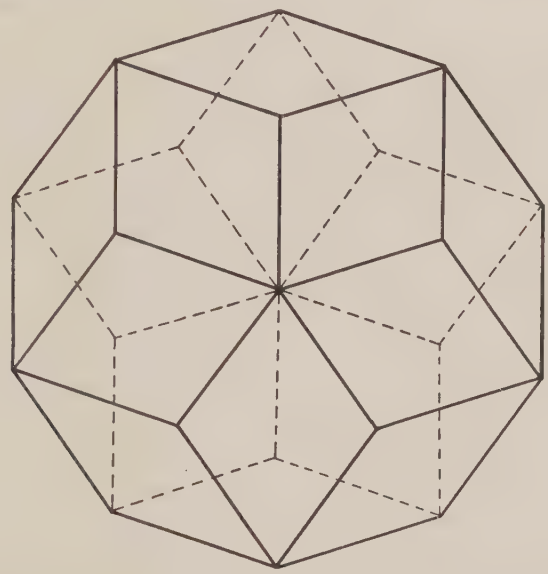

Fig. 1. Diagram of a rhombic triacontahedron, viewed down a fivefold axis. This polyhedron has 32 vertices and 30 identical rhombic faces. It can be seen from the diagram that the vertices on the threefold axes (where 3 edges meet) have as their nearest neighbours a set of 6 vertices, 3 of them on threefold axes and 3 of them on fivefold axes. The pentakis dodecahedron has very similar characteristics, except that the vertices on threefold axes lie further out from the centre of the polyhedron, so that the planar rhombic-shaped faces become pairs of triangular faces, with a dihedral angle of 156° 43′. It thus also has 32 vertices, but 60 identical triangular faces.

Views of the models looking down a threefold axis are shown in Plate II(b) & (c). It will be seen that the resemblance to a hexagonal arrangement is very close, and that the appearance closely imitates that of the virus particles shown in Plate II(a), provided that the subunits around the edge of the particle, as it faces the observer, are not seen. This is the effect we would expect to get with particles only partially immersed in the sheet of phosphotungstic acid.

The appearance of the models when viewed in a direction in between two threefold axes is shown in Plate II(e) & (f); these show two intersecting groups of 6 subunits each with a central subunit, with 2 subunits shared between them at their common edge; again, the agreement with the appearance of virus particles shown in Plate II(d) is very satisfactory.

A view of the models looking down a twofold axis is shown in Plate III(b) & (c). This view is characterized by two overlapping hexagonal sets of subunits forming the diamond. It may be compared with the appearance of selected particles of TYMV in Plate (III(a)), and it will again be seen that the correspondence is very close indeed.

Another distinctive feature of such an arrangement is the presence of subunits which lie at the centre of a group of 5 subunits. This can be seen in several views of the models, and particles showing this feature particularly clearly are illustrated in Plate III(d). Such an appearance provides a very strong and specific indication of the presence of fivefold symmetry. We have not seen a ring of 5 near the centre of the particle, but this would only happen if the particle were sitting on a fivefold axis, and, as the subunits on these axes protrude considerably above their 5 neighbours, we need not be surprised.

3. Discussion

Thus we find that either the pentakis dodecahedron or the rhombic triacontahedron gives excellent agreement with all the observed appearances of the particles; but the arrangement of the subunits does not of necessity have to adopt either of these precise forms. As we have already mentioned, the degree of "puckering" of the hexagons can be varied without destroying the cubic symmetry, and even when fivefold axes are present as well, the subunits at the centres of sets of 5 may be moved radially, independently of those at the centres of sets of 6. There is thus a continuous spectrum of models which include, as special cases, the ones we have already mentioned and also the face-centred dodecahedron and the face-centred icosahedron. These latter two are not satisfactory in their detailed appearance—for instance in the face-centred dodecahedron the 2 types of subunit which occur in the rings of 6 differ in their distances from the central subunit by more than 20% in projection and this divergence conflicts strongly with the experimental observations. And, in the face-centred icosahedron, subunits on the fivefold axes protrude outwards too far to be readily compatible with either the apparent near-planarity of the hexagons, or with the detailed appearance seen when looking down a twofold axis. However, it is much more difficult to distinguish between the less extreme possibilities; there is some slight evidence in favour of arrangements like the pentakis dodecahedron—for instance, a number of cases are seen where the subunits on threefold axes in the "diamonds" show up a little more strongly than those on the fivefold axes, as though they were protruding outwards slightly further. On the other hand, the fact that the particles so often do appear to lie on a "diamond" suggests that this set of subunits does not diverge very far from planarity and would favour the rhombic triacontahedron. In general, then, we can only say that the particles approximate to one of these two polyhedra and that to a close approximation they have 532 symmetry, but we cannot say whether either the second or both of these relationships is precisely true. The X-ray evidence shows that 23 symmetry is fully developed, and that the virus particle has strong icosahedral features attributable to the protein component (Finch, 1959; Klug & Finch, 1960) but by its nature it cannot prove that *all* the protein is arranged strictly in accordance with this symmetry.

It is of interest that the visible subunits often appear ring-shaped, which would be a natural consequence of their being built up of smaller "structural" units arranged around a rotation axis. If the particles have true 532 symmetry, then the subunits on the 12 fivefold axes must each contain $5m$ identical structural units, and those on the 20 threefold axes $3n$ identical structural units, where m and n are non-zero integers. Thus the number of fundamental structural units must be $60(m+n)$, the minimum number therefore being 120. We may also note that both types of subunit seen in the

electron micrographs appear to be very similar in size. If these subunits are built up from a common, or similarly sized, structural unit it would be more likely that the numbers involved were 5 and 6 rather than 5 and 3. The minimum number of structural units would then be 180. However, the use of a common structural unit would place extremely high structural requirements on such a unit (to form all the necessary inter- and intra-subunit bonds), and it may be more reasonable to suppose that two differing structural units are involved.

The subunit structure can also be detected in the "empty" particles which are present in the preparations. To some extent, the appearance of these particles is anomalous for, even when photographed under appropriate conditions of contrast, they show little sign of substructure except at the edges. A possible explanation might be that the unsupported shells tended to have their immersed face flattened when they were dried in the sheet of PTA, while the intact virus with its RNA core was more rigid and preserved its surface protrusions. We do not think it likely, however, that the structure seen in the intact particles has been imposed on them merely by their outer shell drying down onto the nucleic acid core, for the "empty" particles look very similar to the intact ones at their periphery, where their general shape and number of subunits correspond closely. The subunits seen in profile in the "empty" shells often appear disc-shaped.

The separation between the subunits in our preparations is about 65 to 75 Å, and the particles themselves have diameters of about 230 to 240 Å. If the subunits were located with their centres on the vertices of the two polyhedra we have named, then the mean diameter of the spherical shell would be about 190 Å. If we take account of the thickness of the shell, then the values are reasonably compatible. In undried particles with a diameter of 280 to 300 Å, the distance between the centres of the subunits would be about 90 Å.

The structure we have found is a different one from that tentatively suggested by Klug *et al.* (1957) (which consisted of 60 approximately spherical protein subunits of diameter about 60 Å situated at the vertices of a snub dodecahedron and in contact, each with its nearest neighbours), although of course the two arrangements have the same symmetry. The X-ray evidence which supported a model in which the subunits were about 60 Å apart came from observations of intensity modulations in the powder diagrams of TYMV, suggesting a predominant spacing of 60 Å in the protein particle. At first sight, this result might appear to conflict with any model in which the subunits were 90 Å apart. However, we would like to put forward the suggestion that what the modulation of the X-ray diagram is showing us is the characteristic spacing between the *holes* in the structure, i.e., the spaces in between the subunits. In the model we have described there are 60 of these holes (if the subunits are roughly spherical or cylindrical), and the characteristic spacing between them is 55 to 60 Å. They will lie very approximately on the vertices of a truncated icosahedron (the dual of a pentakis dodecahedron). It is a well known feature of wave optics that the non-zero order diffracted rays from a structure cannot enable us to distinguish between the structure and its complement (Babinet's principle), and so the X-ray diffraction results give equally strong support to structures in which either holes or subunits are about 60 Å apart.

An arrangement of spherical or circular disc-shaped subunits on the vertices of a pentakis dodecahedron or a rhombic triacontahedron has another interesting feature, and one that may be of particular value if it is to provide a protective coat for the RNA; not only is the *average* packing in the shell rather close but, perhaps more

important, there are no large gaps at all in the structure, the holes we have mentioned being relatively small ones as far as access through the shell is concerned.

We are indebted to Professor Katz for the encouragement and support he has given this work, to Dr. Klug and Dr. Finch both for stimulating us to consider some of the issues dealt with in this paper and for supplying us with samples of TYMV, and to Miss Pamela Dyer for her assistance at many points. One of us (G.Z.) acknowledges with appreciation the support of a postdoctoral fellowship from the National Institutes of Health (U.S.A.).

REFERENCES

Bernal, J. D. & Carlisle, C. H. (1948). *Nature*, **162**, 139.
Brenner, S. & Horne, R. W. (1959). *Biochim. biophys. Acta*, **34**, 103.
Caspar, D. L. D. (1956). *Nature*, **177**, 475.
Crick, F. H. C. & Watson, J. D. (1956). *Nature*, **177**, 473.
Cundy, H. M. & Rollett, A. P. (1951). *Mathematical Models*, pp. 112–117. Oxford University Press.
Finch, J. T. (1959). Ph.D. Thesis, University of London.
Hall, C. E. (1955). *J. Biophys. Biochem. Cytol.* **1**, 1.
Hodgkin, D. C. (1949). *Cold Spr. Harb. Symp. Quant. Biol.* **14**, 65.
Huxley, H. E. (1957). *Proc. Stockholm Conference on Electron Microscopy*, 1956. Stockholm: Almqvist & Wiksell.
Huxley, H. E. & Zubay, G. (1960). *J. Mol. Biol.* **2**, 10.
Klug, A., Finch, J. T. & Franklin, R. E. (1957). *Biochim. biophys. Acta*, **25**, 242.
Low, B. (1953). *The Proteins* **1**, 235. New York: Academic Press.
Markham, R. (1951). *Disc. Faraday Soc.* **11**, 221.
Schmidt, P., Kaesberg, P. & Beeman, W. W. (1954). *Biochim. biophys. Acta*, **14**, 1.
Steere, R. L. (1957). *J. Biophys. Biochem. Cytol.* **3**, 45.

J. Mol. Biol. (1960) **2**, 197-200

Electron Microscope Observations on the Structure of Turnip Yellow Mosaic Virus

H. L. Nixon and A. J. Gibbs

Rothamsted Experimental Station, Harpenden, Hertfordshire, England

(*Received 2 May 1960*)

Electron micrographs of turnip yellow mosaic virus particles prepared by the negative staining technique show clearly defined internal structure, which indicates that the protein shell of this virus is constructed of 32 subunits in an icosahedral arrangement. The structure inferred from the electron micrographs satisfies the X-ray data, and contains subunits which occupy two structurally distinct sites.

Turnip yellow mosaic virus (TYMV) reaches a high concentration in infected plants, from which it can be extracted and crystallised by simple methods (Markham & Smith, 1949), so it is not surprising that it is one of the most studied of the "spherical" plant viruses. Markham & Smith (1949) and Markham (1951) obtained evidence that their preparations of TYMV contained components of different density but similar size. They showed that the lighter component, which is non-infective and contains no nucleic acid, is serologically indistinguishable from the heavy component which contains nucleic acid, and concluded from this that the nucleic acid is carried within a hollow protein shell. Klug, Finch & Franklin (1957*a*, 1957*b*) obtained evidence from X-ray diffraction studies of icosahedral symmetry within the particles, and suggested that their X-ray diffraction patterns would be most simply explained if the virus particles had a protein shell consisting of 60 identical subunits arranged in rings of five. Caspar (1956) obtained X-ray evidence for a similar symmetry within the particle of tomato bushy stunt virus, as did Finch & Klug (1959) with poliomyelitis virus, which was thus perhaps identical in structure and form, although not in size, with TYMV and tomato bushy stunt particles. Magdoff (1960) obtained evidence of icosahedral symmetry within the particle of southern bean mosaic virus, and recent X-ray work with TYMV (Klug, private communication) has confirmed the icosahedral symmetry of that particle. Steere (1957), using a special replica technique, obtained electron micrographs of TYMV particles showing rings of six knobs with one in the centre, but he did not attempt to relate these images to the structure postulated by Klug *et al.* on the basis of the X-ray data. With the notable exception of the early work of Markham & Smith, none of these studies provided any evidence about the location of the nucleic acid or about the way in which it is bound to the protein subunits. All the detailed structures suggested for the protein shell have been based solely on the X-ray results, and except for the single electron micrograph published by Steere no definite information on the internal structure of any of these particles has been provided by electron microscopy.

We have now obtained pictures of TYMV, by a negative staining technique (Brenner & Horne, 1959), which show clear internal structure. Analysis of the images

suggests that TYMV particles have 32 subunits, which are therefore structurally (but not necessarily also chemically) of two different kinds (Plate I). These pictures were obtained from particles in an old crystalline preparation of the virus obtained in 1956 from Dr. Markham of the Virus Research Unit, Huntingdon Road, Cambridge. The preparation has been stored as a suspension of crystals in one-third saturated ammonium sulphate solution at 4°C since reaching our laboratory. Samples for electron microscopy and other tests were withdrawn and dialysed against 0·01 M-phosphate buffer at pH 7·5. After centrifuging briefly to remove insoluble material, the supernatant fluid containing the virus particles was diluted suitably, mixed with 2% neutral sodium or potassium phosphotungstate and then sprayed on to carbon-coated platinum discs using an all metal spray gun (Nixon & Fisher, 1958). Little infectivity had survived the long storage, for out of four turnip plants inoculated with the dialysed sample only two developed the symptoms of TYMV; clarified sap from these plants reacted specifically with an antiserum prepared against TYMV in rabbits.

TYMV extracted from diseased plants and examined immediately showed the same internal structure as that shown by the old virus preparation used in our work, but none of the particles in the freshly made preparations showed the subunit structure so clearly. The sprayed mounts were examined directly in the electron microscope at a magnification of 80,000, and yielded pictures of the kind reproduced as Plate I(a). Many particles that were only superficially penetrated by the stain show evidence of internal structure at both the edges and inside. The surface is composed of what appear to be subunits, roughly circular in outline and approximately 6 mμ in diameter. Not more than 12 subunits are visible on any one particle, and if the mounting technique permits only half or slightly fewer than half the total number of subunits to be seen this suggests that the shell contains 25 to 40 subunits, or roughly half the number in the 60 unit structure suggested from X-ray data by Klug *et al.* Possible arrangements containing about this number of subunits and at the same time having icosahedral symmetry, which is necessary to satisfy the X-ray diffraction observations, are very few. Experiments with models constructed from table tennis balls showed that all the features of the electron microscope images could be reproduced by a shell made from 32 subunits. In this structure 20 subunits are arranged in twelve rings of 5, each subunit being shared between three adjacent rings. The remaining 12 subunits are placed at the centres of the rings, and thus occupy sites which are structurally distinct. Other arrangements, containing 20 or 42 subunits, although having the symmetry required by the X-ray results, nevertheless fail to show the observed features. Plate I(f) shows a photograph of our model, oriented to present a ring of 6 subunits with one in the centre towards the observer.

In our electron micrographs the subunits are always arranged in one of two patterns. In one of these, a single subunit is surrounded by a ring of 6 others as shown on particles near the centre of Plate I(b) and I(c). In the other pattern, 4 subunits are arranged as if at the corners of a parallelogram, and are surrounded by 8 other subunits, most clearly seen on particles close to the centre of Plate I(d) and I(e). The major and minor axes of this parallelogram are approximately 12·5 and 8·5 mμ long respectively; it can be seen that this pattern has rings of 6 subunits round each of the subunits forming the ends of the minor axis of the parallelogram, and rings of 5 subunits round each of the subunits forming the ends of the major axis of the parallelogram. In the 60 unit structure suggested by Klug *et al.* all the subunits are arranged in separate rings of 5 without sharing, and this arrangement, however

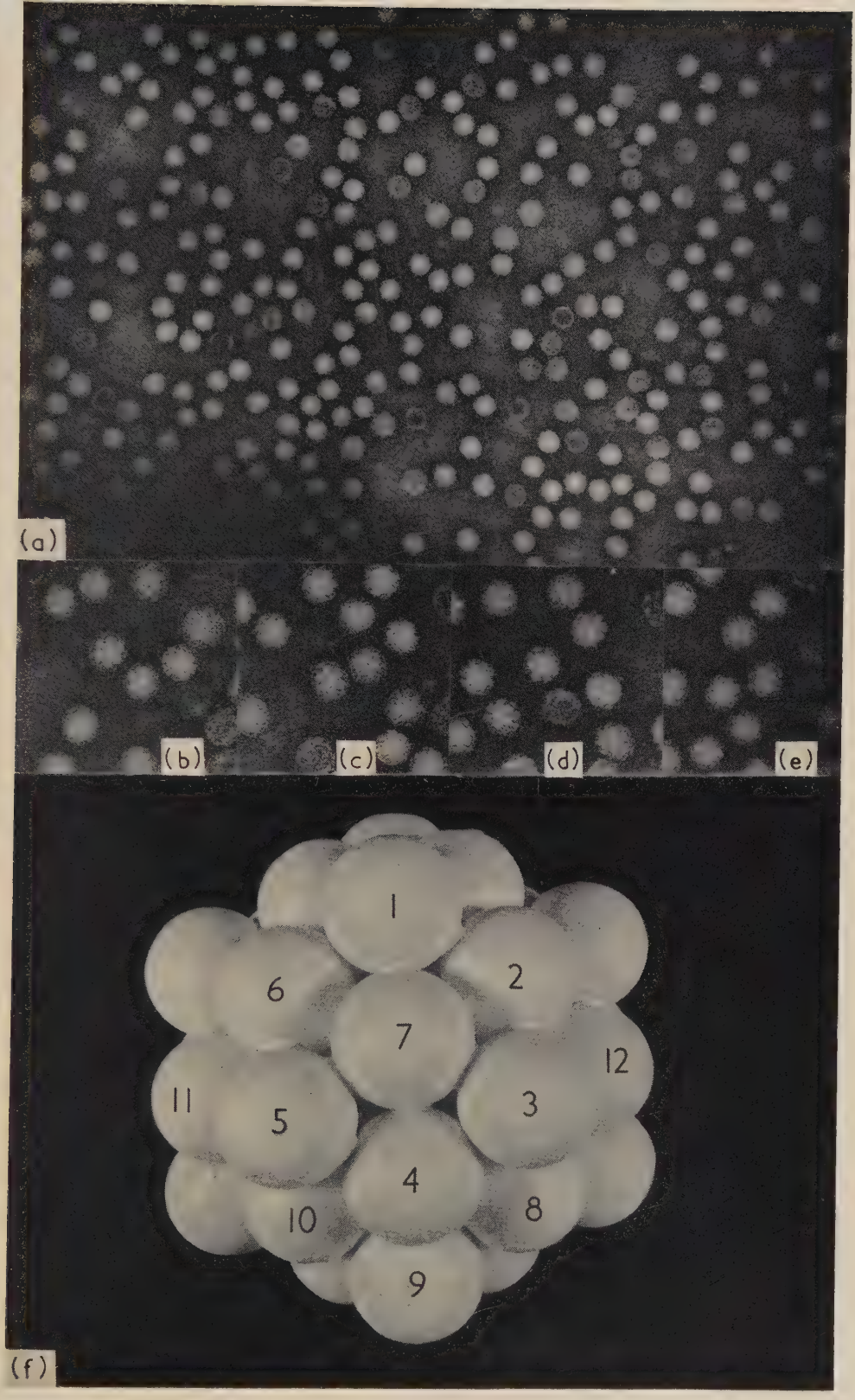

PLATE I(a). Particles of turnip yellow mosaic virus, negatively stained with phosphotungstate. × 120,000.

I(b), I(c), I(d), I(e). Selected parts of the same field at a higher magnification, showing the two characteristic patterns found on the particles (see text). × 240,000.

I(f) Model constructed from table tennis balls to show the suggested structure. A ring of six subunits surrounds the central one, and units numbered 1, 2, 6 and 7 outline the diamond pattern.

[*To face page* 198

oriented, cannot show the patterns we find. A search of many thousands of particles showed that whenever internal structure of any kind was visible, it was invariably one or the other of the two patterns described.

It is not known whether the images of virus particles seen in negatively stained preparations are of the upper or the lower surface of the particles, and indeed the ability to see subunit structure in some virus particles but not in others in the same preparation has sometimes been claimed to be due to increased contrast resulting from the superimposition of the images from subunits in the upper and lower halves of the shell. In our proposed 32 unit structure, if either of the patterns we find were oriented symmetrically, then the patterns on the upper and lower parts of the particle would coincide exactly and thus the image contrast would be increased. However, on most of the patterns the subunits are slightly off centre, so that their images cannot be exactly superimposed. The fact that the subunits can still be seen clearly and that their shape is apparently not distorted by imperfect superimposition suggests that the images are derived from one surface of the particle only, but it is not clear whether this is the upper or the lower part.

The exact position occupied by the 12 subunits at the centres of the rings of five other subunits is not determined by the symmetry, which merely requires these subunits to be located on the fivefold axes. However, no particles can be found showing a pattern with one subunit in the centre of the particle surrounded by 5 others. This suggests that the subunit at the centre of a ring of five projects beyond the plane of the ring so much that the particle cannot rest upon it. If these 12 subunits on the fivefold axes do protrude (Plate I(f), subunits 1, 3 and 5), certain other features of the patterns can be explained, for 3 of the subunits in each ring of 6 are at fivefold axes, and if protrusive enough will act as points on which the particle can rest and show the ring-of-6 pattern. The fact that this pattern is invariably off centre suggests that the central subunit (Plate I(f), subunit 7) protrudes slightly beyond the plane, which would rest on the 3 subunits at the fivefold axes, and therefore the particles will always rest on the subunit at the centre of a ring of 6 (i.e., a subunit at a threefold axis, Plate I(f), subunit 7) and 2 subunits at fivefold axes (Plate I(f), subunits 3 and 5). Thus in Plate I(f) the model is resting on the subunits on the opposite side of the particle which correspond to subunits 3, 5 and 7, and when moved slightly is most likely to rest next on those corresponding to 1, 3 and 7, or 1, 5 and 7, or 3, 4 and 5. In all these positions it will show a ring-of-6 pattern. If, however, there are any impurities in the virus preparation a virus particle may become propped in an intermediate position, which would be such as to show a parallelogram of four subunits surrounded by eight subunits (Plate I(f), subunits 3, 4, 5 and 7, surrounded by subunits 1, 2, 12, 8, 9, 10, 11 and 6) as can be seen in the electron micrographs.

Dr. Klug has told us that the 32 unit structure would satisfy the demands of symmetry imposed by the X-ray data just as well as the 60 unit structure originally proposed, and the electron microscope images agree so well with the 32 unit arrangement that we feel justified in concluding that the protein shell of TYMV has in fact 32 subunits arranged in the manner just described and not 60 as originally proposed. It is important to notice that in our suggested 32 unit structure the subunits occupy two structurally distinct positions, at the point of emergence of either a threefold or a fivefold axis. Such an arrangement does not necessarily imply any significant chemical or morphological difference between the units which occupy different sites. In suggesting a 60 unit structure, Klug, Finch & Franklin deliberately excluded the possibility of a structure of this kind with two different kinds of

subunit, and sought instead one in which all the subunits occupied structurally identical positions.

Sometimes at the edges of the particles the subunits project radially in a way which suggests a prismatic rather than a roughly spherical shape (Plate I(d), lower left), and sometimes the images of the units are surrounded by a white line suggesting that the units themselves may perhaps be hollow (Plate I(d), upper right). Apart from this our pictures give no direct information about the exact shape of the subunits, nor do they throw any light upon their mode of attachment to the nucleic acid. The external diameter of the particles in our pictures is estimated to be 24·8 mμ, a rather smaller value than that generally accepted for TYMV and obtained from shadowed preparations (Cosentino, Paigen & Steere, 1956). In our experience many other plant virus particles appear smaller when mounted by the negative staining technique, probably because the outer parts of the particles are penetrated by the stain, so that they appear dark in a positive print and are not seen. Plate I(a) also contains images of several particles which appear to have been deeply penetrated by the stain. These "empty" particles are apparently of two kinds, one of which only shows a roughly circular outline, and a second in which traces of subunit structure can still be seen, although the whole particle appears much darker than most of those in the field. Presumably one or both of these represents the "top component" of Markham & Smith; if it is only one, we do not know which, and neither do we know whether any of these "empty" particles are the product of long storage or of the specimen mounting techniques. The study provides another example of the value of the negative staining procedure, and shows that electron microscopy may be able to provide useful information at a level which will help in the interpretation of X-ray diffraction data bearing upon the internal structure of plant viruses.

We wish to thank Dr. R. Markham, Cambridge, for the sample of TYMV used in most of this study; Dr. A. Klug, London, for helpful discussions, and Mr. R. D. Woods, Rothamsted, for his able assistance with the electron microscopy.

REFERENCES

Brenner, S. & Horne, R. W. (1959). *Biochim. biophys. Acta*, **34**, 103.
Caspar, D. L. D. (1956). *Nature*, **177**, 475.
Cosentino, V., Paigen, K. & Steere, R. L. (1956). *Virology*, **2**, 139.
Finch, J. T. & Klug, A. (1959). *Nature*, **183**, 1709.
Klug, A., Finch, J. T. & Franklin, R. E. (1957*a*). *Nature*, **179**, 683.
Klug, A., Finch, J. T. & Franklin, R. E. (1957*b*). *Biochim. biophys. Acta*, **25**, 242.
Magdoff, B. S. (1960). *Nature*, **185**, 673.
Markham, R. (1951). *Disc. Faraday Soc.* No. **11**, 221.
Markham, R. & Smith, K. M. (1949). *Parasitology*, **39**, 330.
Nixon, H. L. & Fisher, H. L. (1958). *Brit. J. Appl. Phys.* **9**, 68.
Steere, R. L. (1957). *J. Biophys. Biochem. Cytol.* **3**, 45.

J. Mol. Biol. (1960) **2**, 201-215

The Symmetries of the Protein and Nucleic Acid in Turnip Yellow Mosaic Virus: X-Ray Diffraction Studies

A. Klug and J. T. Finch

Birkbeck College Crystallography Laboratory (University of London), Torrington Square, W.C.1, England

(*Received 28 May 1960*)

Turnip yellow mosiac virus (TYMV) is an approximately spherical plant virus having a (hydrated) spherically-averaged diameter of 280 Å and containing about 60% protein and 40% RNA (Markham, 1951). The protein is in the form of a spherical shell with the RNA contained inside. Associated with the virus is the "top component" which consists of empty protein shells containing no RNA. Previous X-ray diffraction studies (Klug, Finch & Franklin, 1957) of crystals of TYMV have shown that the virus particles have the symmetry of the tetrahedral point group (23), with a very strong tendency towards icosahedral (532) symmetry. It was suggested that the icosahedral symmetry was due to the protein component. We have now extended these studies on the virus crystals to higher angles of diffraction. Our previous observations are confirmed and it is shown that some part of the virus particle has 532 symmetry developed to a resolution of at least 4 Å.

We have now also obtained photographs of a single crystal of the top component and these confirm that the protein shell has 532 symmetry. It is therefore made up of 60 asymmetric (structurally equivalent) units so that the number of chemical units of any one kind must be a multiple of 60. Recent electron microscope observations presented in the accompanying papers (Huxley & Zubay, 1960; Nixon & Gibbs, 1960), show that the virus is composed of 32 protuberances arranged so that 20 fall at the vertices of a pentagonal dodecahedron and 12 at those of an icosahedron. The relation between the X-ray and the electron microscope results and the available chemical evidence is discussed. All the present data can be reconciled if the protein shell is made up of 180 (or, less likely, 120) chemical subunits arranged regularly in 20 groups of 6 (or 3) at the dodecahedral vertices and in 12 groups of 5 at the icosahedral vertices, but other, only statistically regular, models cannot be ruled out.

Differences are observed between the X-ray diffraction patterns of crystals of the virus and of the top component. These must be due directly or indirectly to the RNA, and show the RNA to possess, at least in part, some kind of regular structure. The differences observed are consistent with a configuration having 23 symmetry, which, if correct, would imply that the RNA is made up of 12 geometrical subunits. This could still be reconciled with a single *chemical* chain. The problem of packing such a chain into a spherical particle with cubic symmetry is discussed. However, the apparent 23 symmetry of the RNA may arise as a statistical average over the many virus particles in a crystal, the RNA in a single particle having lesser symmetry. The various possibilities are discussed.

1. Introduction

Turnip yellow mosaic virus (TYMV) is of considerable interest because it was discovered (Markham & Smith, 1949; Markham, 1951) that the infective virus is accompanied in the plant by protein particles—the so-called top component. These are

physically similar to the virus particles except that they are non-infective and contain no RNA. The protein particle has the approximate form of a hollow spherical shell which, in the intact virus, is filled with RNA. Both the virus and the top component can be crystallized from ammonium sulphate solution (Markham & Smith, 1949) and the two crystal forms are the same and the unit cells very similar (Bernal & Carlisle, 1948). The existence of these two associated particles therefore seems to provide a striking opportunity for studying by X-ray diffraction methods the substructure of both the protein and the RNA in a spherical virus on the lines of the investigations by Franklin (1956; see Franklin, Caspar & Klug, 1959) on tobacco mosaic virus and repolymerized A-protein.

In a previous paper (Klug, Finch & Franklin 1957, hereafter referred to as KFF for brevity) we have already reported on the first stages of an X-ray study of single crystals of the virus. However, at the time, crystals of top component large enough for single crystal work were not available, and our X-ray investigations were confined to "powder" photographs of a sludge of very small, wet crystals. More recently, we have obtained X-ray precession photographs of a small, single crystal of top component from a batch kindly prepared for us by Dr. Markham. In this paper we describe this investigation and the results that have emerged. We also describe some further work on crystals of the virus (Finch, 1959) relevant to the problem of the particle symmetry.

In our earlier paper (KFF) the crystal structure of the virus was deduced, and it was shown that the virus particle had the symmetry of the cubic point-group 23 (tetrahedral symmetry). It was also shown that there was a strong indication of additional pseudo-symmetry corresponding to the point-group 532 (icosahedral symmetry), and it was suggested that this situation arose from the fact that a *part* of the virus particle had true 532 symmetry. (This is in accord with the theoretical predictions of Crick & Watson (1956) on the symmetry likely to be possessed by a small spherical virus particle.) Reasons were given for identifying this part with the protein component of the virus. The results reported here on the symmetry of the protein shell confirm this suggestion, so that the overall 23 symmetry of the virus particle must be ascribed to the RNA.

2. Further Observations on the Virus Crystals

(a) *Summary of previous observations*

The crystal structure has already been described (KFF). The centres of the virus particles fall on a simple body-centred cubic lattice with a cube edge of 350 Å, but the particles may have either of two orientations which alternate in a regular manner. This means that the true unit cell is larger than the simple one corresponding to the virus centres. However, viewed at low resolution, so that the two orientations of the virus particles are indistinguishable from each other, the crystal structure is a simple body-centred cubic one, with an interparticle distance of 304 Å, and therefore similar to that of bushy stunt virus (Caspar, 1956). Formally, the structure may be thought of as made up of two interpenetrating diamond-type lattices, i.e. the space-group is $F4_132$ with the two independent special positions (*a*) and (*b*) (International Tables, 1952) occupied by virus particles rotated 90° to each other about the cube edge of the unit cell. For short, we shall call this crystal structure a "double diamond lattice".

Precession photographs of TYMV showed concentrations of strong reflections in certain directions ("spikes"). It was found that these spikes could be resolved into two identical sets such that the relative directions of the spikes within a set are those of the symmetry axes of the point group 532, and such that the two sets correspond to the two particle orientations present in the lattice. This is strongly suggestive that the virus particle has 532 symmetry. However, the complexity of the TYMV lattice fortunately permits the possibility of determining directly whether this 532 symmetry is fully present or not. Members of a certain class of reflections (*hhh*, with *h* odd) were observed, which, if the particle had true 532 symmetry, would be absent. It was therefore concluded that the virus particle as a whole does not have strict 532 symmetry.

(b) *Experimental limitations*

The intensities on the X-ray photographs of a virus crystal fall off very rapidly with angle and the photographs described in our earlier paper (KFF) were generally confined to precession angles of less than 2°, corresponding to a maximum spacing of about 25 Å. With the Hilger semi-microfocus X-ray unit used for this work, exposures of 2 to 3 days were necessary. It is pertinent to mention here that the task of collecting intensity data is enormous. The simplest virus crystal with a unit cell side of about 350 Å and cubic symmetry 23 (cf. bushy stunt) would give approximately 1,800 independent reflections (allowing for the cubic crystal symmetry) to a spacing of 10 Å and 14,000 out to 5 Å. For TYMV with a unit cell side of 700 Å (and crystal symmetry 432) the corresponding numbers are about 7,000 and 56,000. Even allowing for the special absences found, these figures are very large compared with even complex crystals of small globular proteins. Furthermore the crystal reflections are extremely weak (except at very low angles, where the whole virus particle or each of its subunits is scattering as a body), the average intensity to be expected being approximately inversely proportional to the volume of the unit cell.

A further difficulty is that after the prolonged exposure necessary for even a small-angle precession photograph the crystal suffers a good deal of radiation damage. On subsequent photographs of the same crystal, the general fall-off in intensities is even more pronounced, and, moreover, the intensities of some individual reflections are changed relative to one another. The particle structure is a little less sensitive to radiation damage than the crystal structure, as can be seen from the diffuse areas characteristic of the particle transform which are still present on the photographs (see Fig. 1 of KFF). Generally, therefore, a fresh crystal must be used for each new exposure.

(c) *A low-resolution Patterson function*

In view of these problems, the systematic collection of intensities has so far been confined to spacings greater than about 25 Å, since this could be done largely by means of 2° precession photographs of the zero layers corresponding to a relatively small number of zone axes, viz [100], [110], [111], [112], [103]. Higher layer photographs were avoided as far as possible because of the less favourable Lorentz factor effect.

From this data a three dimensional Patterson map has been computed (Finch, 1959). The map is dominated by the closely spherical nature of the virus particles, and very similar to the Patterson expected from uniform density spheres in a body-centred cubic lattice. The main departures are all consistent with vectors expected from particles exhibiting 532 point-group symmetry.

This rather more formal analysis therefore confirms that the virus particle has a high measure of 532 symmetry. In the previous work this was deduced from the appearance on the X-ray photographs themselves of "spikes" of reflections with high intensities in the directions of the symmetry axes of this point group. It should be stressed that, since the reasoning used in either form of deduction is essentially statistical in nature, it cannot be concluded that 532 symmetry is strictly present.

(d) *Moderate angle precession photographs*

Besides the systematic 2° precession photographs referred to above, 3° photographs have been taken of the [111] and [112] zero layers, and 5° photographs of [100] and [110] zero layers, in order to obtain some idea of the distribution of intensity in reciprocal space at higher angles. The two latter are reproduced in Plates I and II. The use of these larger precession angles was made possible by access to a 3 kw rotating-anode tube at the Royal Institution, which enabled the photographs to be taken in a practicable time. Using as large crystals as we had available (0·5 to 1·0 mm), the 3° photographs were obtained with exposures of about 10 hr and the 5° photographs in 30 hr. Further experimental details may be found elsewhere (Finch, 1959).

On the [100] photograph (Plate I) it can be seen that the strong reflections tend to be concentrated in the directions of the rotation axes of the point-group 532 and that these "spikes" extend to the limit of the photograph (0·11 $Å^{-1}$). A noticeable feature is the group of strong spots clustered about the reflection 52,32,0 close to the direction of the five-fold axis. (The direction ratios of the five-fold axes relative to the crystal (Cartesian) axes are 1·618 : 1 : 0.) These reflections lie at spacings close to 11 Å, a region where scattering from proteins is characteristically strong.

Likewise, on the [110] photograph, spikes of strong intensity occur in the direction of the two- and three-fold rotation axes of the point-group. The strongest reflections of the type *hhh* are those with $h = 16$, 24, 32 and 40 respectively, and the difference in the reciprocal spacings of adjacent reflections is $0{\cdot}0172 = 1/58$ $Å^{-1}$. The strongest reflections of the type *hh*0 have $h = 14$, 24, 34, and 44, and the reciprocal spacing difference is $0{\cdot}020 = 1/50$ $Å^{-1}$. The presence of a modulation of period about 1/60 $Å^{-1}$ is also visible on the 3° [111] zero layer photograph referred to above.

These modulations are undoubtedly characteristic of the transform of the virus particle and may be traced to the same cause as the spherically averaged modulation of about 60 Å observed in powder photographs of top component (see KFF) which we shall discuss below. There are variations of intensity visible in other directions where the average intensity is strong, but these are much less regular and can hardly be said to constitute a modulation. The reason why the modulation is so well defined in the crystallographic directions *hh*0 and *hhh* is that, in each case, the projection of a particle of 532 symmetry on to the line in question is the same for both of the orientations present in the crystal structure. The projections of the particles in the two different orientations on to other lines (such as the five-fold or non-crystallographic three-fold directions) are not the same.

The [110] photograph (Plate II) also shows that the reflections with *h*,*k*,*l* all odd are very weak to the limits of observation (0·11 $Å^{-1}$). The reflections of the type *hhh* with *h* odd, whose presence shows that the virus particle as a whole cannot have 532 symmetry (see KFF), are clearly visible.

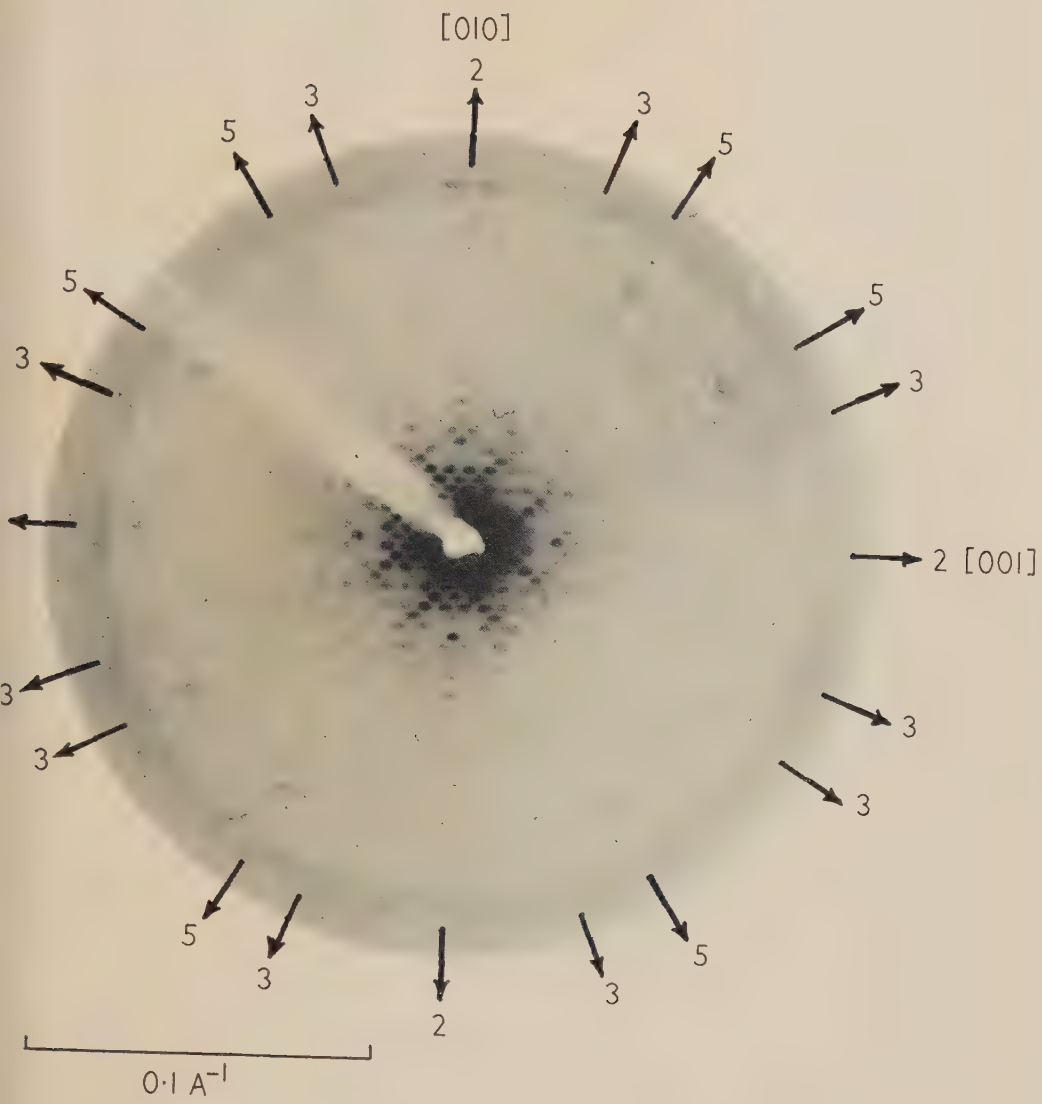

PLATE I. Zero layer precession photograph of TYMV crystal taken with the X-ray beam parallel to a cube edge, [100].

The precession angle was 5° and the exposure time was 30 hr on a rotating-anode tube run at 3 kw. The edge of the photograph corresponds to spacings of about 9 Å. The directions of those five-, three- and twofold rotation axes of particles with 532 point group symmetry which lie in this plane are indicated by arrows. The twofold axes shown are in the directions of the fourfold axes of the crystal. The inner region of the photograph is shown in Plate III(b).

[*To face page* 204

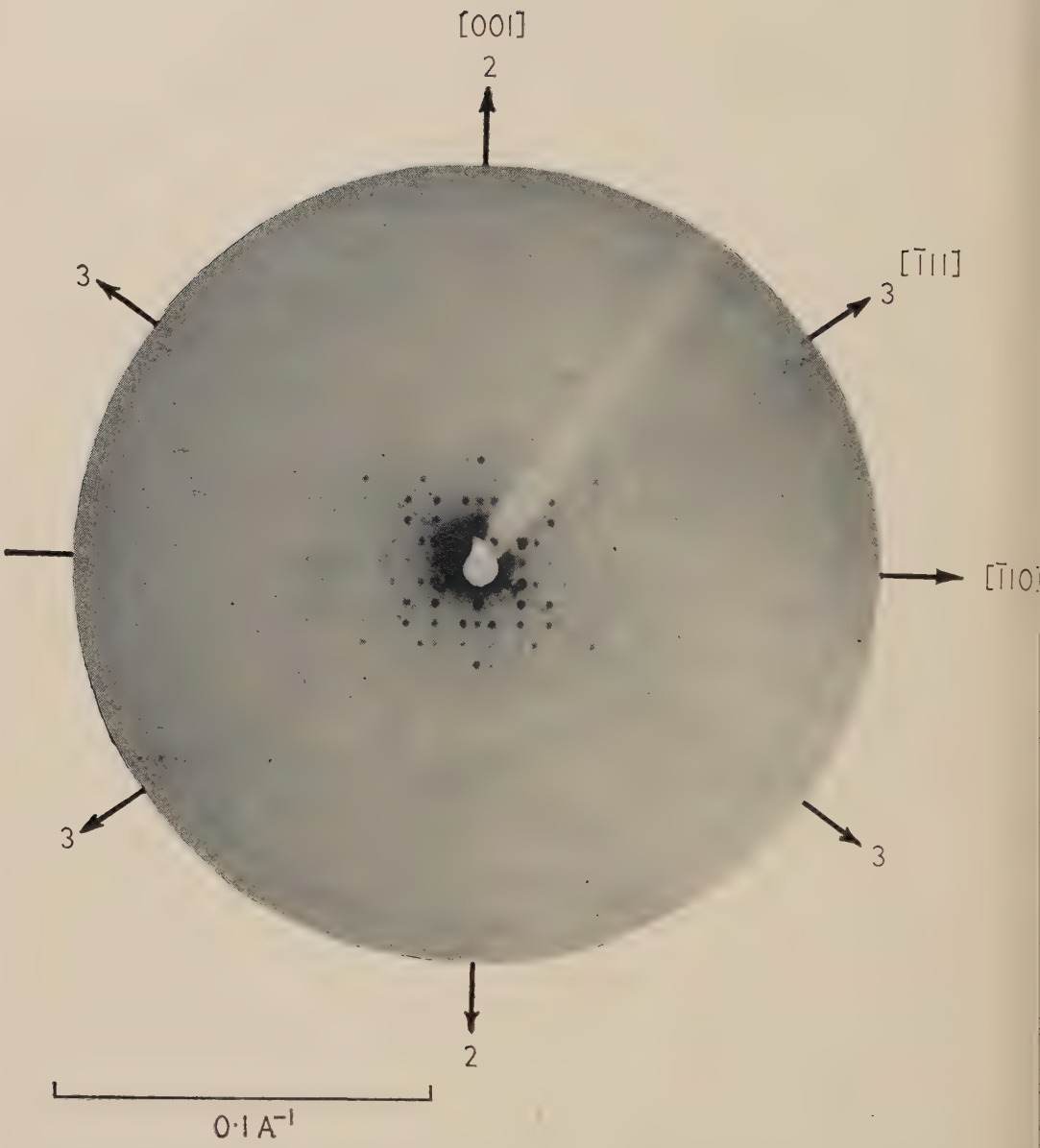

PLATE II. Precession photograph of a TYMV crystal with the X-ray beam in the direction of the twofold axis of the crystal, [110]. The precession angle was 5°.

Spikes of reflections of strong intensity occur in the directions of the two- and threefold rotation axes of the point group 532 (or 23), the four- and threefold axes of the crystal respectively.

The reflections in the direction of the threefold axis show a marked modulation in intensity, indicating a prominent spacing of about 60 Å within the virus particle.

Several reflections with odd indices occur, particularly those of the form *hhh*, which would be absent if the point group of the virus particle were strictly 532.

(e) *High-angle reflections*

In the course of the collection of intensity data, a number of 1° to 2° precession photographs were taken without using layer-line screens. Provided the exposure is sufficient, very narrow annular regions of higher layers of the reciprocal lattice are observable, and except for the appearance of a lattice in the zero layer, the whole photograph resembles a "still" in which the systems of circles have become annuli. A set of such photographs, taken with the X-ray beams close to the directions of the zone axes mentioned earlier, provides a random but rather sparse sampling of reciprocal space out to high angles. The sampling, although restricted, is representative. Thus we have observed that the higher layers visible on a number of 1° to 2° precession photographs taken at slightly different angles of offset to the [112] zone axis show only one (independent) outstandingly strong reflection. This reflection, of index 54,32,2 on the sixth layer of the reciprocal lattice, is located very close to the group of strong reflections lying on the fivefold axis in the 11 Å region visible on the [100] zero layer photograph (Plate I). It is striking that the only strong intensities that we have observed at spacings less than 10 Å are sets of 5 broad spots lying very close to the directions of the fivefold symmetry axes at a reciprocal spacing of about 0·25 $Å^{-1}$. Each spot represents a small group of unresolved strong reflections, and it was possible to assign an approximate index to the central reflection in each group. The indices found were 78,126,0; 84,136,0; 88,144,0; 92,152,0; and 96,160,0.

This fairly regular succession of strong spots, almost as close to the irrational direction of the fivefold axes as the rational sampling on the lattice permits, is so striking and singular and occurs at such low spacings that it is highly unlikely that it could arise from something in the particular structure which did not have true 532 symmetry. We cannot give a good quantitative measure of its strength and say what proportion of the whole virus particle has this 532 symmetry, but we can say that the 532 symmetry is exact to a resolution of at least 4 Å. The fact that the scattering is particularly strong in the 11 Å and 4 Å regions is strongly suggestive that the seat of the 532 symmetry is the protein of the virus, but we cannot, in all rigour, conclude that the whole of the protein component necessarily has this symmetry.

3. Observations on Single Crystals of Top Component

The question of whether or not the virus *protein* has full 532 symmetry, and therefore consists of 60 identical asymmetric units, can best be answered by studying single crystals of the top component. The crystals sent to us by Markham were rather small, had very poorly developed faces, and some were obviously polycrystalline; and our first attempts to obtain single crystal photographs all failed. More recently, after being stored for about a year at 4°C, the preparation was found to contain a few crystals of about 150 μ diameter. One of these crystals, a thin plate of thickness about 50 μ, was found to give good X-ray photographs.

The diffraction from a crystal of top component is much weaker than that from a virus crystal, weak as that is already, so that the work was only made possible by the use of the rotating-anode tube at the Royal Institution, mentioned above. Since only a very limited part of reciprocal space can be explored using one crystal, we decided to limit ourselves to taking very small angle precession photographs ($1\frac{1}{3}$°)—such photographs took about 18 hr. The crystal could not be set even roughly by eye, and this was done by a combination of still and precession photographs which enabled us to find and identify the [115] and [552] zone axes. The orientation of the crystal being

thus determined, it was set, using a stereogram, successively for the four major zone axes, [100], [110], [111] and [112], and small angle precession photographs were taken (see Plates III(a) and IV).

These photographs showed that the top component crystals are strictly isomorphous with those of the complete virus to the limits of the patterns recorded. No difference can be detected in the cell dimensions and the two crystals have the same lattice symmetry and space group $F4_132$. The non-space-group absence of reflections with $h + k + l = 4n + 2$ and the absence or weakness at low angles of reflections with h, k, l all odd, characteristic of the virus crystal structure, are also shown by the top component. Corresponding precession photographs of two crystals are overall very similar, but there are specific differences in intensity of a number of reflections.

Thus in Plate III we have compared the [100] photograph with one from a crystal of the complete virus. The spikes of strong intensity in the directions of the five-fold rotation axes are much more striking in the case of the virus protein, and we believe that this shows the 532 symmetry to be enhanced with respect to that of the complete virus particle.

The intensity differences in the [110] zero layer may be seen by comparing Plates II and IV. The most important changes are in the *hhh* reflections with h odd, which, in the virus crystal photographs, tend to be stronger than the general reflections of the type $h + k + l =$ odd (see Plate II), but which either vanish or are very much reduced in the top component crystal photographs. (This effect is also visible in the [112] photograph not reproduced here.) This is most noticeable in the case of the 555 reflection which in the virus crystal is the strongest of all the reflections with odd indices, but which is very much weaker in the top component. These are exactly the reflections which, as predicted in KFF, would vanish for particles of strict 532 symmetry arranged in the "double diamond" lattice. The fact that the 555 reflection does not entirely disappear we attribute to the fact that the top component crystals contained a small fraction of complete virus, of which it is very difficult to remove all traces from a preparation of top component.

Although the systematic data on the top component intensities go out only to a spacing of about 35 Å, we have observed in the outer regions of the [115] precession photograph (which was taken without a layer-line screen, and which, being the first precession photograph taken, shows least deterioration) a number of strong reflections which fall nicely on the direction of the two distinct fivefold axes lying close to the basal reciprocal lattice plane of this zone axis. These are the reflections $10,\overline{16},2$ and $22,30,\bar{4}$ close to one fivefold axis, and $24,16,0$ and $54,32,\bar{2}$ close to another. The last mentioned reflection has also been observed as strong in the case of the virus crystals (see section 2(d)), suggesting a close similarity in the arrangement of the protein in the two materials.

Thus, all the observations we have on the top component show that it has 532 symmetry. That this symmetry is now probably strictly present in the protein is shown by the virtual disappearance of the *hhh* reflections with h odd; but since only a small number of reflections are involved in this observation, this evidence must be treated with some caution. However, taken together with the observations on the virus crystal showing that some part of it has 532 symmetry developed to a resolution of at least 4 Å, it is hard to escape the conclusion that most, if not all, of the protein of the virus particle possesses strict 532 symmetry. Some of it *must* have, but until the location of all the chemical subunits is determined, we cannot be sure that there is not a part of the total protein that is organized differently.

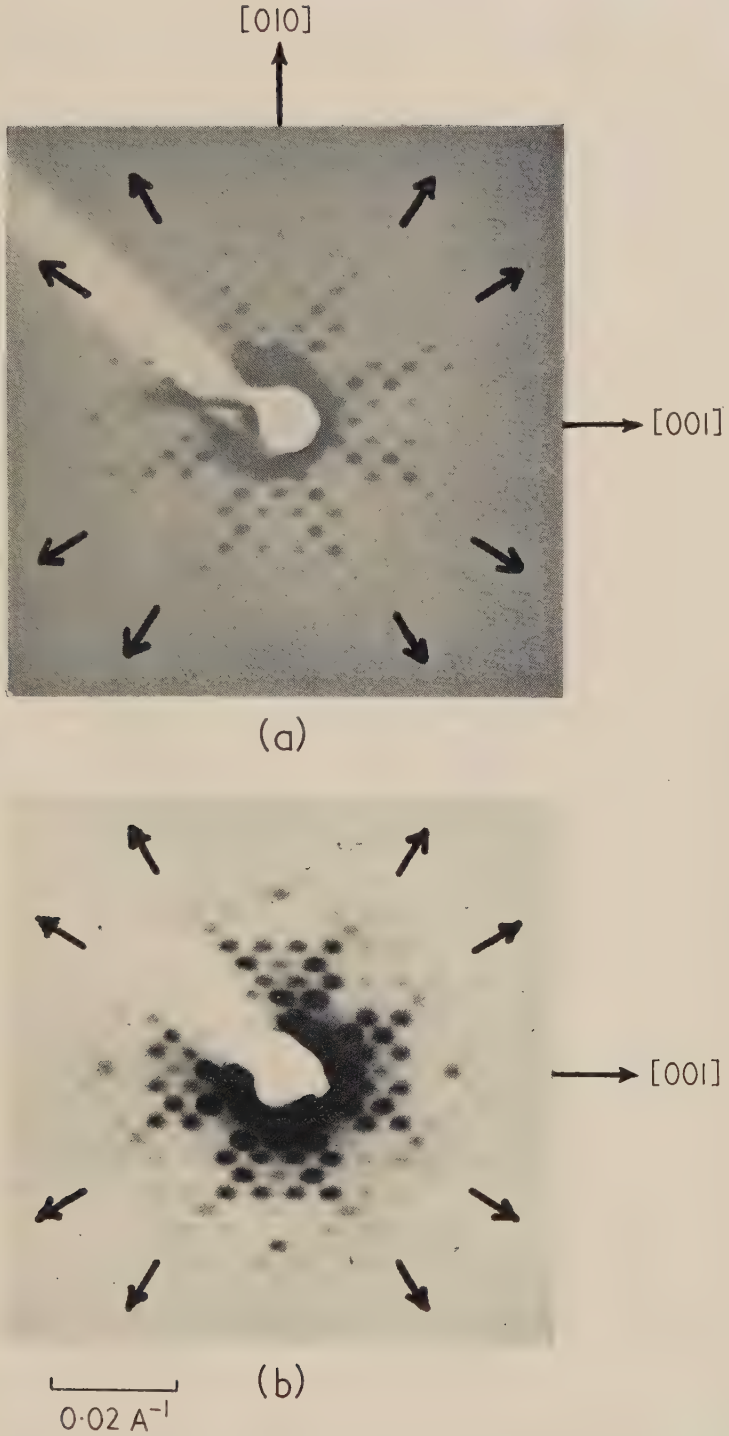

PLATE III. Comparison of the [100] axis precession photographs (in the same orientation and to the same scale) of crystals of (a) the top component, and (b) the virus.

The spikes of reflections of high intensity in the directions of pairs of adjacent three- and five-fold rotation axes (unresolved at these low angles) are much more marked in the case of the top component. The directions of the fivefold axes are marked by arrows.

[*To face page* 206

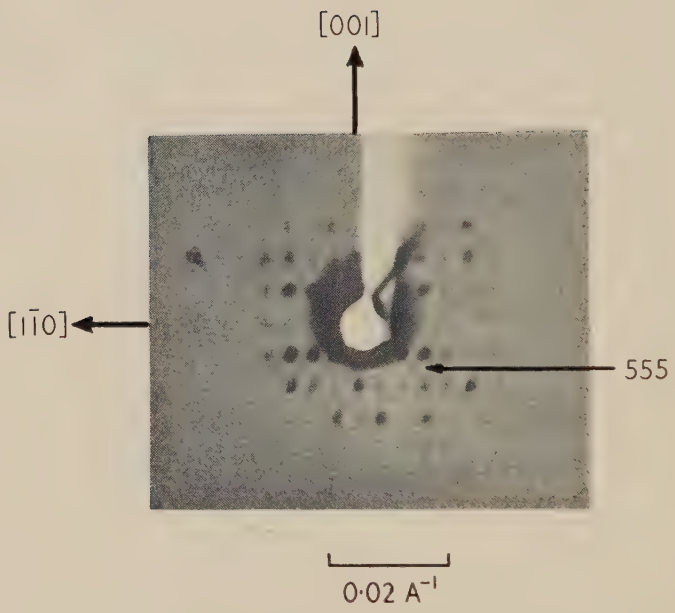

PLATE IV. A [110] axis precession photograph ($1\frac{1}{3}°$) of the top component crystal.

The arrow marks the 555 reflection which is very much weaker than in Plate II, where it is the strongest of the reflections *hhh* with *h* odd.

4. The Structure of the Protein Shell

In our earlier paper we tentatively put forward the suggestion that the 60 asymmetric units required by the X-ray results were arranged at the vertices of a snub dodecahedron of edge length 60 Å. This model was based on a marked modulation of period approximately 1/60 Å observable in the intensity pattern which we have referred to above. This indicates a predominant spacing of 60 Å in the particle, and the latter was taken to correspond to the centre-to-centre distance between subunits packed to form the protein shell. From some recent electron microscope observations on TYMV, Huxley & Zubay (1960) have suggested that the 60 Å spacing is characteristic of the distance between holes in the structure (i.e. the spaces between subunits) rather than between protuberances (i.e. the subunits themselves). The fact, which formed the physical basis of our suggestion, that 60 globular units packed 60 Å apart on the surface of a sphere give a model having the correct dimensions for the protein shell of the top component, is now seen to be a geometrical coincidence.

Huxley & Zubay (1960) and Nixon & Gibbs (1960) have examined TYMV in the electron microscope by the negative staining method, and have found that regularly disposed protuberances may be discerned on the surface of the particles. These appear to be the morphological subunits forming the protein shell. From an analysis of the characteristic patterns of knobs observed in different views of the particles, and using the fact (known from X-ray results) that the particles must have the cubic symmetry 23, Huxley & Zubay concluded that there are 32 such subunits on the surface of the virus particle. As a rough first approximation, the structure resembles an arrangement of subunits placed at the vertices and at the centres of the hexagonal faces of a truncated octahedron. This arrangement has 432 symmetry which is forbidden by the X-ray data. By a careful study of the electron micrographs, Huxley & Zubay showed that a slightly different arrangement of 32 units accounted for the patterns seen much more satisfactorily, and this was one which had 532 symmetry, as required by our X-ray results. The arrangement approximates closely to either a pentakis dodecahedron or a rhombic triacontahedron (see, for instance, Cundy & Rollett, 1951). The latter are semi-regular polyhedra having 532 symmetry, and in view of the latest X-ray results discussed above it seems very likely that the polyhedron with 32 vertices does in fact have *strict* 532 symmetry.

Nixon & Gibbs likewise conclude that there are 32 subunits arranged at the vertices of a polyhedron with 532 symmetry, but refer to the polyhedron concerned as approximating to a face-centred pentagonal dodecahedron. This polyhedron is different in detail from the two just mentioned. However, all the possible models considered are part of a series of polyhedra with 32 vertices, whose basic feature is that each has 12 vertices arranged at the vertices of an icosahedron (i.e. in fivefold positions) and 20 at the vertices of a dodecahedron (in threefold positions). The relative radii of the two sets of vertices is variable giving rise to a continuous spectrum of polyhedra having the same 532 symmetry.

Since approximations to these polyhedra cannot be distinguished in the electron micrographs, it is the X-ray evidence that compels us to assume that the 32-vertex polyhedron has true 532 symmetry. Furthermore, if the particles have true 532 symmetry, the subunits seen in the electron micrographs—which we may call morphological subunits—must be further divided into small "structural" units arranged around the rotation axes of the polyhedron. Since the subunits occupy two different types of position, they can be of two different species. Thus the subunits on the 12

fivefold axes must each contain 5 identical structural units, and those on the 20 threefold axes, 3 identical structural units. Thus the number of structural units would be 120, arranged in two sets of 60 each. The structural units within a set of 60 must be identical in all respects, but those of the two different sets need not be. The X-ray crystallographic unit (or strictly, asymmetric unit) contains a pair of structural units, one from each set. Furthermore, according to the way we have defined "structural unit," each of these may be divided into chemical subunits (i.e. distinct polypeptide chains) which may not be chemically identical. The total number of chemical subunits possible is therefore $(60m + 60n)$where m and n are non-zero integers. It should

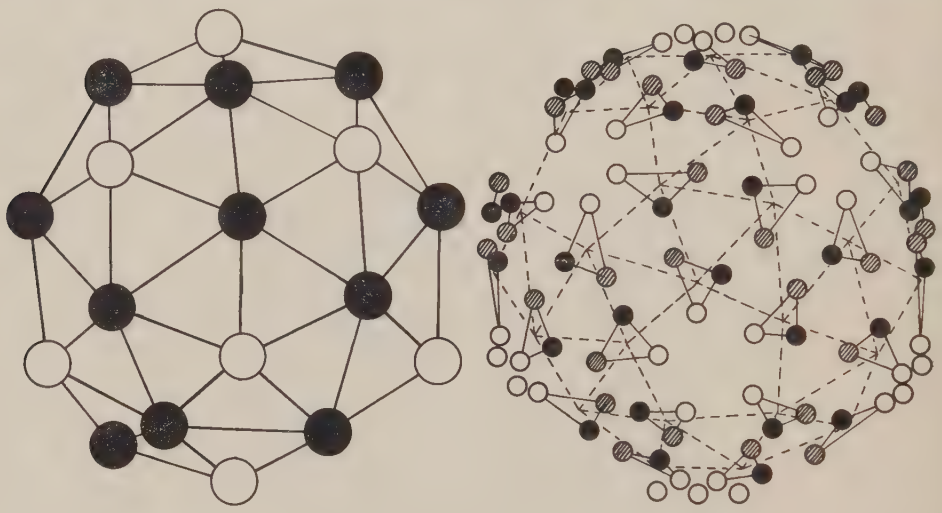

(a) (b)

FIG. 1. Schematic diagram of the structure of the protein shell of TYMV, combining the electron microscope, X-ray diffraction, and chemical evidence at present available.

(a) An arrangement of 32 units consisting of 12 (white) placed at the vertices of a regular icosahedron and 30 (black) at the centres of the faces of a slightly larger icosahedron. This is the type of arrangement seen in the electron microscope (Huxley & Zubay, 1960; Nixon & Gibbs, 1960). This arrangement would have strict icosahedral symmetry only if each unit were subdivided: each white unit into 5 identical structural subunits, and each black into 3, making 60 each of black (12×5) and of white (20×3) structural subunits. These structural units may be further divided into chemical subunits.

(b) A sub-division of (a) resulting in an arrangement possessing strict icosahedral symmetry and consisting of 180 chemical subunits of possibly three kinds (black, white, and shaded). Each white unit of (a) has been divided into 5 white structural (and, in this case, chemical) subunits. Each black unit of (a) has been divided into 3 structural subunits, each of which has been further subdivided into a pair (one black and one shaded) of chemical subunits. The symmetry does not require the three kinds of subunit to be the same chemically, but even if identical, they are still differently situated in the structure (i.e. they are not structurally equivalent).

The asymmetric unit (or X-ray crystallographic subunit) is a group containing one chemical unit of each kind, shown by the triangles in the diagram, although the choice of the group is quite arbitrary. The dotted lines joining the centres of these triangles (asymmetric units) form a polyhedron with 60 vertices which has, of course, icosahedral symmetry.

be noted that even if all the chemical units are identical chemically, they are still differently situated in the structure (i.e. they are not structurally equivalent). The relation between the various kinds of unit is illustrated in Fig. 1, which also serves schematically to indicate the structure of the protein shell of TYMV.

It is clear from the interpretation of the X-ray photographs that a model of 32 spherical, or even globular, units at the vertices of the rhombic triacontahedron or

any of the other similar polyhedra will not account for the radial Patterson function constructed from the intensities measured on powder photographs of top component crystals (see KFF). All such models would give a predominant 85 to 90 Å spacing which is not observed. The units must therefore be different from spheres. Indeed Huxley & Zubay (1960) have noted that the morphological units often appear to be ring- or disc-shaped, and that this would be a natural consequence of their being built up of smaller units arranged about the rotation axes. In this case the predominant spacing would almost certainly correspond to the distance between the spaces left between discs in contact. As mentioned earlier these spaces are about 60 Å apart and there would be 60 of them in all.

The total number of chemical subunits is therefore a multiple of 60, but the chemical evidence on the substructure of TYMV is still far from complete. The amino acid analyses of TYMV (see Markham, 1959; M. W. Rees, private communication) give by calculation a minimum subunit size of molecular weight 20,000, and the preliminary end-group analysis (J. I. Harris, private communication) indicates that the chemical unit is indeed of this size. Using the value of 5×10^{10} for the particle molecular weight published earlier (Markham, 1951) of which 60% is protein, the number of chemical units would seem to be 150, but more recent determinations of the particle weight (Markham, private communication) indicate that the published value must be revised upwards. It therefore seems likely that the number of chemical units is 180, but the figure of 120 cannot be ruled out at present. As a consequence it is probable that each of the 20 subunits in the three-fold positions of the rhombic triacontahedron consists of 6 rather then 3 chemical subunits. In that case, the number of chemical units at the 32 vertices of the polyhedron would be either 6 or 5, so that the morphological units at each position would be similar in size. The converse argument has been used by Huxley & Zubay (1960). They noted that the knobs at each position appeared very similar in size in the electron micrographs so that the numbers of smaller subunits involved were more likely to be 6 and 5, rather than 3 and 5, in which case the minimum total number would be 180.

A schematic diagram of the structure of the protein shell of TYMV, incorporating the electron microscope, X-ray, and chemical evidence at present available, is shown in Fig. 1. This also serves to illustrate the various kinds of unit picked out by different methods. The relation between these various units is more fully discussed elsewhere (Klug & Caspar, 1960).

The structure immediately raises the question as to how, in fact, the shell is built, i.e. what are the actual *building units* out of which the three-dimensional structure of top component is assembled in the infected plant. Are they the 60 groups of 3 structurally non-equivalent chemical units (forming the asymmetric units), or, as appears to be more likely, are they the 32 morphological subunits seen in the electron microscope? If the latter, is there then a prior aggregation into rings of, say, 5 and 6, respectively, which then come together to build the shell? It should be noted that in that case a very simple building rule would account for the resultant structure, namely that a 5-ring fits into good contact with a 6-ring. The protein shell could thus be assembled ("crystallized") out of building units without the mediation of any further organizing principle or agency. In particular an empty protein shell could be built by itself without the need for the prior formation of a core of RNA. This is a rather attractive picture and would explain the occurrence of top component as shells assembled from, say, a pool of protein subunits, when the latter are present in excess over the RNA, at some stage during the process of virus replication. A complete

picture of the process would, however, also have to explain how the same fundamental chemical unit can aggregate into 5- or 6-rings (in the same medium); there might, for instance, be an equilibrium between the two modes. Or are there, in fact, two very similar but not quite identical chemical units which make both modes possible?

Another, and even more difficult, hypothesis to test is that all the building units are identical 6-rings (say). Twenty of these form a skeletal framework having strict 532 symmetry at the vertices of a pentagonal dodecahedron, and the 12 gaps in the framework (the icosahedral positions) are filled by like building units, rather more loosely bound, so that there are 32 such units in all per particle. The configuration of 12 units at the icosahedral position could be made so as to possess statistical 532 symmetry. This model would agree with the appearance of the electron micrographs, and also with the X-ray result that most of the virus protein possesses strict 532 symmetry.

It is to be hoped that physico-chemical methods will reveal the nature and size of the protein building unit. Kaper & Steere (1959) have reported an alkaline degradation method by means of which small soluble protein fragments could be obtained from TYMV. Very recently, Kaper (1960) has presented evidence on the sequence of events during the degradation. Intact empty protein shells resembling top component are formed first, and these then dissociate into fragments of smaller size. These have an apparent sedimentation coefficient of 11 s under Kaper's experimental conditions, but have not yet been sufficiently well characterized to permit their identification with any of the units discussed above.

The actual arrangement of chemical units present in the protein shell could in principle be found by the heavy-atom method used by Franklin & Holmes (1958) in determining the helical parameters of tobacco mosaic virus. If the chemical subunits were specifically labelled with a heavy-atom, the coordinates of these atoms could be determined. It is hoped that this result will eventually emerge when a successful isomorphous replacement has been achieved.

5. The Question of the Configuration of the RNA in the Virus Particle

The observed specific differences between the X-ray patterns of crystals of virus and of top component could arise not only directly from the absence of RNA in the latter, but possibly also indirectly from some modification in the arrangement of the protein shell when the RNA is not present. We believe that the latter, indirect effect is small for the reason that the crystal structure of the virus and top component are identical and that the X-ray precession photographs are very much alike, apart from the intensity changes described above. Bernal & Carlisle (1948, 1951) reported the unit cell side of the top component to be about 2% greater than that of the virus, but the difference is probably within the range of experimental error. As the external shapes and sizes of the particle are very similar, the virus protein apparently keeps the same configuration whether or not the nucleic acid is present. If this is the case, the differences in intensities must be directly related to the structural arrangement of RNA in the virus.

The fact that the observed differences are not spherically symmetrical indicates that at least to a resolution of 30 Å (at which spacing the present top component photographs end) the RNA has a definite structure. Although a comparison to a greater resolution cannot be made at present, there are two further observations which shed light on this question:

(1) Wide-angle powder diagrams from preparations of crystals of the virus and the top component are shown as densitometer curves in Fig. 2. The main difference between the two curves is the very broad maximum in the virus curve at a spacing of about 30 Å. There are smaller changes in the neighbourhood of the 10 Å region, where the intensity of the virus scattering increases near a spacing of 11·5 Å, decreases at 9·6 Å and increases at about 5 Å, relative to the top component. While the differences near 30, 12, and 5 Å are found in regions where isolated RNA shows broad diffraction bands (Klug, Finch & Holmes, in preparation), the scattering curve from the virus particle is not simply the sum of the top component curve plus that of 40% free RNA. Thus it seems that the RNA in the virus particle, or at least a good deal of it, has a structure different from that of isolated RNA and presumably one imposed upon it by the virus protein. The situation, therefore, may in some respects be analogous to that of tobacco mosaic virus, despite the large proportionate difference in RNA content.

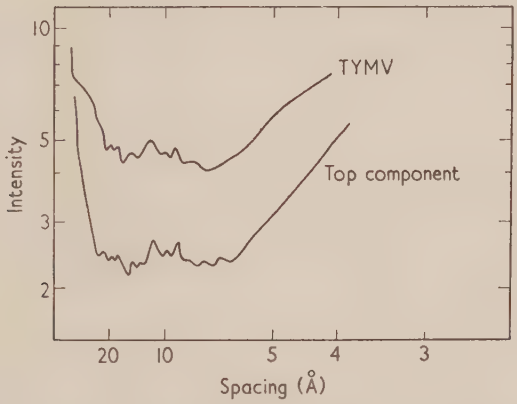

FIG. 2. Photometer curves of the scattered intensity obtained in powder photographs of wet crystals of the complete virus and of the top component.

(2) The fact that the virus particle as a whole has 23 symmetry is shown by the presence of the *hhh* reflections with *h* odd. On the photographs so far obtained these extend to a spacing of about 40 Å. If the protein has strict 532 symmetry, the 23 symmetry of the virus particle must in some way be produced by the presence of RNA.

This not only strongly implies that the RNA has a definite structure, but, taken at face value, would also suggest that it might have 12 (geometrical) subunits. This does not, of course, mean that chemically the RNA cannot be a single chain, for in this case the "subunits" would refer to the mode of winding of the chain. However, we cannot yet be definite on the number of asymmetric units of RNA, since the 23 symmetry suggested for the RNA refers to the *average* throughout the crystal. One can easily conceive of a situation where the RNA in each particle has a symmetry lower than cubic, e.g. orthorhombic (222) or monoclinic (2) or even no symmetry, in which case it could take up, in each particle, one of a number of possible orientations with respect to the particle (and hence crystal) axes. If these occur at random in different particles, the net effect would be to make the RNA, statistically, appear to have the same symmetry as the crystal. This difficulty can, however, eventually be settled when more data are available.

We cannot even be sure at present that the RNA has no symmetry, but it would seem to us that, in this case, it is likely that the statistical averaging over the virus particles in the crystal would so smear out the contribution that the *hhh* reflections with *h* odd would simply fall off with increasing angle. Table 1 shows that this is

TABLE 1

Reflection	Intensity	Reflection	Intensity
111	110	999	44
222	0	10,10,10	0
333	v. weak	11,11,11	53
444	300	12,12,12	v.w.
555	113	13,13,13	v.w.
666	0	14,14,14	0
777	16	15,15,15	v.w. or 0
888	26	16,16,16	173

not the case to the spacing of the 11,11,11 reflections, namely 45 Å, beyond which point the intensities of the *hhh*, *h* odd, reflections on our photographs obtained to date fall off so as to be immeasurable. It seems to us that this rules out some gross structure for the RNA, e.g. a ball of coiled RNA in the centre of the virus, without any symmetry. However, some configuration with 222 or 2 symmetry (cf. Figs. 3(a) and 3(c)) might be possible, as the diffraction effects would not be smeared out by the cubic averaging so drastically as a configuration with no symmetry.

If the RNA does have the symmetry of one of the point groups 23, 222, or 2, yet another problem is raised. An object with 222 or 23 symmetry (the RNA configuration) has one Cartesian triad of twofold axes at right angles which must coincide with one of the 5 such Cartesian triads possessed by an object with 532 symmetry (the protein shell), if the two objects are to conform to one another in symmetry. However, when the crystal is formed—and it is the contacts between outsides, i.e. the protein shells of the different particles, that are involved—there is no geometrical reason why the Cartesian triad of the protein shell which coincides with the crystal axes should be the same as that which coincides with the twofold axes of the 23 object (the RNA) inside. It might be any one of the other four, and if the triad is chosen at random, the result would be that, *in the crystal*, the RNA would appear to have, statistically, 532 symmetry. Since this is at variance with the X-ray observations, it seems that we have to explain why the virus particles in the crystal are all aligned with their included RNA in the correct orientations required by the crystal symmetry. A simple answer, for instance, might be that the RNA inside distorts the protein shell somewhat so that the Cartesian triad common to both is picked out above the other four possible *a priori*. Similar reasoning applies to the case where the RNA has 2 symmetry. There is no experimental information to enable us pursue these arguments further.

It should perhaps be pointed out that even should the symmetry of the RNA be determined, this does not in any way establish how the polynucleotide chain(s) is (are) packed within the framework of protein subunits. One cannot simply make a list of the *a priori* geometrical paths possible, as could be done in the case of tobacco mosaic virus (see Franklin *et al.*, 1959) where the helical symmetry lends itself naturally to the accommodation of a long chain molecule. The problem is part of the more general

one of putting *one* long fibrous molecule into a spherical particle possessing, say, cubic symmetry. It is interesting to note that it is impossible to form a closed continuous curve (a three-dimensional knot or coil) having cubic symmetry. The highest symmetry possible appears to be orthorhombic (222) symmetry, and in Figs. 3(a) and 3(b) we have drawn by way of illustration examples of a continuous curve (chain)

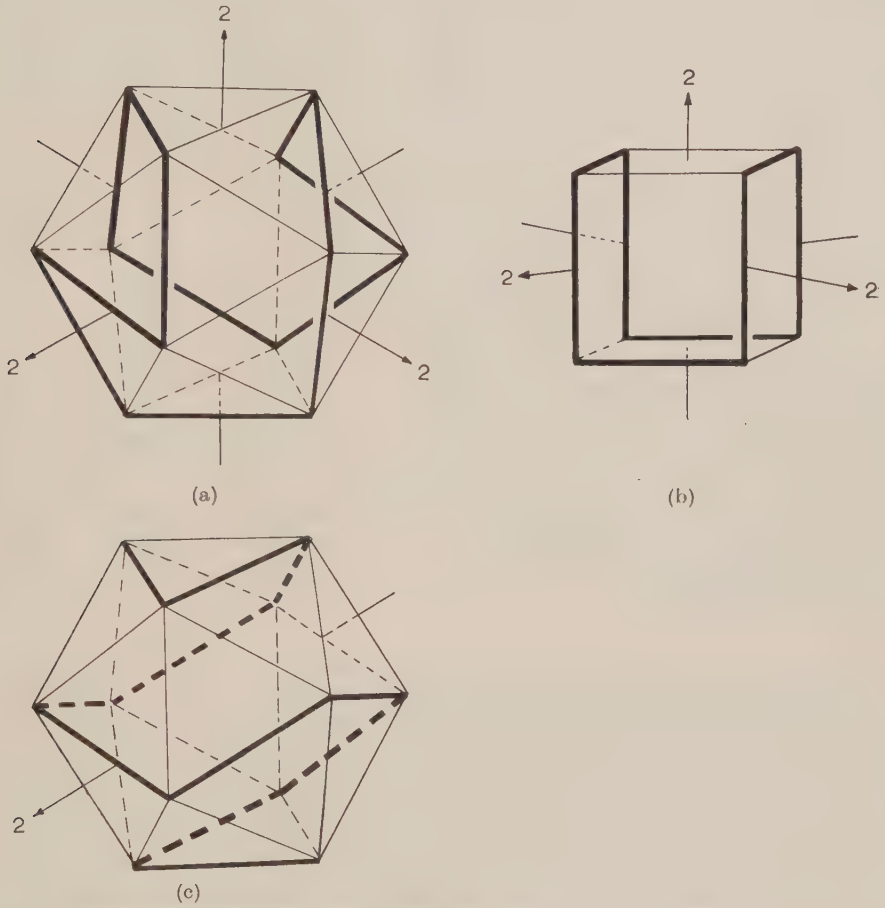

FIG. 3. Continuous curves passing once through each vertex of (a) an icosahedron and (b) a cube. These curves have 222 symmetry which is the highest symmetry that may be possessed by a continuous curve in three dimensions. Such curves are necessarily closed.

(c) A continuous (and open) curve with 2 symmetry passing through each of the vertices of an icosahedron once.

with this symmetry passing through all the vertices of a cube and of an icosahedron to show how this could be accommodated to cases of 23 or 532 symmetry respectively. We have also drawn in Fig. 3(c) a possibly more realistic continuous curve, having 2 symmetry, which does not close back on itself, but which also touches each vertex of an icosahedron once. It is also possible to draw a curve of this kind possessing no symmetry at all. These examples can be extended to the cases of other and more complex polyhedra. At each vertex of the polyhedron a loop might be inserted so that one would finally have a set of loops possessing as a whole cubic symmetry which would conform to the symmetry of the protein shell. However, the segments joining these into one continuous curve (chain) must still have 222 or 2

symmetry. The latter segments can, of course, be made very short relative to the loops, so that it would be difficult (by X-ray methods) to tell whether the symmetry of the whole was not in fact cubic.

The amino acid analysis of the virus (see Markham, 1959) shows that there are not enough basic residues present (as there are in the case of tobacco mosaic virus protein) to neutralize the charge on the RNA. In any case, since the RNA is mainly located within the protein shell, all of it cannot presumably be in contact with protein. It is probably coiled inside the virus, and Markham (1959) suggests that it is probably cross-linked by means of polyvalent bases. This general kind of structure with parts of the RNA in contact with the protein (and presumably having a symmetry consistent with the protein) and a part coiled differently, can be nicely reconciled with the considerations presented in the last paragraph, for folding one long chain molecule into a spherical virus. It will, however, also be clear that the same considerations show that it would be a much easier problem to pack the RNA so as to conform to a protein shell with cubic symmetry, if it were made up of distinct subunits.

We have dealt at some length with this problem because of the possible existence of chemical subunits of RNA, i.e. not linked by covalent bonds, in spherical viruses. We may perhaps be permitted to raise the question here whether in fact the *raison d'être* of spherical viruses is that they can accommodate subunits of RNA, whereas in the rod-shaped helical viruses the RNA is in the form of a single chain. The question will presumably have to be resolved by physico-chemical means. The present evidence is that although RNA extracted from TYMV has a sedimentation coefficient of 28 s (Cheng, 1959) suggesting that all the RNA in the virus comes out in one piece, very mild treatment of this RNA results in its breakdown into a smaller component (Haselkorn, private communication).

We should like to thank Dr. R. Markham for supplying us with preparations of virus and of top component and for his continued interest; Sir Lawrence Bragg and the members of the Davy Faraday Laboratory of the Royal Institution for putting at our disposal a rotating-anode tube; Drs. Huxley and Zubay and Drs. Nixon and Gibbs for communicating their electron microscope observations before publication; and Professor J. D. Bernal for his interest and encouragement. We are indebted to Professor H. S. M. Coxeter for some correspondence in connection with the problem of the symmetry of curves in three dimensions. This work was supported by a research grant No. E-1772 from the National Institute of Allergy and Infectious Diseases, U.S. Public Health Service. We also wish to acknowledge financial assistance by the Agricultural Research Council to one of us (J. T. F.) and a grant by the Wellcome Foundation for the purchase of a precession camera.

REFERENCES

Bernal, J. D. & Carlisle, C. H. (1948). *Nature*, **162**, 139.
Bernal, J. D. & Carlisle, C. H. (1951). *Disc. Faraday Soc.* **11**, 227.
Caspar D. L. D. (1956). *Nature*, **177**, 475.
Cheng, P. (1959). *Proc. Nat. Acad. Sci., Wash.* **45**, 1557.
Crick, F. H. C. & Watson, J. D. (1956). *Nature*, **177**, 473.
Cundy, H. M. & Rollet, A. P. (1951). *Mathematical Models*, p. 115. Oxford University Press.
Finch, J. T. (1959). Ph.D. Thesis, University of London.
Franklin, R. E., Caspar, D. L. D., & Klug, A. (1959). *Plant Pathology: Problems and Progress, 1908–1958*, p. 447. Golden Jubilee Volume of the American Phytopathological Society, University of Wisconsin Press.

Franklin, R. E. & Holmes, K. C. (1958). *Acta Cryst.* **11**, 213.
Huxley, H. E. & Zubay, G. (1960). *J. Mol. Biol.* **2**, 189.
International Tables for X-ray Crystallography (1952). **1**, 319.
Kaper, J. M. (1960). *Nature*, **186**, 219.
Kaper, J. M. & Steere, R. L. (1959). *Virology*, **8**, 527.
Klug, A. & Caspar, D. L. D. (1960). *Advanc. Virus Res.* **7**, in the press.
Klug, A., Finch, J. T. & Franklin, R. E. (1957). *Biochim. biophys. Acta*, **25**, 242.
Markham, R. (1951). *Disc. Faraday Soc.* **11**, 221.
Markham, R. (1959). *The Viruses*, vol. **2**, 33. New York: Academic Press.
Markham, R. & Smith, K. M. (1949). *Parasitology*, **39**, 330.
Nixon, H. L. & Gibbs, A. J. (1960). *J. Mol. Biol.* **2**, 197.

J. Mol. Biol. (1960) **2**, 216-225

On the Expression of a Structural Gene†

Monica Riley,‡ Arthur B. Pardee,§ François Jacob, and Jacques Monod

Biochemistry Department and Virus Laboratory, University of California, Berkeley, California, U.S.A.

and

Services de Physiologie Microbienne and Biochimie Cellulaire, Institut Pasteur, Paris, France

(*Received 16 May 1960*)

Experiments were made on the kinetics of β-galactosidase production by zygotes formed upon mating of inducible, *lac*$^+$(Hfr z^+i^+), and constitutive, *lac*$^-$(F^- z^-i^-), strains of *Escherichia coli* K12. Enzyme formation commenced within two minutes of the time of injection of the z^+ gene. The zygote thereafter produced β-galactosidase at a rate similar to that by an induced bacterium, and no increase in rate of enzyme production per zygote was observed in the first thirty minutes after mating. Therefore, the time required for the injected genetic material to become active in the functional apparatus of the F^- cell, for formation of any possible intermediates between genetic material and enzyme, and for formation of the enzyme itself, are each less than two minutes.

The Hfr strain of *E. coli* was labeled with ^{32}P and was mated with the non-radioactive F^- bacteria. A segment of ^{32}P-labeled genetic material containing the z^+ locus was transferred to the recipient. ^{32}P decay in the newly acquired genetic material was found to decrease the enzyme-forming capacity of zygotes even when it occurred some time after initiation of enzyme synthesis.

These results appear to indicate that integrity of the genetic material is required not only for an initial transfer of genetic information, but actually for enzyme synthesis to continue.

1. Introduction

Very little is known as yet about the mechanism by which structural specificity is transferred from gene to protein. Many variations can be written on such a theme. For our present purposes, we need only consider two elementary models.

(1) *No stable intermediates are formed.* According to this model, the gene acts directly as a template for protein synthesis. For many experimental purposes, the assumption that the gene acts *via* an *unstable* intermediate is equivalent.

(2) *Stable intermediates are formed.* According to this model, the gene forms stable intermediates (for instance RNA particles) which in turn synthesize the enzyme.

In order to distinguish between these two models, the ideal experiment would consist of transferring into a cell, hitherto lacking it, a gene controlling the synthesis of a protein and then removing it. By studying the kinetics of synthesis of the protein by the recipient cell following entry of the gene, one may expect to obtain some insight into the mechanisms which operate in the expression of the gene. Furthermore,

† This work was aided by a grant from the Jane Coffin Childs Memorial Fund.

‡ U.S. Public Health Service Predoctoral Fellow.

§ National Science Foundation (U.S.A.) Senior Postdoctoral Fellow.

by removing the gene after allowing a delay for expression, one might hope to detect the presence of stable intermediate catalysts.

For such a study to yield significant results, a certain number of requirements must be met:

(a) It must be established that the gene involved governs the *structure* of the protein. This requirement is essential, since it is now apparent that certain "regulatory" genes affect the synthesis of certain proteins indirectly, by setting up a control mechanism, which does not involve any transfer of structural information to the protein itself, the structure of which is governed by a "structural" gene distinct from the "regulatory" gene. The kinetics of expression of a regulatory gene have been analyzed in a recent paper in this Journal (Pardee, Jacob & Monod, 1959).

(b) The transfer of the gene, from donor to recipient cell, should as much as possible not involve nonchromosomal material.

(c) The time of entry of the gene into the recipient cell must be determined with precision.

The system which we have used appears to meet these requirements. It involves the sexual transfer from donor (Hfr) to receptor (F^-) of *E. coli* of a gene (z^+) which governs the synthesis of the enzyme β-galactosidase. That this gene determines the structure of the protein is established by the observation that mutations of this gene result in the formation of an altered protein. Moreover, in stable heterozygote diploids carrying the wild type z^+ and a mutated allele, both normal β-galactosidase and altered β-galactosidase are formed (Perrin, Bussard & Monod, 1959). The expression of the z^+ gene is controlled by another gene (i^+) which governs the synthesis of an intracellular repressor. The inhibitory effect of the repressor must be antagonized by an inducer for β-galactosidase to be formed.

Concordant evidence indicates that sexual transfer of chromosomes in *E. coli* does not involve cytoplasmic constituents. The most significant fact, in this respect, is that neither low molecular-weight metabolites, nor the cytoplasmic repressor are transferred from Hfr to F^- during conjugation (Pardee *et al.*, 1959).

The time of entry of the z^+ gene following mating can be determined rather accurately by separation of the mating bacteria at appropriate times and determination of recombinants (Wollman, Jacob & Hayes, 1956).

This system allows one to determine accurately the kinetics of β-galactosidase synthesis in zygotes of *E. coli* which have inherited their cytoplasm from an F^- carrying an inactive (z^-) allele of the z gene, and which have received a chromosome segment containing the z^+ allele from the Hfr. This study forms the subject of the first part of this paper. We have also attempted to study the effect of "removing" the z^+ gene. Since it is not possible actually to extract the gene from the cell, we have approached the problem by using the ^{32}P-decay method: the genetic material of the z^+ Hfr is heavily labeled with ^{32}P; after transfer of this material into unlabeled $F^- z^-$ bacteria, the zygotes are frozen and kept at low temperature to allow ^{32}P-decay in the transferred genetic material, in the absence of cell metabolism (Fuerst, Jacob & Wollman, 1956); the rate of enzyme synthesis after thawing is then determined (McFall, Pardee & Stent, 1958). This experiment is discussed in the second part of the paper.

2. Materials and Methods

The kinetic experiments were carried out with *E. coli* strain K12 growing exponentially in a glycerol-salts medium. The Hfr strain (4,000) carried the alleles z^+ (β-galactosidase

positive), i^+ (inducible for this enzyme), and Sm^S (sensitive to streptomycin). The F^- strain carried the z^-, i^- (constitutive for β-galactosidase) and Sm^r alleles. Composition of the medium, conditions of growth, and techniques used for enzyme assay have been described in a previous publication (Pardee *et al.*, 1959).

The experiments involving ^{32}P-decay were performed under slightly different conditions from the above. The Hfr strain used in the kinetic studies was unsuited for the ^{32}P experiments since it is lysogenic for the phage λ, and would be induced by ^{32}P-decay. The $z^+i^+Sm^S$ Hfr strain CS101 (kindly supplied by Dr. J. Tomizawa) was used instead. Injection of the z^+ gene by this strain commences at 10 min under the conditions described below.

Composition of the low phosphate-casein hydrolysate medium "H" and techniques of ^{32}P-labeling and low temperature storage were similar to those described by Stent & Fuerst (1955). The Hfr parent was grown for 2 to 2·5 divisions in a medium containing 4 μg P/ml. at a specific activity of 90 mc/mg P. This culture was centrifuged, resuspended in fresh non-radioactive medium and mixed with a suspension of exponentially growing $F^- z^- i^- Sm^r$ bacteria in 0·1 M-phosphate buffer at pH 6·3 and 15 mg/ml. asparagine. After an interval for mating, the Hfr was killed and further mating was prevented by the addition of 130 μg/ml. streptomycin and 10 μg/ml. Duponol C (sodium lauryl sulfate). The zygote suspension was diluted into minimal storage medium (Fuerst & Stent, 1956) further enriched to 10% glycerol and samples were frozen at — 196°C.

The use of the "H" medium does not qualitatively alter the kinetics observed in the minimal M63 medium, but the events in the zygote following conjugation appear to proceed at a faster rate in the richer medium. Times of formation of repressor and onset of replication do not appear comparable in the two media.

Methods for the determination of enzyme-forming capacity of the zygote suspension were similar to those described previously for unmated bacteria (McFall *et al.*, 1958). Samples of the frozen zygote suspension were thawed from day to day, separated from the high-glycerol storage medium by centrifugation, and resuspended in fresh "H" medium containing streptomycin and Duponol to prevent remating and induction of β-galactosidase in the Hfr. After 5 min preincubation, *iso*propyl-β-D-thiogalactoside (IPTG) was added to a final concentration of 5×10^{-4} M together with phosphate buffer at pH 7 at a final concentration of 4×10^{-3} M. The rate of induced β-galactosidase synthesis was determined by assay at intervals of the β-galactosidase in portions of induced culture containing about 5×10^4 zygotes.

Recombinant viability was measured on lactose-streptomycin plates and on broth-lactose-tetrazolium plates (Lederberg, 1948).

3. Kinetics of Gene Expression upon Transfer

(a) *Preliminary experiments*

Since the experiments to be performed concerned the synthesis of enzyme by zygotes or by exconjugant cells, it was necessary to determine the effects of mating upon enzyme-forming mechanisms independently of gene transfer itself. For this purpose, wild type F^- cells (z^+) were mixed with an excess of Hfr (z^-) cells, and inducer was added 30 min later. As a control, a portion of the F^- (z^+) population was mixed with an excess of F^- (z^-) cells (with which they do not mate). Fig. 1 shows that the mated population synthesized the enzyme 30 to 50% slower than the unmated one. The complementary experiment, where Hfr (z^+) were mated to F^- (z^-), gave similar results. These results are not surprising, since it is known that zygotes and exconjugant Hfr cells grow more slowly than normal cells. However, the kinetics of galactosidase synthesis are not seriously distorted in the mated as compared with the unmated population. In both cases, the accumulation of enzyme with time appears quasi-linear, at least within the first 60 min from addition of inducer. This apparent linearity, when one would expect an exponential increase, is due to the comparatively

slow growth of these cells. Even when unmated their generation time was about 90 min. The exconjugants do not divide for 3 to 4 hr. Most of the z^+ bacteria must have mated since the rate of enzyme synthesis was reduced by one-half to one-third.

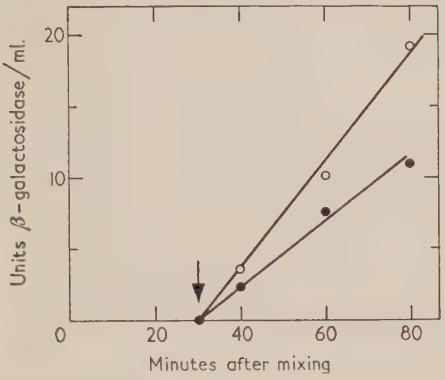

FIG. 1. Inhibition of induced enzyme production in mating bacteria.

F^- z^+ bacteria were mixed with a threefold excess of Hfr z^- bacteria, under the conditions normally used for mating. At 30 min the inducer IPTG was added and β-galactosidase was determined at intervals (●). As a control the F^- z^+ were mixed with an F^- z^- culture under the same conditions (○).

(b) *Kinetics of gene penetration and enzyme synthesis*

In order to study the kinetics of expression of the z^+ gene following its entry into the zygote, the time of entry must be determined as precisely as possible. It is known (Wollman *et al.*, 1956) that chromosome injection commences at random in the mating pairs. At the high bacterial densities used here, collision frequency does not appear to be the limiting factor. Following the commencement of injection, a finite and apparently fairly constant time is required for a given gene to enter into the zygote. The increase in zygotes containing z^+ can be estimated, in a mating of the type:

$$\text{Hfr } z^+Sm^s \times \text{F}^- z^-Sm^r$$

by shaking the culture to break the conjugating pairs at suitable times, and counting the z^+Sm^r recombinants by plating on lactose-streptomycin medium. (It should be recalled that the Hfr types used in the present experiment inject the z^+ gene some 60 to 70 min earlier than the *Sm* sensitivity gene.) As it may be seen from Fig. 2, the accumulation of z^+Sm^r recombinants follows quite accurately a linear course, allowing a fairly precise extrapolation down to the time of appearance of the first z^+ containing zygotes at 18 min. As long as unmated cells remain in large numbers, the increase in zygotes having received a specified gene follows a linear course, reflecting the formation of new mating pairs with time and the delay required for gene penetration.

Let us consider the kinetics of enzyme synthesis by the zygote population (Fig. 3). Enzyme begins to be formed very soon after the time of appearance of the first z^+-containing zygotes, and accumulates thereafter at a rate which increases with time for at least 30 to 50 min. In order to analyze these kinetics more precisely, the accumulation of z^+ zygotes in the population must be taken into account. Accumulation is linear with time, as long as unmated cells remain (Fig. 2). We may therefore write, for the number n of z^+-containing zygotes as a function of time (in this interval)

$$n = \alpha(t - t_0)$$

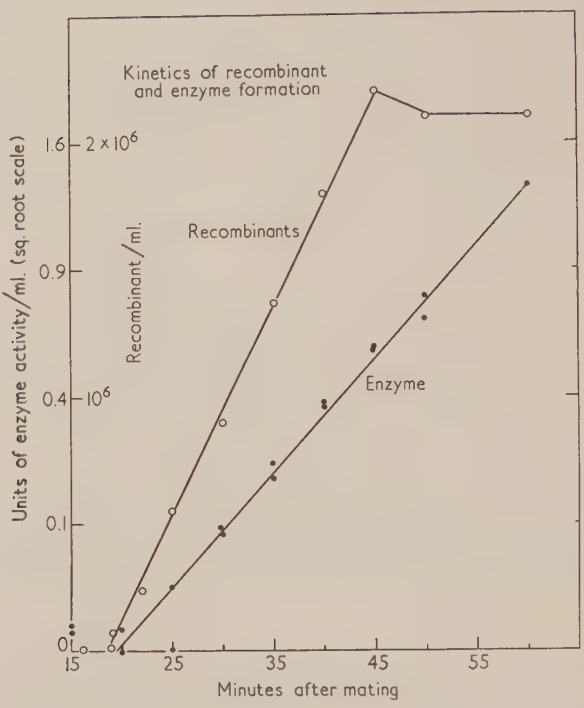

FIG. 2. Recombinant production and enzyme formation by zygotes.

Mating was performed as described under Methods, and samples were taken for blending and plating, and for enzyme estimation, at the times shown. Enzyme/ml. is plotted on a square root scale for reasons stated in the text.

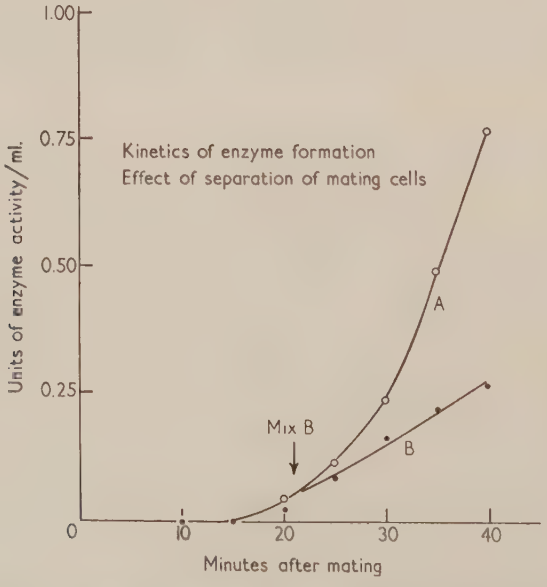

FIG. 3. Kinetics of enzyme production in undisturbed and mixed cultures.

Mating was performed as described under Methods. Sample A was undisturbed during the experiment; sample B was vigorously agitated at 21 min to disrupt the mating couples. Enzyme activity/ml. is shown *vs* time of mating.

where t_0 is the time between conjugation and penetration of the z^+ gene and α is a constant which depends upon the experimental conditions.

The rate of enzyme synthesis in the culture is equal, at any time, to the number of z^+ zygotes, and to the rate r of enzyme synthesis per z^+ zygote. We may write therefore:

$$\frac{dZ}{dt} = r\alpha(t - t_0) \tag{1}$$

where Z is the amount of enzyme in the culture. An assumption concerning the rate of synthesis per zygote must now be made. The simplest assumption is that the rate

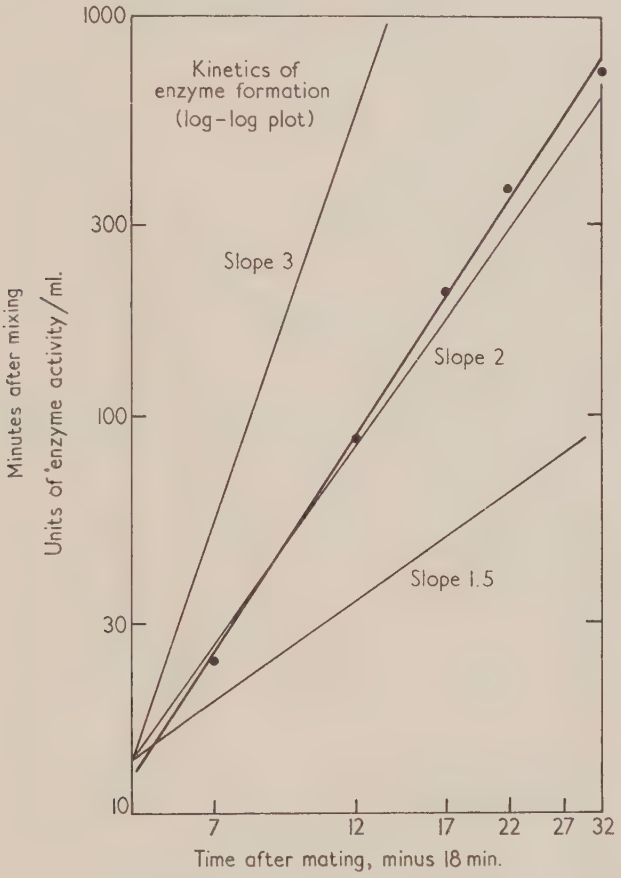

FIG. 4. Log-log plot of enzyme *vs* time.

The data shown in Fig. 2 are plotted on log-log coordinates as amount of enzyme/ml. (in arbitrary units) *vs* time. Slopes of 1·5, 2 and 3 are shown for reference.

is independent of time. The next simplest is that the rate increases linearly with time counted from entry of the z^+ gene, as would be the case if the gene synthesized an intermediate catalyst in a linear fashion.

Integrating equation (1) under the first assumption (r = constant) we obtain:

$$Z = H(t - t_0)^2 \tag{2}$$

where H combines the different constant factors.

Under the second assumption ($r = k(t - t_0)$), one obtains:

$$Z = H'(t - t_0)^3$$

To test whether one or the other assumption agrees with the data, it is convenient to plot log of enzyme *versus* log of time (counted from the time of entry of the first z^+ genes). The slope should be 2 if the relation is quadratic, 3 if it is cubic. Figure 4 shows that slope 3 is quite incompatible with the data, which give a good fit with slope 2. In a number of repetitions of this experiment, the slopes all lay within the range 1·7 to 2·1. As Fig. 2 shows, a plot of square root of enzyme synthesis *versus* time gives an excellent fit, allowing a fairly accurate extrapolation to the origin, which is found to coincide, within experimental error, with the time when the first z^+ zygotes appear.

These results therefore show that the rate of enzyme synthesis by the zygotes is constant from the time of entry of the z^+ gene, up to at least 40 or 50 min later.

The constancy of the rate of enzyme synthesis per zygote can also be demonstrated by interrupting the mating process a few minutes after the appearance of the first z^+ zygotes. As shown in Fig. 3, the rate of enzyme synthesis, after interruption of mating, is constant and equal to the rate achieved at the time of interruption.

The rate of enzyme synthesis by the z^+ zygotes should be compared with the rate obtained with wild type bacteria under similar conditions. The experimental value of the constant in equation (2) corresponds to $1{\cdot}9\times10^{-8}$ units of enzyme synthesized per minute per z^+Sm^r recombinant ultimately found. Since there are probably 4 to 5 times as many z^+ zygotes as z^+Sm^r recombinants (Wollman *et al.*, 1956), the rate per z^+ zygote is about $0{\cdot}4\times10^{-8}$ min^{-1}. Induction of Hfr bacteria in the process of mating (cf. preliminary experiments) give $1{\cdot}5\times10^{-8}$ units min^{-1} per bacterium, or $0{\cdot}5\times10^{-8}$ min^{-1} per nucleus (i.e. per z^+ gene) for trinucleate bacteria. These values are close enough, in view of the assumptions made, to support the conclusion that the z^+ gene functions nearly as effectively in the zygotes as in normal bacteria.

The precise coincidence in time between the appearance of the first z^+Sm^r recombinants and initiation of enzyme synthesis constitutes proof that the effect is not due to the transfer of cytoplasmic constituents from Hfr to F^-. As further evidence on this point, it is worth reporting that when certain types of Hfr were used, which inject the z^+ gene at a very late time (and into only a negligible fraction of the zygotes, because most of the conjugant pairs separate before that time), no enzyme formation at all was detected.

4. Effects on Enzyme Synthesis of ^{32}P Disintegration occurring in the Transferred Material

In order to determine whether enzyme synthesis can proceed after gene inactivation, we have used the ^{32}P-decay method. When Hfr bacteria heavily labeled with ^{32}P are mated with nonradioactive F^- bacteria, the production of recombinants remains sensitive for some time to ^{32}P-decay in the zygotes (Fuerst *et al.*, 1956). These experiments show that ^{32}P-decay destroys the capacity for replication of the transferred genetic material. One may similarly determine the effect of ^{32}P-decay on phenotypic expression of the z^+ gene, as measured by its effect on the rate of β-galactosidase synthesis.

For such experiments, zygotes were formed from radioactive Hfr and nonradioactive F^- bacteria, and ^{32}P-decay was allowed to occur as described under Methods. Figure 5 shows the results of an experiment in which mating was arrested 35 min after mixing the parents, and zygotes were allowed to develop until 60 min; i.e. for 50 min after penetration of the first z^+ gene. In the nonradioactive control culture

there was no decrease in the rate of enzyme synthesis during the period of storage. But, in contrast, the radioactive zygotes suffered a progressive loss of enzyme-forming capacity which must be attributed to the effects of ^{32}P-decay in the injected genetic material.

The effect of allowing different times of expression for the z^+ gene before decay is shown in Fig. 6. Mating was arrested at 35 min, as above, and the resulting zygotes

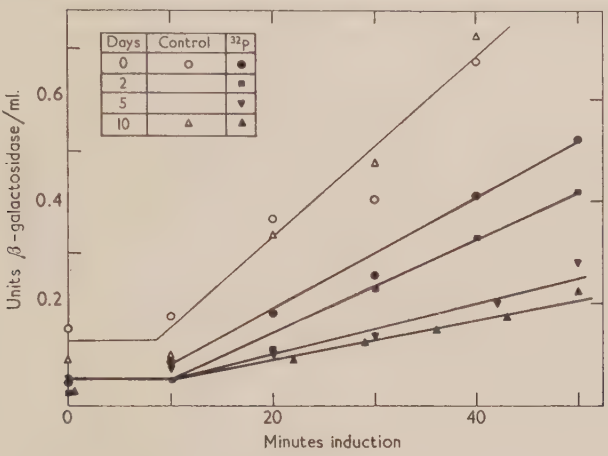

FIG. 5. Kinetics of enzyme formation as influenced by decay of ^{32}P.

E. coli CS101 grown on ^{32}P of specific activity 90 mc/mg P were mixed with nonradioactive F- bacteria. Mating was arrested at 35 min and zygotes were allowed to develop further for 25 min before storage in liquid nitrogen. The procedures are described under Methods.

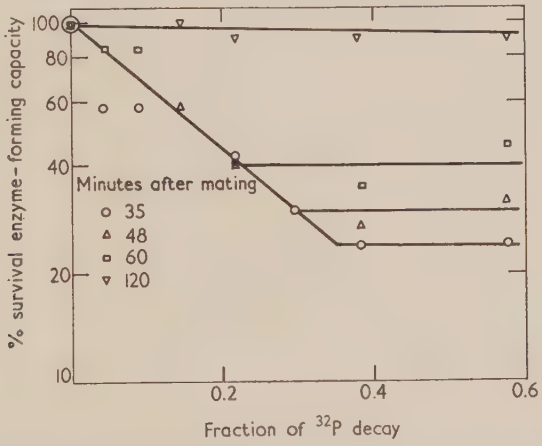

FIG. 6. Inactivation of β-galactosidase formation with progressive ^{32}P decay in zygotes.

Conditions were the same as those described in Fig. 5. After the mating was arrested at 35 min, portions were removed for low temperature storage immediately and at 48, 60 and 120 min after mating commenced. Each Hfr bacterium contained about 2×10^4 ^{32}P atoms in the nucleic acid fraction, or about 5×10^3 ^{32}P atoms in the DNA; therefore, each zygote probably received less than 500 ^{32}P atoms.

were allowed to develop further in the nonradioactive medium before freezing. In the samples taken at 25, 38, and 50 min after injection of the first *z* gene, the initial rates of decrease in enzyme formation appeared to be roughly similar, but a progressively larger fraction of the enzyme-forming capacity became stable with time. Finally, by

110 min, enzyme formation had become completely refractory to ^{32}P-decay. The stability of this last sample provides an internal control which shows that the ^{32}P disintegrations had no indirect effects on enzyme synthesis.

In any case, the stabilization cannot reflect a process which involves transfer of specificity from the injected piece to a stable catalyst which is necessary for phenotypic expression. The kinetic analysis presented above has shown that the class of zygotes examined 35 min after mating (25 min after injection of the z^+ gene) are virtually all fully functioning to produce β-galactosidase, and yet 75% of these zygotes are sensitive to ^{32}P-decay in the genetic material containing the z^+ gene. Similarly the z^+ genes of the 60 min sample had all achieved full expression for 30 to 50 min before freezing, yet 50% of this population was susceptible to the effects of ^{32}P-decay. Therefore the slow development of resistance, which probably resulted from the onset of replication of the genetic material, does not affect the conclusion that ^{32}P-decay in the genetic material suppresses enzyme synthesis.

Ability of the zygotes to give rise to recombinants was affected similarly to enzyme formation, both when measured on plates having lactose as the only carbon source and on nutrient-tetrazolium plates that allowed growth of F^- as well as recombinant bacteria. The correspondence of loss of ability of the injected material to replicate and to permit enzyme synthesis leaves little doubt that the sensitive material transferred from Hfr to F^- is indeed the genetic material.

The rates of inactivation of viability and enzyme formation of totally labeled, induced, Hfr were about ten times greater than the similar rates for zygotes formed from donors labeled at the same specific activity. It should be recalled at this point that according to McFall *et al.* (1959) the rate of inactivation of enzyme-forming capacity in totally labeled cells is the same as the rate of inactivation of the capacity to multiply. Moreover, their results indicated that the effective disintegration occurs in the DNA. The tenfold difference which we observe in the rate of inactivation of enzyme-forming capacity between totally labeled cells and zygotes would therefore appear to result from the fact that only a fraction of the labeled genetic material of the donor is introduced into the zygotes. This interpretation implies that ^{32}P-decay occurring in the genetic material *outside* of the z^+ gene itself may prevent enzyme formation.

5. Discussion

The problem we want to consider here is whether the experiments reported above allow a choice between the two extreme models of protein synthesis, involving or not the formation of stable intermediates.

The main conclusion to be drawn from the kinetic study of enzyme synthesis following gene transfer may be stated as follows: the z^+ gene which determines the structure of β-galactosidase in *E. coli* functions without significant delay, at maximal rate, when it is transferred by sexual recombination into the cytoplasm of a cell which possessed only an inactive allele of this gene.

This result evidently agrees with the model involving no stable intermediates, whether the gene itself acts directly as a template or *via* an *unstable* intermediate. The result is not compatible with the model involving the formation of stable intermediate templates, since these templates would accumulate in the cytoplasm and the rate of enzyme synthesis should start at zero and increase gradually.

This last model can be reconciled with the findings, however, by the further assumption that the gene forms very rapidly (in less than two minutes) a limited number of

stable intermediate templates, and thereafter stops functioning. Such an assumption may at first sight appear surprising, although perhaps not any more than the alternative one that the gene acts more or less directly in the synthesis of the protein. In any case, the kinetic data cannot tell more and do not discriminate between the two models.

From the ^{32}P-decay experiments one may conclude that under the conditions used, in a cell where the enzyme-forming system is already fully functioning, inactivation of the gene abolishes enzyme synthesis without delay. These findings cannot be explained by the assumption that the transfer of structural specificity from the *z* gene to the protein involves the formation of a stable intermediate catalyst such as cytoplasmic RNA. This model of gene action is excluded. Two qualifications should be noted. First, the experiment does not exclude the possibility that an information-bearing RNA closely associated with the DNA of the gene is transferred as a part of the genetic unit. Secondly, the interpretation advanced here would not be valid if the experimental conditions introduced an artifact such as the selective destruction of cytoplasmic RNA particles as a result of freezing and thawing. However, this seems unlikely in view of the fact that the procedure involves only a single freezing and thawing in a medium which preserves viability.

The assumption that the *z* gene acts *directly* as a template in the synthesis of β-galactosidase would of course account perfectly for the observations. This assumption appears unlikely, however, in the face of a growing body of evidence suggesting that the seat of protein synthesis, in many types of cells including bacteria, is not the nucleus, but rather certain cytoplasmic constituents (ribosomes). We are therefore left to consider the only other alternative, namely that the transfer of information involves functionally *unstable* intermediates, and to ask which cell constituents might be likely candidates for such a function. Surprisingly enough, particulate RNA appears as an unlikely candidate, since it has repeatedly been shown to be chemically stable in intact bacterial cells (although there is no evidence regarding its functional stability which cannot be observed by chemical tests). Ribosomes are not present in sufficient numbers in bacteria for a large fraction of their number to be inactive. No data of this kind are available for other RNA fractions, in particular for the "soluble" fraction, where a high rate of renewal might remain undetected by usual procedures, if it did not involve liberation of small nucleotides. The difficulty here is of another kind: the molecular weight of soluble RNA (as prepared by present methods) appears much too small for it to carry all the information concerning a long polypeptide chain, such as that of the monomer of β-galactosidase. These experiments therefore appear to define an interesting dilemma.

REFERENCES

Fuerst, C. R., Jacob, F. & Wollman, E. L. (1956). *C.R. Acad. Sci., Paris,* **243,** 2162.
Fuerst, C. R. & Stent, G. S. (1956). *J. Gen. Physiol.* **40,** 73.
Lederberg, J. (1948). *J. Bact.* **56,** 695.
McFall, E., Pardee, A. B. & Stent, G. S. (1958). *Biochim. biophys. Acta,* **27,** 282.
Pardee, A. B., Jacob, F. & Monod, J. (1959). *J. Mol. Biol.* **1,** 165.
Perrin, D., Bussard, A. & Monod, J. (1959). *C.R. Acad. Sci., Paris,* **249,** 778.
Stent, G. S. & Fuerst, C. R. (1955). *J. Gen. Physiol.* **38,** 441.
Wollman, E. L., Jacob, F. & Hayes, W. (1956). *Cold Spr. Harb. Symp. Quant. Biol.* **21,** 141.

J. Mol. Biol. (1960) **2**, 226-240

The Physical Properties of DNA from T2 and T4 Bacteriophage

JULIAN B. FLEISCHMAN †

The Biological Laboratories, Harvard University, Cambridge, Massachusetts, U.S.A.

(*Received 12 February 1960, and in revised form 20 May 1960*)

The project was designed to provide a molecular characterization of the DNA of the T-even bacteriophages, T2 and T4. It also attempted to clarify the problem of a possible bipartite distribution suggested by autoradiographic experiments.

The phage were grown on *E. coli* strain B in synthetic glycerol medium. Highly purified phage stocks were obtained by premature lysis and centrifugation. DNA was released from the phage by osmotic shock and cadmium cyanide-lysine treatment. The DNA solutions were deproteinized (except for whole shockates) by treatment with chloroform-amyl alcohol.

Sedimentation studies on purified DNA preparations revealed a single, fairly sharp boundary with a median sedimentation coefficient of 30 s. The intrinsic viscosity was 114 dl./g. The molecular weights determined by light scattering and by density gradient centrifugation were 14×10^6 and 11×10^6 respectively. These values are within the range expected for DNA with the above sedimentation coefficient and intrinsic viscosity. The molecular weight distribution calculated from the sedimentation boundary was found to be much narrower than a Flory (most probable) distribution. An analysis of the sedimentation patterns of whole shockates revealed no evidence for a discrete, large component as suggested by the autoradiograph experiments.

A subsequent investigation (Davison, 1959) suggests that the use of a syringe in sedimentation studies may degrade large molecules of DNA. The relationship between the 30 s DNA and that existing within the phage may therefore be uncertain.

1. Introduction

Although considerable work has been done on the problem of DNA replication in T2 and T4 infected bacteria, there have been few direct attempts to determine the molecular organization of phage DNA. The evidence to date, consisting mostly of by-products of replication studies, is fragmentary and often conflicting.

Stent, Sato & Jerne (1959) attempted to determine whether DNA replicates by a "conservative" or a "dispersive" process by studying the transfer of ^{32}P DNA from parental to progeny phage particles. Their results suggested that the phage DNA may be functionally bipartite, consisting of a portion which is conserved during replication and transferred intact to the progeny, and of another portion which is dispersed and transferred in small fragments.

Levinthal & Thomas (1957*a*), using the technique of molecular autoradiography, observed "stars" in osmotically shocked T2 preparations which represented a uniform fragment of DNA comprising about 40% of the total phage DNA complement, and corresponding to a molecular weight of about 45 million. The remaining 60% of the

† Present address: Department of Biochemistry, Stanford University School of Medicine, Palo Alto, California, U.S.A.

DNA consisted of pieces too small to produce stars. Thomas (1959) has estimated the maximum size of the small pieces to be 12 million. However, the autoradiograph method is not sufficiently sensitive to detect stars smaller than this, and no accurate estimate of the size and number of the small pieces has been made.

The large star-forming unit was found to be resistant to proteolytic enzymes, but it was destroyed by DNase and by deproteinization with chloroform-octanol (Thomas, 1959). Thomas & Knight (1959) reported a sedimentation coefficient of 41 $\pm$ 5 s for the star-forming unit using a fixed partition cell. Such a value might be expected for DNA of molecular weight 45 million (Thomas & Knight, 1959; Doty, McGill & Rice, 1958). Among first generation progeny phage studied by autoradiography, stars were found which appeared to comprise about 20% of the parental DNA, or approximately half of the large subunit (Levinthal & Thomas, 1957*b*). The 20% piece seemed to be preserved intact through a second cycle of infection. Genetic crosses revealed that markers for host range specificity appear to be associated with the parental large subunit.

The experiments of Meselson, Stahl & Vinograd (1957), while not conflicting with the foregoing replication schemes, give rise to a different picture of phage DNA organization. Photometric examination of a band of T4 DNA in a cesium chloride density gradient revealed a Gaussian distribution of DNA molecules over the band. According to the authors' theory, this implies a homogeneous assortment of molecules monodisperse with respect to their molecular weight which was calculated to be 14 million.

In view of these conflicting pictures of phage DNA and of the uncertainties accompanying the new techniques of molecular autoradiography and density gradient centrifugation, the problem was approached using classical methods of direct physical observation: sedimentation velocity, viscosity, and light scattering. It should be mentioned that in a subsequent investigation, Davison (1959) found that the use of a syringe in sedimentation studies could degrade very large molecules of DNA. This technique was used in the present work, and it is thus uncertain whether or not our results represent DNA molecules as they actually exist within the phage. This point will be considered further in the discussion.

2. Materials and Methods

(a) *Preparation of phage stocks*

The phage strains used were T2H (obtained from Dr. A. D. Hershey) and T4r_{102} (from Dr. E. Freese). No difference in the physical properties of the DNA from these two phages was observed. For the purposes of these experiments, they will be considered physically identical. Phage titers were determined by the agar plating method (Adams, 1959).

Phage stocks were grown on *Escherichia coli* strain B in glycerol medium (Fraser & Jerrel, 1953) in 10 liter quantities. The bacteria were grown to a count of 2 to 3×10^8 cells/ml. and then infected with phage to a concentration of 2×10^7 plaque-forming units per ml. In the preparation of T4 lysates, L-tryptophan (10 μg/ml.) was added with the infecting phage. The culture was lysed prematurely (Hershey, 1957) by the addition of 100 to 150 ml. of chloroform. Premature lysis substantially increases the final purity of the phage stocks, although the yields were generally lower than those of spontaneous lysates. Prematurely lysed cultures yielded phage titers of 4 to 8×10^{10}/ml.

The lysates were clarified by filtration through No. 42 Whatman filter paper using hi-flow celite. The maximum loss of titer resulting from filtration was 10 to 15%. The phage were then concentrated by batch-wise centrifugation at 15,000 g for 2 hr. The pellets were resuspended and combined in 500 ml. of glycerol medium, aerated at 37°C to remove

traces of chloroform, and incubated with 1 μg/ml. ribonuclease and 1 μg/ml. pancreatic deoxyribonuclease (Worthington) for $\frac{1}{2}$ hr at 37°C to degrade non-phage nucleic acids. $MgSO_4$ was added to a concentration of 0·002 M as a cofactor for the DNase. The phage were then purified by 5 subsequent cycles of low and high speed centrifugation. After each high speed centrifugation (23,000 ***g*** for 1 hr) the pellets were resuspended in 100 ml. of a solution of 0·2 M-NaCl + 0·01 M-phosphate buffer (pH 7) + 0·001 M-$MgSO_4$. The presence of magnesium ions was necessary for the stability of the phage stocks. The titers of the final, purified stocks ranged from 1 to 3×10^{12}/ml., representing a net recovery of about 40% of the original lysate. The optical density per plaque-forming unit of these stocks was consistently between 0·6 and $0{\cdot}7 \times 10^{-11}$. This compares favorably with similar values obtained by Hershey (1957) and Meselson (1957) and with 1 to 2×10^{-11} for stocks prepared from spontaneous lysates. The purified phage exhibited a single sharp peak when examined with an ultraviolet absorption optical system in the analytical ultracentrifuge. The sedimentation coefficient was 704 S which agrees well with values obtained by other workers (Hook, Beard, Taylor, Sharp & Beard, 1946).

(b) *Preparation of DNA*

(i) *Osmotic shock.* Phage were concentrated to a titer of 5×10^{12}/ml. by high speed centrifugation. The salt concentration was raised to 4 M by the slow addition of crystalline NaCl, and the suspension incubated for $\frac{1}{2}$ hr at room temperature. The loss of infectivity at this stage was less than 5%. The phage were shocked by rapid dilution in 20 vol cold distilled water. Over 99% of the phage was inactivated, and the solution became quite viscous due to the release of DNA.

(ii) *Cadmium cyanide.* The procedure described by Kozloff & Lute (1957) was followed. Cadmium cyanide digestion inactivated over 99% of the phage. The DNA was released from the protein coat by adding two vol 0·3 M-DL-lysine hydrochloride buffered with tris to pH 8·75 and incubating for $\frac{1}{2}$ hr at 37°C. Protein ghosts were removed by centrifugation at 32,000 ***g*** for $\frac{1}{2}$ hr. The supernatant contained 85 to 90% of the DNA originally present in the phage as measured by the diphenylamine reaction. The cyanide and lysine were removed by dialysis against pH 7 phosphate buffer. All DNA solutions were routinely stored in the presence of 0·01 M-sodium citrate.

(iii) *Deproteinization.* For many of the physical measurements it was desirable to minimize the effects of protein contaminants. DNA solutions prepared by the above methods were treated with one-third their volume of chloroform plus one-thirtieth their volume of amyl alcohol (Sevag, Lackman & Smolens, 1938). The mixture was shaken by hand in a separatory funnel for 10 min. The protein gel was removed and the procedure repeated until a protein gel was no longer visible. The level of protein contamination after this treatment was usually 2 to 3% of the final DNA concentration. (Mechanical degradation of the DNA can occur if the mixtures are shaken by machine for longer periods of time (Litt, 1958; Fleischman, 1959). The manual method, however, yielded DNA preparations with sedimentation patterns identical to those of non-deproteinized DNA prepared by the cadmium cyanide treatment.)

(iv) *Quantitative determinations.* All DNA concentrations were determined by a modification of the diphenylamine reaction (Burton, 1956). The precision of this method was $\pm$ 3% in the range 2 to 250 μg/ml. of DNA. Protein concentrations were estimated by a modified biuret reaction (Zamenhof, 1957). Concentrations could be determined down to 10 μg/ml. with a precision of $\pm$ 8%.

(c) *Physical measurements*

(i) *Sedimentation.* All sedimentation studies were performed on a Spinco model E analytical ultracentrifuge using the ultraviolet absorption optics. This feature, when used in combination with a cell of 30 mm path length, permitted runs to be made on DNA solutions of concentrations between 9 and 14 μg/ml. At these concentrations the measured sedimentation coefficient is within 5% of its value at infinite dilution (Litt, 1958). All runs were made at 29,500 rev/min at or near 20°C. Photographs on Kodak commercial

film were taken at the beginning of each run and at 8-min intervals thereafter. Exposure times were "calibrated" so that the film response was linearly related to the concentration of DNA in the cell. Photographs were analyzed with a Spinco RA Analytrol equipped with a microanalyzer attachment. All sedimentation coefficients were corrected to conditions of water at 20°C. Sedimentation coefficient distributions were calculated from the concentration *versus* distance plots on the Analytrol charts after correction for radial dilution (Litt, 1958; Schumaker & Schachman, 1957).

(ii) *Viscosity.* Measurements were made in a Ubbelohde multi-gradient capillary viscometer mounted in a water bath regulated to 25·00 ± 0·01°C. Flow times for each sample were measured at 4 gradients for each of 3 dilutions between 10 and 30 μg/ml. An extrapolation to zero gradient was made for each concentration to determine the specific viscosity. The intrinsic viscosity $[\eta]$ of the sample was found by extrapolating the reduced specific viscosity to zero concentration. The relative error in the final intrinsic viscosity determination ranged from ± 3 to 5%.

(iii) *Light scattering.* All measurements were made on a Brice-Phoenix light scattering photometer at a wavelength of 436 mμ. Angular intensity measurements were made between 20° and 135° in an Erlenmeyer-shaped cell. Solvents for measuring background scattering were clarified with a millipore HA filter membrane. DNA solutions were clarified by centrifugation for 1 hr at 35,000 *g* in a Spinco model L ultracentrifuge. The solutions were then carefully removed by pipetting and introduced into the scattering cell. The Zimm plot extrapolations to 0° were independent of the DNA concentration in the range 20 to 70 μg/ml. (Rice & Doty, 1957; Doty & Bunce, 1952). Envelopes were accordingly measured at only one concentration. This appreciably reduced the possibility of dust contamination and DNA aggregation which could occur while measuring several concentrations. Data were plotted according to the method of Zimm (1948). Molecular weights were determined by linear extrapolation of the scattering envelope to 0°. Assuming that the extrapolation is correct, the relative error in these molecular weight determinations is ± 16%.

(iv) *Density gradient centrifugation.* The procedure of Meselson *et al.* (1957) was followed except that a deproteinized DNA sample was used. 0·7 ml. of an 8 molal cesium chloride solution containing 3 μg/ml. of T4*r* DNA was centrifuged at 27,690 rev/min in the Spinco model E ultracentrifuge for 90 hr at 25·0°C. Photographs taken on Kodak commercial film were photometered using a Joyce-Loebl double-beam recording microdensitometer at a slit width of 0·03 cm.

3. Results

(a) *Sedimentation constants and heterogeneity of phage DNA*

A total of 15 separate DNA samples prepared from T2 and T4*r* stocks by the osmotic shock and cadmium cyanide methods were run in 0·2 M-NaCl + 0·01 M-Na citrate or in M/15-phosphate buffer (pH 7) + 0.01 M-Na citrate. These yielded an average sedimentation coefficient of 29·5 s with a mean deviation among the samples of ± 1·4 s. The extreme values in this group were 31·4 s and 27·2 s. Nine of the fifteen, including both osmotically shocked and cadmium cyanide preparations, had been deproteinized by manual shaking with chloroform-amyl alcohol. The average sedimentation coefficient of this group was 29·4 ± 1·5 s. The remaining six, all prepared by the cadmium cyanide method, were not deproteinized and yielded an average sedimentation coefficient of 29·6 ± 1·3 s. The boundaries in all the samples were fairly sharp and appeared identical for both deproteinized and non-deproteinized DNA. A typical boundary is shown in Fig. 1. Typical sedimentation coefficient distributions are shown in Figs. 2 and 3.

The apparent uniformity of the sedimentation pattern in all preparations regardless of the method of preparation suggests that the 29·5 s material consists of single molecules of DNA. However, subunits smaller than 29·5 s could conceivably be held together by stable protein links which are resistant to the chloroform-amyl alcohol treatment. To check this, a sample of T2 DNA prepared by the cadmium cyanide

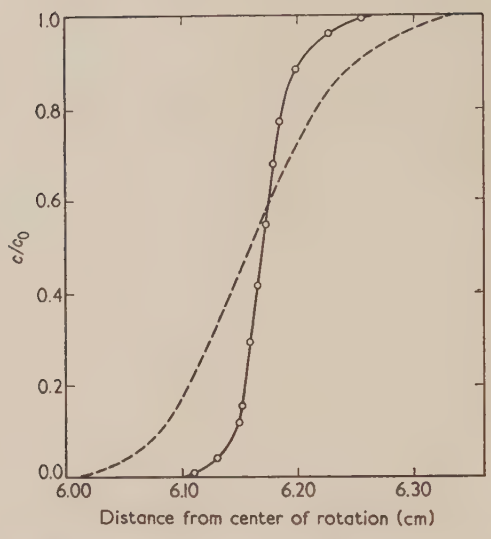

FIG. 1. Sedimenting boundary of T4*r* DNA in 0·2 M-NaCl + 0·01 M-Na citrate after 25·0 min at 29,500 rev/min. DNA concentration = 14 μg/ml. Dashed line is a calculated Flory (most probable) distribution.

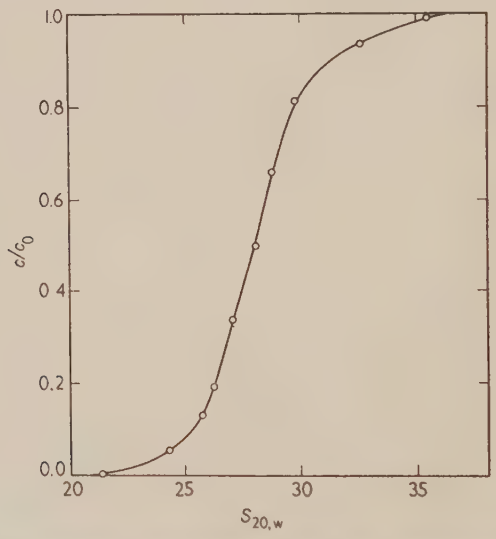

FIG. 2. Sedimentation coefficient distribution of T4*r* DNA in 0·2 M-NaCl + 0·01M-Na citrate. This distribution was calculated from the boundary in Fig. 1. Median $S_{20,w}$ = 28·0 S. 80/20 ratio = 1·18.

method was dialyzed against 0·2 M-NaCl + 0·01 M-Na citrate, deproteinized, and divided into 3 portions. The first was run in the ultracentrifuge as a control. The second was heated to 72°C for 1 hr, a treatment which should partially denature some proteins but which would leave the DNA unharmed (see Fig. 8). The third portion was similarly heated, and after cooling to room temperature was treated with 2 μg/ml. each of trypsin and chymotrypsin (Mann) and incubated at 37°C for half an hour. The sedimentation coefficients observed are summarized in Table 1.

No change in the spreading of the boundaries was observed. There appears to be no large-scale breakdown of the DNA under the above conditions and thus no evidence that there are small subunits held together by protein.

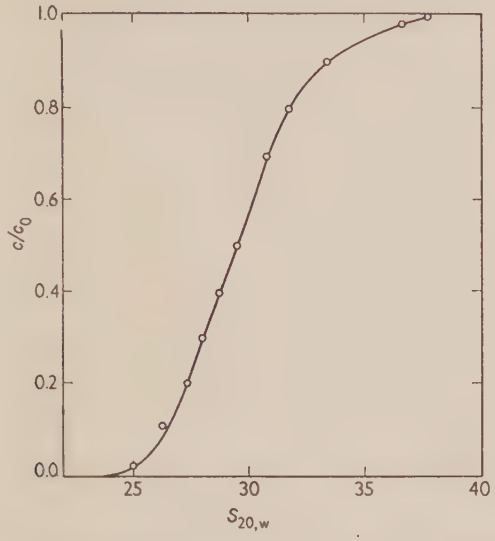

FIG. 3. Sedimentation coefficient distribution of non-deproteinized T2 DNA in M/15-phosphate buffer (pH 7) + 0·01 M-Na citrate. DNA concentration = 11·7 μg/ml. Median $S_{20,w}$ = 30·2 S. 80/20 ratio = 1·20.

Subunits might also be held together by ionic bonds. To see if any breakdown of the preparation would occur in high ionic strengths, a portion of the control sample in the above experiment was raised to a concentration of 3·0 M-NaCl. The sedimentation coefficient observed, corrected for the density of the concentrated solvent, was 30·5 S, indicating no disaggregation.

TABLE 1

	$S_{20,w}$
T2 DNA (Control)	30·9
T2 DNA heated (1 hr at 72°C)	29·0
T2 DNA heated (1 hr at 72°C) + trypsin and chymotrypsin	28·0

In view of the results of Levinthal & Thomas discussed above, several attempts were made to see if a large 40% subunit could be detected in the sedimentation pattern of an osmotically shocked preparation, i.e. in conditions identical to those under which stars are found. A separate series of 8 freshly prepared whole shockates were diluted to the appropriate concentration in 0·2 M-NaCl + 0·01 M-Na citrate. None of these whole shockates were deproteinized. The boundaries observed in the ultracentrifuge were in general more diffuse than those of other samples, with a higher average sedimentation coefficient of 34·8 ± 1·9 S. A typical sedimentation coefficient distribution is shown in Fig. 4. In no case could a distinct, rapidly sedimenting 40%

component be detected. These results suggest that the DNA in whole shockates may be randomly associated with residual protein material of the phage, causing a more rapid sedimentation and a broader peak.

The sedimentation coefficient distributions shown in Figs. 2, 3, and 4 are based on the assumption that the boundary spreading is due entirely to heterogeneity of the DNA. However, convection and diffusion may contribute to boundary spreading (Schachman, 1959). The former is usually negligible at rotor speeds similar to the one used in these experiments (Schumaker & Schachman, 1957). Diffusion hitherto has

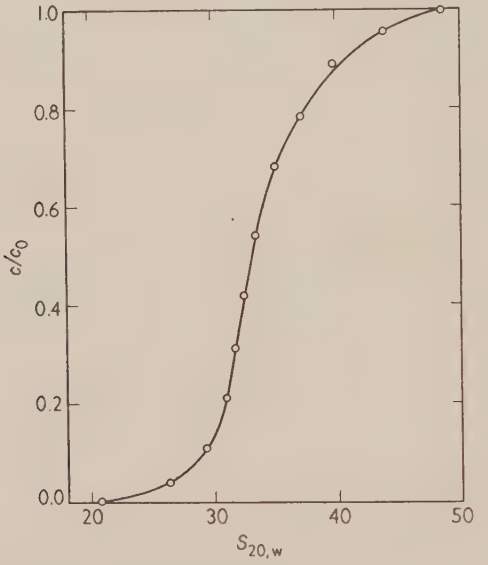

Fig. 4. Sedimentation coefficient distribution of a whole shockate in 0·2 M-NaCl. DNA concentration = 12·0 μg/ml. Median $S_{20,w}$ = 33·0 s. 80/20 ratio = 1·25.

also been considered negligible in sedimentation studies on DNA (Shooter & Butler, 1956; Schumaker & Schachman, 1957; Litt, 1958). However, the investigations were performed on heterogeneous DNA preparations which exhibited considerable boundary spreading due to polydispersity. Since phage DNA may be more homogeneous than DNA from other sources, it is possible that a greater proportion of the boundary spreading may be due to diffusion.

A rough estimate of the extent of diffusion in phage DNA boundaries can be made from the formula $\sigma^2 = 2Dt$ (Williams, Baldwin, Saunders & Squire, 1952) where σ = the standard deviation of the concentration *versus* distance curve due to diffusion, D is the macromolecular diffusion coefficient in cm^2/sec and t is time in sec. A value of D for phage DNA was estimated from the Svedberg equation (Svedberg & Pederson, 1940) assuming a sedimentation coefficient of 30 s and a molecular weight of 14 million (see below). This turned out to be $1{\cdot}2 \times 10^{-8}$ cm^2/sec which is in fair agreement with experimentally determined values of D for DNA from other sources (Shooter, 1957). Values of σ^2 calculated by the above formula were compared with those obtained graphically from the concentration *versus* distance plots of the sedimenting boundary. For boundaries measured between 20 and 60 min of effective sedimentation time, the spread due to diffusion would be about 5 to 15% of the total observed spreading. It is clear that although diffusion may contribute to boundary

spreading in phage DNA sedimentation, the majority of the spread must be attributed to the heterogeneity of the sedimenting material.

The amount of heterogeneity present in phage DNA can be compared with that of DNA from other sources. A convenient criterion of heterogeneity is the "80/20" ratio. This represents the ratio of sedimentation coefficients of material situated at concentration levels of 80% and 20% of the plateau level in the boundary. The average sedimentation coefficients and typical 80/20 values of phage DNA are compared with those of other types of DNA reported by Litt (1958) in the following table.

TABLE 2

Preparation	$S_{20,w}$	80/20 ratio
T2 and T4*r* DNA (osmotic shock and cadmium cyanide; deproteinized)	29·4	1·18
T2 DNA (cadmium cyanide; not deproteinized)	29·6	1·22
Whole shockates (not deproteinized)	34·8	1·25
Calf thymus DNA	23·0	1·5
Salmon sperm DNA	20·0	1·4
Pneumococcal transforming principle	22·0	1·8
Pneumococcal transforming principle sonicates	8·5	1·5
	6·2	1·5

(A value of 1·5 for the 80/20 ratio corresponds closely to a Flory (1953) distribution.) It is evident that phage DNA is more homogeneous than DNA previously studied from other sources.

(b) *The Molecular weight of phage DNA*

The intrinsic viscosities of two deproteinized T2 DNA samples in M/15-phosphate buffer (pH 7) + 0·01 M-Na citrate were 118 ± 5 dl./gm and 109 ± 4 dl./gm respectively. In subsequent discussions, the mean value of 114 dl./gm will be used. A typical extrapolation of reduced specific viscosity to zero concentration is shown in Fig. 5.

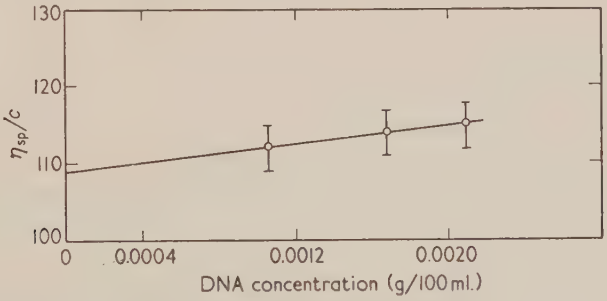

FIG. 5. Concentration dependence of reduced specific viscosity of T2 DNA in M/15-phosphate buffer (pH 7) + 0·01 M-Na citrate.

Doty *et al.* (1958) have developed empirical equations relating sedimentation coefficient and intrinsic viscosity to molecular weight for a series of sonically degraded samples of calf-thymus DNA in 0·2 M-NaCl. The equations are:

$$S_{20,w} = 0{\cdot}063 M^{0{\cdot}37}$$
$$[\eta] = 1{\cdot}45 \times 10^{-6} M^{1{\cdot}12}$$

where S is in svedberg units and $[\eta]$ is in dl./g. Substituting the observed average values of $S = 29{\cdot}5$ and $[\eta] = 114$ for native phage DNA, values of $16{\cdot}5 \pm 2.2$ million and 11.2 ± 0.5 million respectively are obtained for the molecular weight. These values are within the limits estimated below for phage DNA on the basis of light scattering and density gradient equilibrium experiments. Since they agree within a reasonable approximation, phage DNA does not differ radically from calf thymus DNA in its configuration.

The molecular weight distribution of a DNA system must be estimated to interpret light scattering data (Doty, 1957). A molecular weight distribution for phage DNA based on its sedimentation boundary can be calculated if two assumptions are made. The first is that diffusion can be neglected, and that boundary spreading is due to sedimentation coefficient heterogeneity. The second is that all the sedimentation

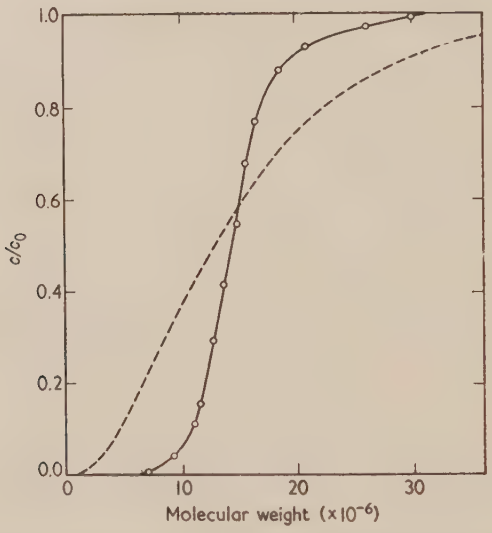

FIG. 6. Molecular weight distribution of T4r DNA calculated from the sedimentation coefficient distribution in Fig. 2. Dashed line is a Flory distribution calculated for $M_w = 15{\cdot}4$ million.

heterogeneity is attributable to molecular weight polydispersity and not to configurational heterogeneity. Although these assumptions are not completely valid, a molecular weight distribution based on them is useful in providing a *maximum* estimate of the molecular weight heterogeneity of the system.

A molecular weight distribution was calculated from the sedimentation coefficient distribution in Fig. 2. The median S_{20} of this particular sample was 28·0 s. It was chosen because its molecular weight was determined independently by light scattering. The molecular weight distribution was calculated from the sedimentation coefficient distribution by applying the relationship $S = 0{\cdot}063M^{0{\cdot}37}$ to the abscissa scale to change values of S to corresponding values of M. The molecular weight distribution is shown in Fig. 6. The weight average and number average molecular weights (M_w and M_n) were calculated directly from this distribution. The values obtained were $M_w = 15{\cdot}4$ million and $M_n = 14{\cdot}0$ million. (The molecular weight obtained for this sample by light scattering was 14·3 million.) The ratio of M_w/M_n is 1·1. This ratio would be 2·0 for a Flory distribution and 1·0 for a monodisperse system. Since the above assumptions make it likely that the distribution overestimates the molecular weight

heterogeneity, it can be concluded that the molecular weight distribution of phage DNA is narrow.

Table 3 summarizes the light scattering molecular weights and radii of gyration (ρ) obtained for three separate deproteinized T4*r* DNA samples.

TABLE 3

Sample	$M_{ls}(\times 10^{-6})$	ρ_{ls}(Å)
K-15	14·3	2910
OS-18	16·0	2630
OS-16	12·0	2850

A typical Zimm plot is shown in Fig. 7. For a polydisperse system, the molecular weight obtained is a weight average (M_w) and the radius of gyration is a z-average (ρ_z) provided the extrapolation is made along the "limiting" (initial) slope (Benoit, 1953; Geiduschek & Holtzer, 1958). However, in the case of DNA, the initial portion of the envelope is usually experimentally inaccessible, and the resulting molecular

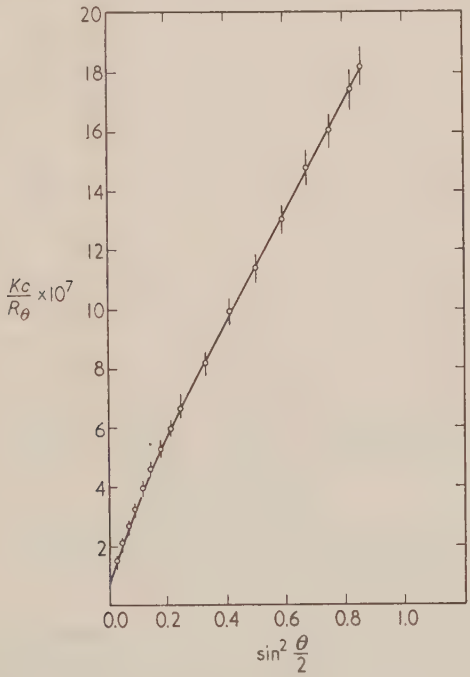

FIG. 7. Light scattering envelope of native T4*r* DNA in 0·2 M-NaCl + 0·01 M-Na citrate. DNA concentration = 25·5 μg/ml. $Kc/R_\theta = 1/14{\cdot}3 \times 10^6$.

weight determinations are often ambiguous. This ambiguity arises from (1) polydispersity, and (2) stiffness of the molecules.

Benoit (1953) and Benoit, Holtzer & Doty (1954) have shown that for most random coil systems curvature due to polydispersity is expected in the scattering envelope. As $\sin^2 \theta/2$ increases, the limiting portion of the envelope will curve and approach an

U

asymptote. Extrapolation of the asymptote to zero angle will give the reciprocal of twice the number average molecular weight (M_n). In monodisperse or very narrow distributions the curvature will be upward, and the asymptotic slope will be steeper than the limiting slope. (In the case of a Flory distribution, both slopes coincide and the scattering envelope is linear.)

When the radius of gyration of the molecule approaches 2000 to 3000 Å as in the case of DNA, the curvature in the envelope will occur below the experimentally available angular range and will not be detected unless readings are made at 10° and below (Benoit *et al.*, 1954; Doty, 1957). Measurements at such low angles are impractical, and the extrapolation must therefore be made from 20° and above. The points in this region are still near the asymptotic portion of the envelope and are not yet on the limiting slope. This means that in the case of phage DNA where the distribution is narrower than a Flory, linear extrapolation from 20° will *overestimate* M_w by about 20 to 40% (Benoit *et al.*, 1954; Doty, 1957) assuming that Benoit's polydispersity considerations for random coils apply.

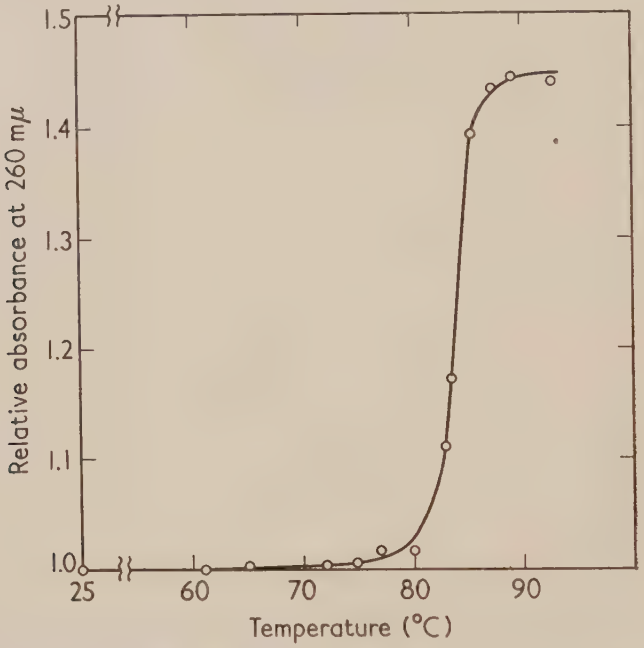

FIG. 8. Heat denaturation profile of T4*r* DNA in 0·15 M-NaCl + 0·015 M-Na citrate. $T_m = 84$°C. The data for this graph were kindly supplied by Dr. Julius Marmur.

On the other hand, Peterlin (1953) has shown that stiffness, or departure from random coil behavior, of the native DNA molecule will produce downward curvature in the scattering envelope. This will occur over a wide angular range for molecules the size of DNA. Butler, Laurence, Robins & Shooter (1959) have pointed out that downward curvature can occur below 30°, and therefore a linear extrapolation from 30° or even from 20° will *underestimate* M_w. The error is minimized as the flexibility of the molecule increases. For the usual degree of stiffness of native DNA, the error ranges from 0 to 25% (Geiduschek & Holtzer, 1958; Butler *et al.*, 1959).

The mean value for the molecular weight of the native T4*r* DNA preparations is 14·1 ± 1·4 million. Because of possible curvature in the envelope below 20°, an

accurate weight average molecular weight cannot be assigned. Nevertheless, the direction and extent of the curvature can be estimated roughly, and it is reasonably certain that the true weight average molecular weight lies between 10 and 18 million. It is also conceivable that upward curvature due to the narrow distribution of phage DNA and the downward curvature due to stiffness may tend to cancel one another, and the linear extrapolation from 20° may be yielding a value fairly close to the true weight average molecular weight.

Both the stiffness and polydispersity problems can be reduced by heat-denaturing the DNA before light scattering (Rice & Doty, 1957). This treatment "collapses" the

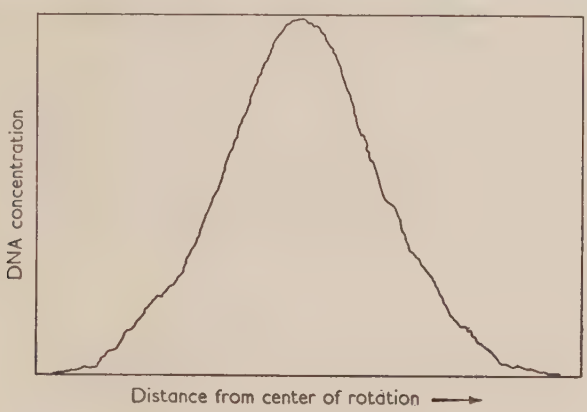

(a)

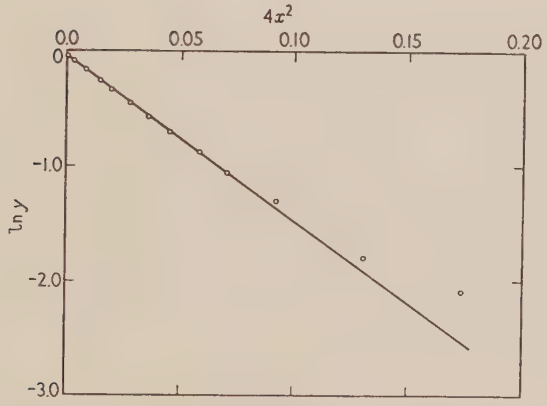

(b)

FIG. 9. (a) Densitometer tracing of T4*r* DNA band after 90 hr at 27,690 rev/min. The density at the center of the band is 1·704 g/ml. (b) Plot of band width (x) squared *versus* logarithm of relative concentration (y). The plot is linear through a 1½-fold logarithmic range implying a nearly Gaussian distribution of DNA.

molecule but does not alter its molecular weight. A preparation of deproteinized T4*r* DNA was heated at 93°C for 30 min in 0·01 M-NaCl + 0·01 M-Na citrate. (The denaturation profile of T4*r* DNA is shown in Fig. 8.) After cooling to room temperature, the extinction at 259 mμ had increased 30% and the intrinsic viscosity was reduced to 30% of its original value. The molecular weight determined by light scattering was $12{\cdot}8 \times 10^6$. This suggests that the extrapolation errors may not be great.

The molecular weight of T4*r* DNA obtained by density gradient centrifugation was 11·1 ± 1·1 million for NaDNA. A densitometer tracing of the band at 90 hr is shown in Fig. 9 together with a plot of ln *y versus* the band width squared. The molecular weight was calculated from the slope of this plot.

Molecular weight determinations by density gradient centrifugation are subject to two important limitations. The first is that any density heterogeneity in the preparation will widen the band, resulting in an under-estimate of the molecular weight (Sueoka, Marmur & Doty, 1959; Baldwin, 1959; Rolfe & Meselson, 1959). The sharpness of the denaturation profile of T4*r* DNA (Fig. 8) suggests that the molecules are fairly uniform in base composition and that density heterogeneity complications are unlikely (Marmur & Doty, 1959). The second limitation of this technique is that in highly concentrated solutions of cesium chloride the DNA may selectively associate either with the electrolyte or with water (Schachman, 1959). This also appears to be unimportant since the density of phage DNA in CsCl (1·704 g/ml.) is similar to that calculated from partial specific volume measurements in NaCl solutions. The molecular weight value of $11{\cdot}1 \times 10^6$ is lower than the 14×10^6 value found by Meselson (1957). This may be due to our use of a DNA sample slightly degraded during purification.

4. Discussion

Our experiments provide no evidence for the existence of both large and small DNA molecules in the T-even phages. Nevertheless there remains the need for an explanation of the autoradiographic results, and it seems likely that this is provided by Davison's (1959) observation that certain manipulative techniques, in particular the use of narrow syringe needles, reduce the size of phage DNA. When a wide bore needle was used to fill the ultracentrifuge cell, reducing hydrodynamic shearing forces to a minimum, he observed 60 s DNA.

This may correspond to all the DNA within T2. Our results may represent, therefore, the disaggregation under hydrodynamic shear of 29·5 s DNA molecules linearly held together by secondary forces, possibly involving protein bridges. Alternatively the shearing forces may transect DNA duplexes and the 29·5 s material may not be a fundamental unit but instead an artifact resulting from the use of a 2 ml. syringe with a no. 22 needle. The uniformity of our results makes us favor the hypothesis of disaggregation of intact DNA molecules, but it is clear that only further experiments will settle this point.

The DNA preparations used for viscosity and light scattering measurements were not put through syringe needles. However, they were routinely deproteinized by manual shaking in chloroform-amyl alcohol. This may have resulted in disaggregation of the DNA to molecules corresponding to the 29·5 s units.

The weight average molecular weight of the 29·5 s DNA based on sedimentation, viscosity, light scattering, and density gradient centrifugation, lies between 11 and 16 million. Molecular weights can also be calculated from sedimentation and viscosity data using the equation of Scheraga & Mandelkern (1953)

$$\beta = \frac{S[\eta]^{1/3}N\eta_0}{M^{2/3}(1 - \bar{v}\rho)}$$

where N = Avogadro's Number, η_0 = viscosity of the solvent in poises (0·010 for saline-citrate), $\bar{v}$ = partial specific volume of DNA = 0·55, ρ = density of the solvent (1·00), $[\eta]$ = intrinsic viscosity of DNA in dl./g, S = sedimentation coefficient in Svedbergs ×

10^{-13}, and β is a value depending on the shape and frictional properties of the molecule. Butler *et al.* (1959), using a value of $2{\cdot}6\times10^{6}$ for β (which is characteristic of a random coil), found that values of M for thymus DNA calculated in this way were consistently higher than those determined by light scattering, often by a factor of two. Substituting the observed values of $S = 29{\cdot}5\times10^{-13}$ and $[\eta] = 114$ for phage DNA, M is calculated to be 21 million. This discrepancy with the light scattering value of 14 million is similar to that observed by Butler *et al.* However, Doty *et al.* (1958) observed that for homologous thymus DNA sonicates β can assume higher values than $2{\cdot}6\times10^{6}$, depending on molecular weight. If β is increased to $3{\cdot}4\times10^{6}$, which is an acceptable value for DNA of the size we have observed, then M calculated from the Scheraga-Mandelkern equation using the above viscosity and sedimentation data is 14 million, in agreement with the light scattering results.

A molecular weight of 11 to 16 million would imply about eight to eleven DNA molecules per phage, assuming a total molecular weight complement of 120 million. It should be stressed that the term "molecule" is one of convenience and should not be interpreted too rigidly. It is possible that covalent bonds other than internucleotide linkages are holding still smaller DNA structures together.

The author wishes to express his gratitude to Dr. James D. Watson for his guidance and advice throughout this work. He is also indebted to Professor Paul M. Doty and his research group for the use of many of their research facilities. The advice and suggestions of Dr. Ernst Freese are gratefully acknowledged. This work was supported by predoctoral fellowships from the National Science Foundation and the National Institutes of Health and by Public Health Service Grant RG-5098.

REFERENCES

Adams, M. H. (1959). *The Bacteriophages*. New York: Interscience Publishers.
Baldwin, R. L. (1959). *Proc. Nat. Acad. Sci., Wash.* **45**, 939.
Benoit, H. (1953). *J. Polym. Sci.* **11**, 507.
Benoit, H., Holtzer, A. M. & Doty, P. (1954). *J. Phys. Chem.* **58**, 635.
Burton, K. (1956). *Biochem. J.* **62**, 315.
Butler, J. A. V., Laurence, D. J. R., Robins, A. B. & Shooter, K. V. (1959). *Proc. Roy. Soc.*, A. **250**, 1.
Davison, P. F. (1959). *Proc. Nat. Acad. Sci., Wash.* **45**, 1560.
Doty, P. (1957). *J. Cell. Comp. Physiol.* **49**, Suppl. 1.
Doty, P. & Bunce, B. H. (1952). *J. Amer. Chem. Soc.* **74**, 5029.
Doty, P., McGill, B. B. & Rice, S. A. (1958). *Proc. Nat. Acad. Sci., Wash.* **44**, 432.
Fleischman, J. B. (1959). Ph.D. Thesis, Harvard University.
Flory, P. J. (1953). *Principles of Polymer Chemistry*. Ithaca, New York: Cornell University Press.
Fraser, D. & Jerrel, E. A. (1953). *J. Biol. Chem.* **205**, 291.
Geiduschek, E. P. & Holtzer, A. (1958). *Advanc. Biol. Med. Phys.* **6**, 431.
Hershey, A. D. (1957). *Virology*, **4**, 237.
Hook, A. E., Beard, E., Taylor, A. R., Sharp, D. G. & Beard, J. W. (1946). *J. Biol. Chem.* **165**, 241.
Kozloff, L. M. & Lute, M. (1957). *J. Biol. Chem.* **228**, 537.
Levinthal, C. & Thomas, C. A. (1957*a*). *Biochim. biophys. Acta*, **23**, 453.
Levinthal, C. & Thomas, C. A. (1957*b*). *The Chemical Basis of Heredity*, ed. by W. D. McElroy & B. Glass. Baltimore: Johns Hopkins Press.
Litt, M. (1958). Ph.D. Thesis, Harvard University.
Marmur, J. & Doty, P. (1959). *Nature*, **183**, 1427.
Meselson, M. (1957). Ph.D. Thesis, California Institute of Technology.
Meselson, M., Stahl, F. W. & Vinograd, J. (1957). *Proc. Nat. Acad. Sci., Wash.* **43**, 581.

Peterlin, A. (1953). *J. Polym. Sci.* **10**, 425.
Rice, S. A. & Doty, P. (1957). *J. Amer. Chem. Soc.* **79**, 3937.
Rolfe, R. & Meselson, M. (1959). *Proc. Nat. Acad. Sci., Wash.* **45**, 1039.
Schachman, H. K. (1959). *Ultracentrifugation in Biochemistry*. New York: Academic Press.
Scheraga, H. A. & Mandelkern, L. (1953). *J. Amer. Chem. Soc.* **75**, 179.
Schumaker, V. N. & Schachman, H. K. (1957). *Biochim. biophys. Acta*, **23**, 628.
Sevag, M. G., Lackman, D. B. & Smolens, J. (1938). *J. Biol. Chem.* **124**, 425.
Shooter, K. V. (1957). *Progr. Biophys.* **8**, 310.
Shooter, K. V. & Butler, J. A. V. (1956). *Trans. Faraday Soc.* **52**, 734.
Stent, G. S., Sato, G. H. & Jerne, N. K. (1959). *J. Mol. Biol.* **1**, 134.
Sueoka, N., Marmur, J. & Doty, P. (1959). *Nature*, **183**, 1429.
Svedberg, Th. & Pederson, K. O. (1940). *The Ultracentrifuge*. Oxford: Clarendon Press.
Thomas, C. A. (1959). *J. Gen. Physiol.* **42**, 503.
Thomas, C. A. & Knight, J. H. (1959). *Proc. Nat. Acad. Sci., Wash.* **45**, 332.
Williams, J. W., Baldwin, R. L., Saunders, W. M. & Squire, P. G. (1952). *J. Amer. Chem. Soc.* **74**, 1542.
Zamenhof, S. (1957). *Methods in Enzymology*, Vol. III, ed. by S. P. Colowick & N. O. Kaplan. New York: Academic Press.
Zimm, B. H. (1948). *J. Chem. Phys.* **16**, 1093, 1099.

J. Mol. Biol. (1960) **2**, 241-242

Letters to the Editor

Über den Einbau Purin-analoger Verbindungen in die Bakterien-Nukleinsäure

2-Aminopurine is transformed by *E. coli* B into adenine and guanine. Both metabolites are used for nucleic acid synthesis, while only a small quantity of unchanged 2-aminopurine is incorporated into DNA and RNA. Adenine or guanine diminish the uptake of 2-aminopurine.

E. coli B converts purine to adenine and guanine. Unchanged purine could not be detected in the bacterial nucleic acids.

In Fortführung der Arbeiten über den Einbau Pyrimidin-analoger Verbindungen in die Bakterien-Desoxyribonukleinsäure (Weygand, Wacker & Dellweg, 1952; Wacker, Kirschfeld & Weinblum, 1960; Wacker, Kirschfeld, Hartmann & Weinblum, 1960) untersuchten wir auch die Aufnahme und den Stoffwechsel Purin-analoger Verbindungen bei Bakterien. Im Nachfolgenden berichten wir über Untersuchungen mit 2-Aminopurin-[T] und Purin-[T] bei *E. coli* B.

Die Markierung von 2-Aminopurin (AP) und Purin erfolgte mit Tritiumgas nach der Methode von Wilzbach (Wilzbach, 1957). Spezifische Aktivität: 2-Aminopurin-[T] 150 mc/mMol; Purin-[T] 1 mc/mMol. Es wird angenommen, daß Tritium im Aminopurin-Molekül gleichmäßig auf die Stellungen 6 und 8 verteilt ist, im Purin-Molekül gleichmäßig auf die Stellungen 2, 6 und 8 (genaue Untersuchungen sind im Gange). *E. coli* B wurde in einem halbsynthetischen Nährmedium (Wacker, Ebert & Kolm, 1958) kultiviert, jedoch ohne Adenin und Guanin. Die Ribotide wurden nach Behandlung der gesamten Bakterien mit 1 N-KOH und anschließender Dialyse aus dem Außendialysat isoliert, die Desoxyriboside wie bereits früher beschrieben (Wacker, Kirschfeld & Träger, 1959). Die Purin- und Pyrimidinbasen wurden nach Perchlorsäure-Spaltung der gesamten Bakterien bzw. der Ribotide oder Desoxyriboside papierchromatographisch isoliert.—Die Bestimmung der Radioaktivität erfolgte in einem Methandurchflußzähler (FH 51). Zur quantitativen Bestimmung der Radioaktivität wurden die Substanzen von den Papierchromatogrammen eluiert, ihre U.V.-Absorption gemessen und dann in unendlich dünner Schicht auf Aluminiumplättchen aufgedampft (Zählausbeute 15 bis 20%).—Lösungsmittelsysteme: I. *n*-Butanol/H_2O, 86:14; II. *n*-Butanol/H_2O/NH_3, 86:13:1; III. H_2O, pH 10.

Wächst *E. coli* B 36 Stdn. in Anwesenheit von 5 μg, 20 μg oder 500 μg AP-[T], so nehmen 100 mg getrocknete Bakterien 10 μg, 33 μg bzw. 230 μg AP-[T] auf. Spaltet man die mit AP-[T] gewachsenen Bakterien mit Perchlorsäure und trennt papierchromatographisch die Purinbasen in den Lösungsmittelsystemen I-III, so sind die dem AP entsprechenden Stellen nur sehr wenig radioaktiv. Dagegen zeigen die Flecke des Adenins eine hohe Aktivität, die des Guanins eine noch höhere.—Wie die Untersuchungen zeigten, wird AP-[T] sowohl in die Ribonukleinsäure (RNS) als auch in die Desoxyribonukleinsäure (DNS) aufgenommen. Nach Angebot von 5 μg AP-[T] pro ml. Nährmedium enthalten 100 mg RNS 0,13 μg AP-[T] und 100 mg DNS 0,03 μg AP-[T]. Die spezifische Aktivität des Adenins beträgt in der RNS $0{,}2\times10^6$ Imp/min/μMol, in der DNS $0{,}6\times10^6$ Imp/min/μMol. Das Guanin hat in der RNS eine spezifische Aktivität von 1×10^6 Imp/min/μMol, in der DNS von $1{,}4\times10^6$

Imp/min/μMol.—In Anwesenheit von 100 μg Guanin oder 100 μg Adenin pro ml. Nährmedium verringert sich die Aufnahme von AP-[T] bei allen Konzentrationen (5 μg, 20 μg und 500 μg) um etwa 20%. In Übereinstimmung mit Befunden bei *Lactobacillus casei* (Elion & Hitchings, 1950) hemmen 500 μg AP das Wachstum von *E. coli* B. (Mit einem ^{14}C-markierten AP von der vergleichsweise geringen spezifischen Aktivität von 1 mc/mMol gestaltet sich der Nachweis des Einbaus von unverändertem AP in die RNS und DNS wesentlich schwieriger.)

Wächst *E. coli* mit 20 μg Purin-[T] pro ml. Nährmedium, so nehmen 100 mg getrocknete Bakterien ungefähr 350 μg Purin auf. Nach Perchlorsäure-Spaltung der gesamten Bakterien und papierchromatographischer Trennung der Purinbasen in dem Lösungsmittelsystem I sind auf dem Papierchromatogramm nur zwei Flecke radioaktiv, nämlich Adenin und Guanin. Die spezifische Aktivität des Guanins betrug 7×10^5 Imp/min/μMol und war doppelt so hoch wie die des Adenins. Radioaktives Purin konnten wir bisher auf den Papierchromatogrammen nicht nachweisen.

In einer vorhergehenden Mitteilung berichteten wir über den Einbau Pyrimidin-analoger Basen in die DNS von *E. coli* B (Wacker, Kirschfeld & Weinblum, 1960). Dabei fanden wir, daß 100 mg DNS etwa 600 μg 5-Bromuracil aufnehmen. Im Vergleich dazu ist die Aufnahme von 0,03 μg AP äußerst gering.—Wie die vorliegenden Ergebnisse zeigen, wird AP bei der Aufnahme von Adenin und auch Guanin verdrängt; beide Purine sind dabei etwa gleich wirksam. Dieser Befund ergänzt und bestätigt die Aufhebung der 2-Aminopurin-Hemmung mit Adenin oder Guanin (Elion & Hitchings, 1950). Da weiterhin AP sowohl in Adenin als auch Guanin umgewandelt wird, kann man annehmen, daß AP in der Bakterienzelle die Rezeptoren des *Adenins und auch Guanins* besetzt.—Die Aufnahme von Purin weist insofern keine Besonderheit auf, da die Verbindung nicht als unnatürlicher Baustein in die Nukleinsäure eingebaut wird, sondern in Adenin und Guanin umgewandelt wird.

Wie diese und die kürzlich mitgeteilten Befunde zeigen (Wacker, Kirschfeld & Weinblum, 1960; Wacker, Kirschfeld, Hartmann & Weinblum, 1960), ist die Spezifität der Basenbausteine der Bakterien-DNS sehr groß (Zamenhof, Reiner, de Giovanni & Rich, 1956). Mit Ausnahme des Ersatzes der Methylgruppe im Thymin durch Brom, Chlor oder Jod konnte bisher noch keine Verbindung gefunden werden, die in größerem Umfange spezifisch nur in die DNS eingebaut wird.

Wir danken der Deutschen Forschungsgemeinschaft und dem Verband der Chemischen Industrie—Fonds der Chemie—für die Unterstützung dieser Arbeit.

Institut für Therapeutische Biochemie
der Universität Frankfurt am Main,
Germany

Adolf Wacker
Sigrid Kirschfeld
Lothar Träger

Received 24 May 1960

REFERENCES

Elion, G. B. & Hitchings, G. H. (1950). *J. Biol. Chem.* **187**, 511.
Wacker, A., Ebert, M. & Kolm, H. (1958). *Z. Naturf.* **13b**, 141.
Wacker, A., Kirschfeld, S. & Träger, L. (1959). *Z. Naturf.* **14b**, 145.
Wacker, A., Kirschfeld, S., Hartmann, D. & Weinblum, D. (1960). *J. Mol. Biol.* **2**, 69.
Wacker, A., Kirschfeld, S. & Weinblum, D. (1960). *J. Mol. Biol.* **2**, 72.
Weygand, F., Wacker, A. & Dellweg, H. (1952). *Z. Naturf.* **7b**, 19.
Wilzbach, K. E. (1957). *J. Amer. Chem. Soc.* **79**, 1013.
Zamenhof, S., Reiner, B., de Giovanni, R. & Rich, B. (1956). *J. Biol. Chem.* **219**, 165.

J. Mol. Biol. (1960) **2**, 243-246

Concerning the Ribonuclease Sequence †

Due primarily to the statistical work of Ycas (1958), it is now felt that globular proteins represent a set of random sequences of amino acids. That is to say, given residue n, no patterns or restrictions govern the selection of the sequentially neighboring residues $n + 1$ or $n + 2$. With the demonstration by Kendrew *et al.*

TABLE 1

n ↓ / $n \pm 3$ and $n \pm 4$ →	CH	OH	Ac	B-A	S	Ar	Total
Found	12	13	13	33	8	18	54·5
CH Expected	13·2	22·7	8·2	29·0	11·1	11·8	
Found	6	11	26	17	15		47
OH Expected	9·8	7·1	25·0	9·6	10·2		
Found		2	3	1	2		17
Ac Expected		1·3	9·0	3·5	3·7		
Found			20	12	6		60
B-A Expected			15·9	12·2	13·0		
Found				2	4		23
S Expected				2·3	5·0		
Found					2		24·5
Ar Expected					2·7		

226

CH includes gly, ala, val, leu, ileu
OH includes ser, thr
Ac includes asp, glu
B-A includes arg, lys, (asp—NH_2), (glu—NH_2)
S includes cys, met
Ar includes his, phe, tyr

† This is publication No. 62 from the Graduate Department of Biochemistry, Brandeis University, Waltham, Massachusetts. This work was supported in part by a grant from the National Science Foundation (NSFG-9743).

(1960) of the existence of the α-helix as the principal symmetry of the secondary structure of a globular protein (myoglobin), the notion of "neighbor" may acquire an additional meaning. Spatially, the nearest neighbors of residue n in an α-helix are residues $n \pm 3$ and $n \pm 4$, and the question may be put: are there any correlations between these positions and position n? With the recent completion of the entire sequence of ribonuclease by Hirs, Stein & Moore (1960), sufficient data are provided to attempt to answer this question.

Table 1 sets forth the total frequency of pairs of the type n and $n \pm 3$, $n \pm 4$ found in the ribonuclease sequence, irrespective of order within the pair. Below each observed frequency is the frequency expected by chance on the basis of the proportionate abundance of each member of the pair. In order to make the statistical procedure more meaningful, the amino acids have been grouped together on the arbitary

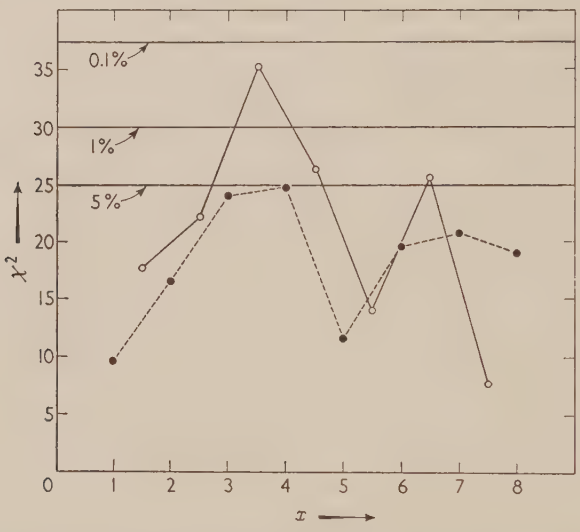

FIG. 1. The ordinate gives with filled circles the value of χ^2 computed for the distribution n *vs* $n \pm x$ as a function of the abscissa x, and with open circles the value of χ^2 for the summed distributions $n \pm x$ and $n \pm (x + 1)$. The latter values are plotted with abscissa midway between the values of x corresponding to the two terms of the sum.

basis of chemical similarity. A single amino acid, proline, has been omitted. The most significant deviations from expectation are underlined. χ^2 is 35·3 which, for these 15 degrees of freedom, is significant between the 1% and the 0·1% level; i.e., a combined deviation of this magnitude could have occurred by chance less than once out of several hundred times. When the same data is tabulated in the same way for sequentially nearest neighbors (n *vs* $n \pm 1$), χ^2 is 9·5 and the sequence appears to be a random one.

Figure 1 shows the dependence of χ^2 (calculated in the same way) on the number of residues from the reference amino acid. Neither $n \pm 3$ nor $n \pm 4$ by itself is as significantly deviant as the sum of the two. For the value of χ^2 in such a sum to be greater than that of either the summands, both distributions must deviate from randomness in the same direction. When $n \pm 7$ and $n \pm 8$ are so summed, the resultant χ^2 is low because the deviations of these two distributions are in opposite directions. The increase in χ^2 for $n \pm 6, 7, 8$ suggests a "second order" influence of the deviations of $n \pm 3, 4$.

Assuming, therefore, that the sequence is *not* random with respect to spatial neighbors in an α-helix (and the data are not yet sufficient to consider the point proved), two main types of reason for the lack of randomness may be offered. The first, purely structural, assumes that ribonuclease has a considerable content of α-helix, and that, in this case, nature in the course of evolution has found it desirable to bring together certain types of side chain, avoiding the juxtaposition of certain other types. Studies of optical rotatory dispersion have, however, indicated a low helical content for this molecule (Yang & Doty, 1957). To investigate the helical possibilities of ribonuclease, a model of the sequence has been built. Using only a right-handed α-helical screw for the peptide links wherever possible, it is found that the sequence can be contained within the crystallographic cell of ribonuclease II (Carlisle, Scouloudi & Spier, 1953) with all —S—S— bridges formed as indicated by Spackman, Stein & Moore (1960), and with a maximum of 80% of the backbone in α-helical fold. The helical segments are here arranged into a right-handed super-coil, with the two longest segments parallel to the *c*-axis. While such a model can serve to place an upper limit on the possible helical content, the actual content must await the outcome of 3-dimensional Fourier syntheses of diffraction data. In any case, one may wonder if ultimate structure provides the whole explanation.

Another possible reason is that the protein-synthesizing machinery (presumably the ribosome) itself may reflect the symmetry of the α-helix. In diffraction terminology this means that, with appropriate choice of vertical scale, the helix net of the template would coincide with that of the α-helix. If this be so, and if the type of coding were related to this symmetry, the observed departure from randomness could occur. Such a relation could be, for instance, some type of interaction between the elements coding residue n and those coding residue $n \pm 3$ or $n \pm 4$ which would restrict the choice of the amino acid for the latter positions to some subset of the entire 20 common amino acids. It is perhaps significant that serine, the most abundant amino acid in ribonuclease, has only 14 different amino acids neighboring it in either the $n + 3$ or $n + 4$ positions, and only 13 in the $n - 3$ or $n - 4$ positions, although it has a total of 28 neighbors of the first kind and 30 of the second. All the remaining residues have fewer kinds of neighbors. It would seem that only more sequential data of a magnitude comparable to that of ribonuclease, or direct evidence concerning the geometry of the template, can decide these questions or elucidate the nature of the code.

The author wishes to thank Dr. Arnold Shapiro for helpful discussions concerning these ideas, and Mildred Iantosca and Jean Roberts for their assistance in tabulating data and constructing the model.

Graduate Department of Biochemistry
Brandeis University
Waltham 54
Massachusetts, U.S.A.

Richard S. Morgan†

Received 7 May 1960, and in revised form 3 June 1960

REFERENCES

Carlisle, C. H., Scouloudi, H. & Spier, M. (1953). *Proc. Roy. Soc.* B. **141**, 85.
Hirs, C. H. W., Stein, W. H. & Moore, S. (1960). *J. Biol. Chem.* **235**, 633.

†Established Investigator of the American Heart Association.

Kendrew, J. C., Dickerson, R. E., Strandberg, B. E., Hart, R. G., Davies, D. R., Phillips, D. C. & Shore, V. C. (1960). *Nature*, **185**, 422.
Spackman, D. H., Stein, W. H. & Moore, S. (1960). *J. Biol. Chem.* **235**, 648.
Yang, J. T. & Doty, P. (1957). *J. Amer. Chem. Soc.* **79**, 761.
Yeas, M. (1958). *Symposium on Information Theory in Biology*, ed. by H. Yockey, p. 70. London: Pergamon Press.

J. Mol. Biol. (1960) **2**, 247–249

Structure of Frizzle Mutant Feather Keratin

One of the central problems which challenges our understanding of the molecular basis of biological phenomena is the genetic control of protein synthesis and structure. While cases are known in which a mutation influences the amino acid sequences in a protein, for example, in the hemoglobin of humans having sickle-cell anemia (Ingram, 1957), there is relatively little evidence on how the structural characteristics of the protein are affected, and even less on how such changes might influence the manner in which the protein functions. Furthermore, little evidence has been presented in these instances on exactly how the physical structure of the protein has been changed, although it has generally been assumed that the chain configuration in the molecule is probably altered (as a result, say, of the exchange of one particular amino acid residue by another). A resulting change in the characteristic spot distribution in the X-ray diffraction pattern is presumed to be a possible consequence of this change in polypeptide chain configuration, although none was found in the case of the sickle-cell anemia hemoglobin (Perutz, Liquori & Eirich, 1951).

The Frizzle mutation in fowl is of interest in connection with this correlation between genetic mutation and protein structure for several reasons. (1) It definitely exhibits in the X-ray diffraction pattern of the feather keratin evidence of the structural influence of a mutation. (2) The alterations in the X-ray pattern, which seem to be associated with changes in amino acid composition, suggest that the change involves the *texture* of this fibrous protein rather than the polypeptide chain structure. (3) It may be possible to connect these structural changes in the protein with the gross effects of the mutation.

The genetic and phenomenological characteristics of the Frizzle mutation in chickens have been discussed in detail (Landauer, 1942). The evidence suggests that frizzling, as compared with normal feather coverage, is a result of a single, incompletely dominant, gene difference. The effect of the mutation is to change the character of the plumage, the change being slight in heterozygous Frizzles but very marked in the homozygous fowl (i.e. both of whose parents are mutants). In the latter case the feathers are quite brittle as compared with the normal bird, and wear off readily, so that the bird may be quite bare for long periods. The feathers also exhibit other structural changes: for example, they tend to be more curled, the barbs are coarser than normal, and the barbules do not interweave as effectively as in a normal feather. As a result of the poorer feather coverage, the bird experiences an increased heat loss, which is followed by a rise in heat production, food consumption, and metabolic activity. Physiological changes result from these adjustments to the environment, and generally lead to increased mortality. That these changes result entirely from excessive heat loss is demonstrated by (1) the fact that no important physiological changes occur if the bird is kept at near thermal neutrality, and (2) if the feathers are removed from a normal bird it develops the same symptoms as does a Frizzle. Therefore it makes no difference whether the defect to body insulation is produced by a hereditary variation (Frizzle mutation) or by experimental procedure (removal of feathers). It may thus be concluded that the immediate effect of the mutation is the production of defective feathers, the secondary consequences to the animal being a result of the associated deficiencies in insulation.

In order to determine if structural changes are correlated with these mutational changes, X-ray diffraction patterns were obtained of the feather keratin from normal,

heterozygous, and homozygous Frizzles. The patterns were obtained using filtered Cu radiation, with the beam incident parallel to the surface of the calamus. The exposures were adjusted for the size of the specimens so that the scattering should be roughly the same in each case. Typical results are shown in Plate I(a) and (b), where Plate I(a) is the pattern of the normal calamus and Plate I(b) is that from a homozygous Frizzle. The pattern due to the heterozygous Frizzle is roughly intermediate between these two. Similar results, obtained with different specimens at a larger specimen-to-film distance, are shown in Plate II(a) and (b), where again Plate II(a) is from the normal calamus and Plate II(b) from the homozygous Frizzle calamus. From the patterns it will be noted that two kinds of differences exist between the normal and mutant feathers: (1) in the mutant calamus pattern there is an indication of a much higher proportion of disordered material, evidenced by the enhancement of

Table 1

Amino acid composition of normal and mutant feathers

(expressed as mg amino acid/g protein)

Amino acid	Normal	Heterozygous	Homozygous
Ala	43·7	43·7	42·9
Arg	56·3	57·2	61·8
Asp	34·8	35·3	34·9
Cys	89·3	85·5	81·8
Glu	89·5	91·5	93·7
Gly	82·5	84·6	85·8
His	4·6	4·8	5·5
Ileu	35·9	38·3	38·2
Leu	97·0	99·2	94·1
Lys	18·1	18·8	23·8
Met	4·9	4·9	4·9
Phe	53·2	53·7	53·2
Pro	112·2	111·8	103·9
Ser	148·1	143·5	142·1
Thr	45·1	43·6	41·2
Try	7·4	7·6	6·8
Tyr	27·5	27·3	28·3
Val	94·4	91·8	84·0

the two halos associated with this component as well as by the weakness of many of the characteristic crystalline reflections; (2) the crystalline component in the mutant feather is much less well oriented than it is in the normal feather. Thus, the mutation gives rise essentially to textural alterations in the protein of the calamus, the basic structure of the crystalline regions remaining unaltered.

To investigate the possibility that these changes may nevertheless reflect variations in the amino acid composition of the protein chains, amino acid analyses were done on the calamus of normal, heterozygous, and homozygous feathers. The results are shown in Table 1. The analyses were done by the microbiological assay method (Henderson & Snell, 1948), and are accurate to better than $\pm$ 5%. Although the changes are small, and, except for valine, are within the experimental error, the numerous progressive changes from normal to heterozygous to homozygous suggest that the diminution in crystallinity is probably correlated with, and may result from, changes in amino acid composition of the polypeptide chains.

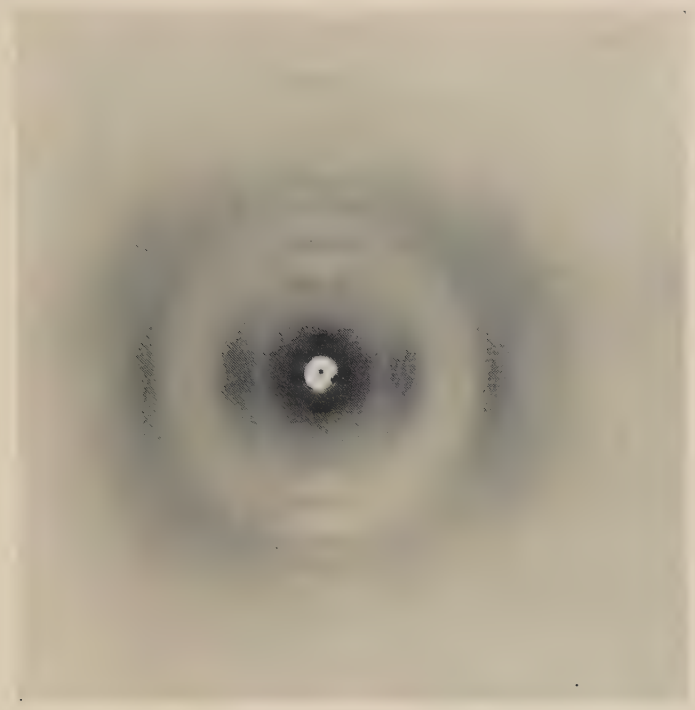

(a)

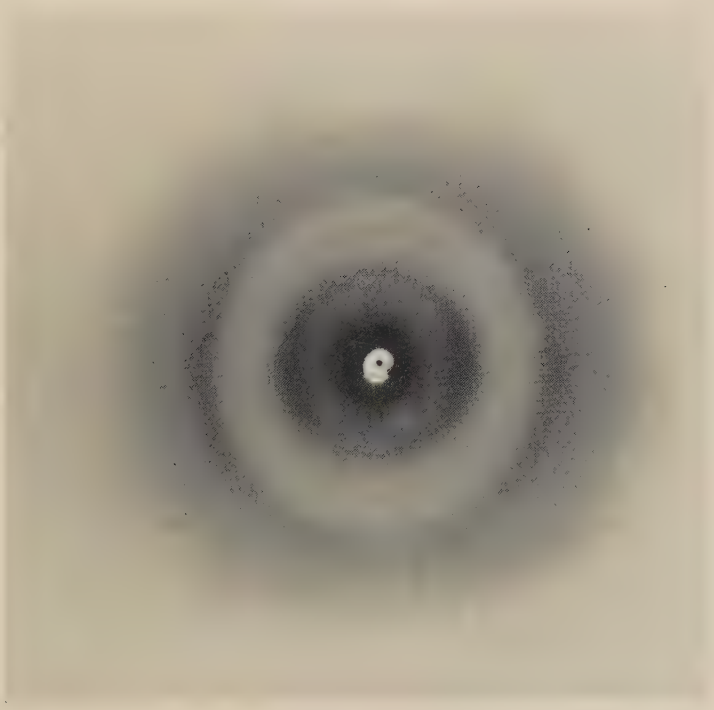

(b)

PLATE I (a) X-ray diffraction pattern of normal chicken calamus. (b) X-ray diffraction pattern of calamus from homozygous Frizzle.

[*To face page* 248

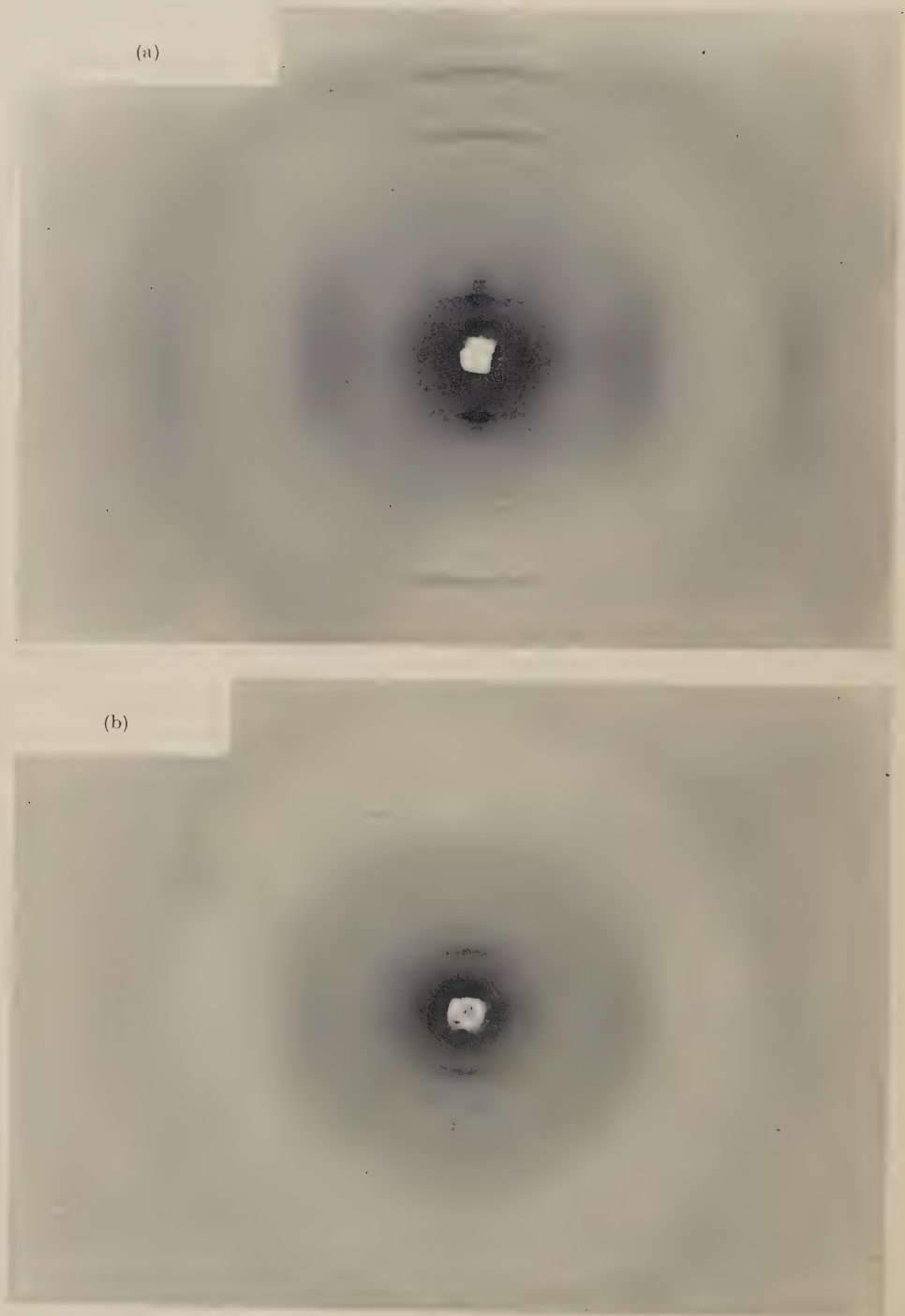

PLATE II. (a) X-ray diffraction pattern of normal chicken calamus. (b) X-ray diffraction pattern of calamus from homozygous Frizzle.

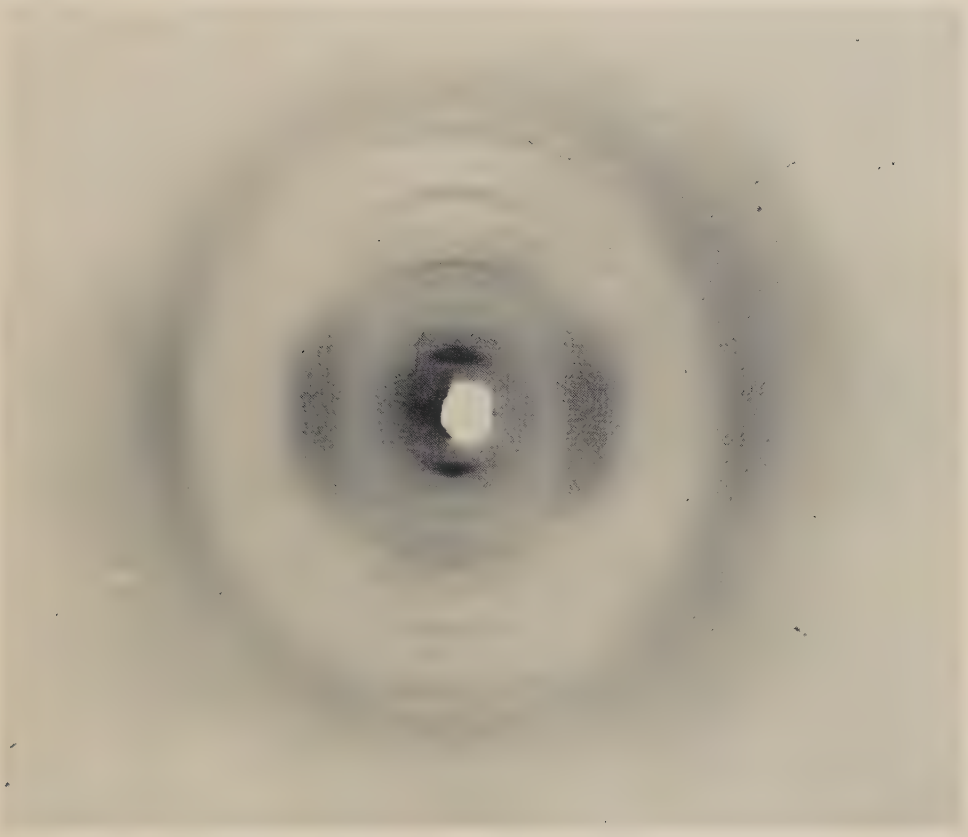

PLATE III. X-ray diffraction pattern of rudimentary feather from a 14-day normal chicken embryo.

It may be pertinent to inquire whether the changes exhibited in Plates I and II are to be considered significant. There are several reasons for believing that they are: (1) X-ray patterns of numerous different feather keratins from different kinds of birds are all basically similar to that of the normal one in Plates I(a) and II(a), none approaching that of the mutant. (2) An X-ray diffraction pattern has been obtained from the rudimentary feathers of a 14-day old normal chicken embryo (M. L. Tiffany & S. Krimm, unpublished results). This pattern, shown in Plate III, already exhibits the essential characteristics of the fully developed normal feather keratin pattern, suggesting that the enhanced disorder evidenced in the mutant pattern is a basic feature of the developed feather. (3) It has been possible to partially solubilize a piece of calamus, a disordered β-keratin component (according to its X-ray diffraction pattern) being removed (Tiffany & Krimm, unpublished results). This disordered component comprises roughly 35% of the normal feather, about 50% of a heterozygous feather, and approximately 75% of the homozygous feather calamus. (4) Polarized infrared spectra of the feather calamus show a significant reduction in the dichroism of NH and CO stretching modes, at 3240 cm^{-1} and 1650 cm^{-1} respectively, in the mutant feather as compared to that in the normal feather. This latter result is consistent with a reduction of the crystalline component and/or its poorer orientation in the mutant feather. All of these facts point to the conclusion that the changes shown in Plates I and II reflect significant characteristics of the specimens and are not artifacts.

While it may be asserted that the Frizzle mutation gives rise to characteristic textural changes in the feather keratin, the source of these changes must be speculative at present. If, as has been recently hypothesized (Krimm & Schor, 1956; Schor, 1958), the characteristic polypeptide chain configuration results from the periodicity of proline residues in the chain, then it might be possible that the mutation is affecting either the amount of proline available for incorporation (which would be consistent with the data in Table 1) and/or its positioning in the chain. In either case the result could well be the formation of a smaller proportion of the crystalline structure in the feather of the mutant. This textural difference may give rise to the altered mechanical properties of the feather which lead to the mutational effects described earlier.

The author is deeply indebted to Professor W. Landauer for providing samples of the mutant feathers. He wishes to thank Mrs. M. L. Tiffany for assistance in the X-ray work, and Mr. T. Onishi for obtaining the infrared spectra. This investigation was supported by a PHS research grant, A-2830, from the National Institute of Arthritis and Metabolic Diseases, Public Health Service.

Harrison M. Randall Laboratory of Physics
University of Michigan
Ann Arbor, Michigan, U.S.A.

S. Krimm

Received 26 January 1960 and in revised form 9 June 1960

REFERENCES

Henderson, L. M. & Snell, E. E. (1948). *J. Biol. Chem.* **172**, 15.
Ingram, V. M. (1957). *Nature*, **180**, 326.
Krimm, S. & Schor, R. (1956). *J. Chem. Phys.* **24**, 922.
Landauer, W. (1942). *Biol. Symp.* **6**, 127.
Perutz, M. F., Liquori, A. M. & Eirich, F. (1951). *Nature*, **167**, 929.
Schor, R. (1958). Ph.D. Thesis, University of Michigan.

INSTRUCTIONS TO AUTHORS

1. The *Journal of Molecular Biology* will publish papers on the nature, production and replication of biological structure at the molecular level, and its relation to function. Suitable subjects are sub-cellular organization: molecular genetics: structure and replication of viruses: molecular structure of muscle, nerve and other tissues: structure of proteins, nucleic acids, carbohydrates, lipids, etc., and their synthetic analogues, as investigated by X-rays, light absorption and other methods: problems of inter- and intra-molecular energy transfer.

2. The Journal will also publish Letters to the Editor (averaging 1000 words), and occasional review articles dealing with a more restricted or immediately topical field than those in review journals. (The Editor should be consulted in advance by anyone who considers submitting such a review.)

3. Communications will often describe results obtained by specialized techniques (for example, those of X-ray crystallography and of genetics), and it is most important that technical terms should be avoided or be clearly defined; in any event the actual results obtained and their implications should be described in a way which does not demand from the reader specialized knowledge of a particular technique.

Papers should contain the maximum density of information compatible with clarity, and every sentence should be scrutinized to ensure that its presence is essential. Authors should include enough experimental details to enable others to repeat the work (these may be printed in small type). Careful preparation of manuscript will aid prompt publication; carelessness will cause delay.

4. *Submission of Manuscripts.* Manuscripts should be sent to Dr. J. C. Kendrew, Peterhouse, Cambridge, England, or to any member of the Editorial Board. The submission of manuscript will be taken to imply that the material is original, and that no similar paper has been or will be submitted for publication elsewhere.

Papers will normally be published in English. Manuscripts in French or German will also be accepted, though the use of these languages may cause delay in publication.

5. *Copy.* Papers should be typewritten in double spacing *throughout* (including tables, legends and footnotes), on one side of quarto paper, with a margin of 1 inch all round. The position of tables and illustrations should be indicated in the text; tables and legends for illustrations should be typed separately at the end of the manuscript. All pages should be numbered serially and securely fastened together. Two copies of each manuscript should be submitted, together with three copies of the summary (see §6) and four copies of the abstract (see §9).

A short running title of not more than 40 characters (including spaces), suitable for page headings, should be indicated if the full title is longer than this.

The name of the laboratory where the work has been done should be indicated on the title page. All typescript (including the references) should be carefully checked for errors.

6. *Summary.* A summary will be printed at the head of all papers (excluding Letters to the Editor); this should generally not exceed 300 words, and should be intelligible to the general reader without reference to the main text. Abbreviations should be avoided. Summaries of papers to be printed in French or German will be in English, and should be longer (up to 1000 words) for the benefit of readers not familiar with these languages.

7. *Conventions.* The conventions used in current issues of the Journal for headings, references, etc., should be followed in preparing manuscripts. References should be listed alphabetically at the end of the paper, and abbreviated according to the *World List of Scientific Periodicals*, except that for periodicals with English names capital initial letters should be used throughout. Citations in the text should read thus: Smith, Brown & Robinson (1957), or (Smith, Brown & Robinson, 1957). When a citation has more than two authors, the names of all of them should be given at the first citation (except for more than five authors), and on subsequent citations thus: (Smith *et al.*, 1957). The conventions (Brown, 1957*a*), (Brown, 1957*b*) should be used where more than one paper by the same author(s) has appeared in one year. Volume number should be indicated in the typescript thus: **35.**

Footnotes should be avoided whenever possible. Essential footnotes should be indicated by superscript figures in the text and collected on a single page placed at the end of the manuscript.

Customary abbreviations will be used; authors may refer to *Chemical Abstracts*, to the *Biochemical Journal*, **66**, 8 (1957), and to *Notes on the preparation of papers to be communicated to the Royal Society* (1951). Certain non-standard abbreviations of chemical substances are convenient, and those listed in the *Journal of Biological Chemistry* may be used without further definition (e.g. DNA, ATP). Any other abbreviations of this kind should be used sparingly, and must be defined in a footnote at the point in each manuscript where the first such abbreviation occurs.

8. *Illustrations.* It is often convenient to make a *drawing* two or three times larger than it will appear in the Journal, but very large drawings should be avoided and it will be helpful if drawings and illustrations are submitted on quarto (or 8½ by 11 inch) sheets. Drawings should be made in

Indian ink on tracing linen, Bristol board, or faintly blue-lined graph paper; the originals should always be submitted with the manuscript, since photo-prints of drawings often cannot be reproduced satisfactorily. Explanations should, as far as possible, be placed in the legend; the drawing itself should contain a minimum of lettering, and this should be inserted lightly in *blue pencil*, in lower case except for proper names, when a capital should be used. It should be remembered that drawings will be reduced to a size not exceeding 8 by 5 inches, and that the final thickness of the lines should be 0·25 to 0·3 mm. If a curve is given merely for illustrative purposes no cross-lines are needed, but the axes should be graduated at intervals, and the diagram should be boxed in. Where possible, related diagrams should be grouped to form a single figure, and should be prepared uniformly and *on the same scale*. Where appropriate and possible a scale should be included in the illustration itself; the magnification may be noted in the legend and adjusted after reduction by the blockmaker.

Whenever possible *photographs* should be supplied the same size as they are to appear in the Journal. The page area available for a plate is 5 by 7 inches or, at the most, 6 by 8 inches.

Line drawings will be referred to as Figure 1, Figure 2, etc., and half-tone blocks as Plate I, Plate II, etc. The name(s) of the author(s) and the number should be written on all illustrations, together with the indication "Top" if necessary. Besides the original illustrations *one* duplicate set must accompany the second copy of the manuscript; these may be photo-prints, and need not be of the same quality as the originals but must be clear and legible. If *oversize* original drawings are submitted (bigger than $8\frac{1}{2}$ by 11 inches) they must be accompanied by *two* sets of small photo-prints.

9. *Abstracts*. Authors should send with their manuscripts *four copies* (typewritten in double spacing) of an abstract, in about 100 words, suitable for inclusion in biological abstracting journals. This abstract will not appear in the *Journal of Molecular Biology* but will be scrutinized by the Editors before being passed for publication. The abstract should outline as briefly as possible the results and definitive conclusions of the work. Details of methods are generally not required.

The abstract should be headed as follows: title of paper; name(s) of author(s); *J. Mol. Biol.*, followed by space for the year, volume and page references; abbreviated postal address (including country of origin) to which applications for reprints may be sent. For example: The isolation and properties of deoxyribonucleoprotein particles containing single nucleic acid molecules. G. Zubay & P. Doty. J. Mol. Biol. . . . . (Dept. of Chem., Harvard Univ., Cambridge, Mass., U.S.A.). —text of abstract follows.

10. *Reprints*. Fifty reprints of each paper will be supplied free of charge; additional copies may be purchased.

METABOLIC PATHWAYS

Edited by **DAVID M. GREENBERG**

Department of Biochemistry, University of California School of Medicine, San Francisco

Completely Rewritten Second Edition of CHEMICAL PATHWAYS OF METABOLISM

In 2 Volumes

THIS WORK contains an up-to-date account of present day knowledge of the metabolic patterns and enzyme systems that carry out the metabolic reactions of living organisms. Each chapter has been written by an outstanding authority.

VOLUME 1: **Carbohydrates, Lipids, and Related Compounds**

September 1960, about 540 pp., illus., $18.00

SPECIAL OFFER, valid until 31 December 1960—$16.50

Free Energy and Entropy in Metabolism
By ARTHUR B. PARDEE and LLOYD INGRAHAM

The Mitochondrial System of Enzymes
By DAVID E. GREEN and SIDNEY FLEISCHER

Glycolysis
By BERNARD AXELROD

The Tricarboxylic Acid Cycle
By H. A. KREBS and JOHN M. LOWENSTEIN

Other Pathways of Carbohydrate Metabolism
By BERNARD AXELROD

Biosynthesis of Complex Saccharides
By WILLIAM Z. HASSID

Fatty Acid Oxydation and Synthesis
By DAVID E. GREEN and DAVID M. GIBSON

Ascorbic Acid
By JOHN J. BURNS

Metabolism of Phosphatides
By ROGER ROSSITER

Metabolism of Sterols
By T. T. TCHEN

Metabolism of Steroid Hormones
By LEO T. SAMUELS

Carotenoids and Vitamin A
By GORDON MACKINNEY

AUTHOR INDEX—SUBJECT INDEX

VOLUME 2: **Amino Acids, Nucleic Acids, Porphyrins, Vitamins, and Coenzymes**

In preparation

Nitrogen Metabolism of Amino Acids
By PHILIP P. COHEN and H. J. SALLACH

Carbon Catabolism of Amino Acids
By DAVID M. GREENBERG

Biosynthesis of Amino Acids
By DAVID M. GREENBERG

Metabolism of Sulfur-Containing Compounds
By ERNEST KUN

Peptide and Protein Biosynthesis
By ILSE D. RAACKE

Purines and Pyrimidines
By MARTIN P. SHULMAN

Nucleotides and Nucleosides
By LEONARD WARREN

Metabolism of Heme and Chlorophyl
By SAM GRANICK

Thiamine
By PETER ALBERSHEIM and JAMES BONNER

Pyridine Nucleotides, Pantothenic Acid and Coenzyme A
By NATHAN O. KAPLAN

Riboflavin
By GERHARD W. E. PLAUT

Pteridines and Vitamin B-12
By THOMAS H. JUKES and HARRY P. BROQUIST

AUTHOR INDEX—SUBJECT INDEX

ACADEMIC PRESS, New York and London
111 Fifth Avenue, New York 3, New York
17 Old Queen Street, London, S.W.1

Announcing a Comprehensive Treatise

IN 3 VOLUMES

Structure and Function of MUSCLE

Edited by G. H. BOURNE, *Emory University*

Volume 1 — Structure

May 1960, 472 *pp.*, 115 *illus.*, $14.00

The Anatomy of Muscles and Their Relation to Movement and Posture, by R. D. Lockhart

The Microanatomy of Muscle, by E. W. Walls

Development of Striated Muscle, by J. D. Boyd

Histochemistry of Developing Skeletal and Cardiac Muscle, by E. B. Beckett and G. H. Bourne

Skeletal Muscle Tissue in Culture, by Margaret R. Murray

The Structure of Striated Muscle As Seen by the Electron Microscope, by H. Stanley Bennett

The Molecular Basis of Contraction in Cross-Striated Muscles, by H. E. Huxley and J. Hanson

Molecular Structure and Function of Smooth Muscle, by Arpad Csapo

Structure and Function of the Contractile Apparatus in the Muscles of Invertebrate Animals, by Jean Hanson and J. Lowy

Motor End-Plate Structure, by R. Couteaux

Muscle Spindles and Other Muscle Receptors, by Sybil Cooper

Intercalated Discs of Heart Muscle, by F. S. Sjöstrand and E. Andersson-Cedergren

AUTHOR INDEX—SUBJECT INDEX

Volume 2 — Biochemistry and Physiology

August 1960, 593 *pp.*, *illus.*, $16.50

Proteins of the Myofibril, by Andrew G. Szent-Györgyi

Biochemistry of Muscular Action, by D. M. Needham

Biochemistry of Sarcosomes, by E. C. Slater

Endocrines and Muscle, by Jane A. Russell and Alfred E. Wilhelmi

The Neuromuscular Junction: Role of the Acetylcholine System, by David Nachmansohn

Some Aspects of the Biophysics of Muscle, by Robert W. Ramsey

Thermodynamics of Muscle, by R. J. Podolsky

Comparative Physiology of Activation of Muscles, with Particular Attention to Smooth Muscles, by C. Ladd Prosser

The Physiology of Muscular Exercise, by Roger G. Bannister

Part I. Some Effects of Fatigue, Temperature, and Training on Muscular Contraction in Man, by O. G. Edholm

Part II. Fatigue of the Working Individual, by E. Hohwü Christensen

The Control of Muscular Activity by the Central Nervous System, by Marion Hines

Selected Topics on the Physiology of the Heart, by W. F. H. M. Mommaerts, B. C. Abbott, and W. J. Whalen

AUTHOR INDEX—SUBJECT INDEX

Volume 3—Pharmacology and Disease

September 1960, 482 *pp.*, *illus.*, $15.00

Effects of Drugs on Smooth and Striated Muscle, by Stephen Thesleff

The Effects of Drugs on Myocardial Contractility, by Neil C. Moran and Marion DeV. Cotten

Virus Infections of Muscle, by E. J. Field

Parasitic Infections, by P. C. C. Garnham

Muscle Regeneration and Repair, by E. J. Field

Effects of Nutritional Deficiencies upon Muscle, by Karl E. Mason

Aging Changes in Muscle, by L. J. Rubinstein

Post Mortem Changes in Muscle, by J. R. Bendall

Histochemistry of Skeletal Muscle and Changes in Some Muscle Diseases, by E. B. Beckett and G. H. Bourne

Myopathy: The Pathological Changes in Intrinsic Diseases of Muscles, by F. D. Bosanquet, P. N. Daniel, and H. B. Parry

Clinical Aspects of Some Diseases of Muscle, by Ronald A. Henson

Genetic Aspects of Muscular and Neuromuscula Diseases, by John N. Walton

Remarks on Muscle, by Albert Szent-Györgyi

AUTHOR INDEX—SUBJECT INDEX

ACADEMIC PRESS, *New York and London*

111 Fifth Avenue, New York 3, New York

17 Old Queen Street, London, S.W.1

"Surely destined to become one of the classics of biochemistry"—SCIENCE

THE ENZYMES

SECOND EDITION *Completely revised and reset*

Edited by **Paul D. Boyer, Henry Lardy, and Karl Myrbäck**

Complete in 7 volumes

Fifteen per cent price reduction on orders for the complete set received before publication of the last volume

Volume 2: Purine and Pyrimidine Nucleotides and Phosphagens

Prosthetic Groups and Cofactors (Part A)

April 1960, 479 *pp., illus.*, $16.00

Contents

Adenine Nucleotides and Properties of Pyrophosphate Compounds By ROBERT M. BOCK

Uridine Nucleotides By LUIS F. LELOIR and CARLOS E. CARDINI

Cytidine Nucleotides By EUGENE P. KENNEDY

Guanosine and Inosine Nucleotides By MERTON F. UTTER

N-Phosphorylated Guanidines By J. F. MORRISON and A. H. ENNOR

Pyridoxal Phosphate By ALEXANDER E. BRAUNSTEIN

Folic Acid By JESSE C. RABINOWITZ

Glutathione By W. EUGENE KNOX

Thiamine Coenzymes By DAVID E. METZLER

Flavin Coenzymes By HELMUT BEINERT

AUTHOR INDEX—SUBJECT INDEX

Volume 3: Prosthetic Groups and Cofactors (Part B)

July 1960, 497 *pp., illus.*, $16.00

Contents

Coenzyme A By L. JAENICKE and F. LYNEN (Translated from the German by Helmut Beinert)

The Pyridine Coenzymes By NATHAN O. KAPLAN

Charge-Transfer Complexing of Pyridinium Rings By EDWARD M. KOSOWER

Lipoic Acid By LESTER J. REED

Metal and Enzyme Interactions: Correlation of Composition, Function, and Structure By EERT L. VALLEE

Heme Compounds in Enzyme Catalysis By K. G. PAUL

Vitamin K By HENRIK DAM and E. SØNDERGAARD

Vitamin E By PAUL D. BOYER

Enzymic Aspects of the Visual Processes By GEORGE WALD and RUTH HUBBARD

L-Ascorbic Acid By J. J. BURNS and GILBERT ASHWELL

Enzymic Equilibria and Thermodynamics By MARVIN J. JOHNSON

AUTHOR INDEX—SUBJECT INDEX

VOLUMES 4 and 5: 1960, *in preparation*

VOLUMES 6 and 7: 1961, *in preparation*

ACADEMIC PRESS, New York and London

FILED IN STACKS

CONTENTS

BOEDTKER, HELGA, Configurational Properties of Tobacco Mosaic Virus Ribonucleic Acid 171

HUXLEY, H. E. and ZUBAY, G., The Structure of the Protein Shell of Turnip Yellow Mosaic Virus 189

NIXON, H. L. and GIBBS, A. J., Electron Microscope Observations on the Structure of Turnip Yellow Mosaic Virus 197

KLUG, A. and FINCH, J. T., The Symmetries of the Protein and Nucleic Acid in Turnip Yellow Mosaic Virus: X-Ray Diffraction Studies . . 201

RILEY, MONICA, PARDEE, ARTHUR B., JACOB, FRANÇOIS and MONOD, JACQUES, On the Expression of a Structural Gene 216

FLEISCHMAN, JULIAN B., The Physical Properties of DNA from T2 and T4 Bacteriophage 226

Letters to the Editor—

Über den Einbau Purin-analoger Verbindungen in die Bakterien-Nukleinsäure, ADOLF WACKER, SIGRID KIRSCHFELD and LOTHAR TRÄGER 241

Concerning the Ribonuclease Sequence, RICHARD S. MORGAN . . 243

Structure of Frizzle Mutant Feather Keratin, S. KRIMM . . . 247

Printed in Great Britain at the Aberdeen University Press